UNIVERSITY OF TRENTO - Italy

International Doctoral School in Biomolecular Sciences

XXV Cycle

"Functional characterization of the RNA binding protein RALY"

Tutor

Professor Paolo MACCHI

CIBIO- University of Trento

Ph.D. Thesis of

Albertomaria MORO

CIBIO- University of Trento

Academic Year 2012-2013

To myself and my little world...

INDEX

.

ABSTRACT

Of 25000 genes encoded from genome, more than 90% are subject to alternative splicing or other post-transcriptional modifications. All these events produce a high number of different proteins that form the basis for the high variety of cells. The RNA-binding proteins (RBPs) play crucial roles in this variability by regulating many steps of biological processes regarding RNA metabolism. The heterogeneous nuclear ribonucleoproteins (hnRNPs) belong to big family of RBPs involved in many aspects of RNA metabolism including RNA stability, intracellular transport and translation. More recently, RALY, a RNA-binding protein associated with the lethal yellow mutation in mouse, has been identified as new member of the hnRNP family even if, its biological function remains still elusive.

My PhD project aimed to characterize human RALY and to assess its function in mammalian cells. Initially I identified the expression pattern of this protein into the cell and I characterized the functional nuclear localization sequence that localizes RALY protein into the nuclear compartment. In order to better understand the role of RALY in the cells, I identified the proteins component of RALY-containing complexes using a new assay named iBioPQ (*in vivo*-Biotinylation-Pulldown-Quant assay). I also performed polyribosome profiling assay to check the presence of RALY in translating mRNAs. Moreover, a microarray assay was performed in order to identify potential mRNAs whose metabolism appears dependent on RALY expression. Taken together, the results that I obtained suggest that RALY is involved in mRNA metabolism. Unfortunately more studies remain to do before shedding some light on the biological role of RALY in mammals

.

1 - INTRODUCTION

According to the central dogma of molecular biology, a particular segment of DNA, called gene, is transcribed into RNA (precisely messenger-RNA) and then it is converted, through a process called translation, into a protein. In this scheme, the mRNA had been viewed as a passive component which carries the protein blueprint from the nuclear DNA to the cells' "machines" which drive protein synthesis. However, this is a very simply way to see gene expression, because gene expression is a very complex and highly regulated process, especially relating to mRNA. Differential gene expression is crucial for growth, differentiation, development and cell survival in various situations, including environmental stress. It is very important, therefore, that all these processes are tightly controlled, not only in order to minimize cell energy, but also to reduce errors that might affect survival of the cell or even of the entire organism. For these reasons several interconnected steps have been evolved to control gene expression.

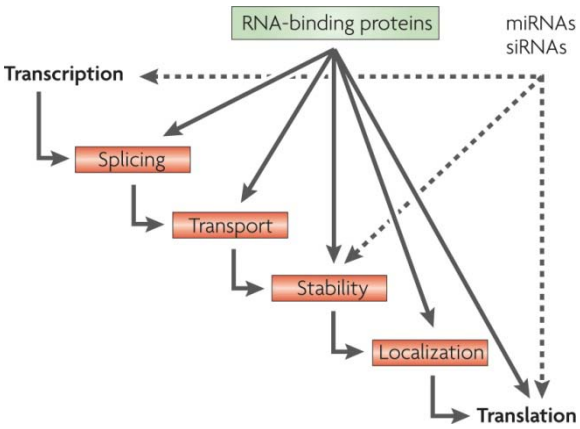

Figure 1 Interconnected steps of post-transcriptional regulation and its potential coordination (Keene 2007)

In the last few years, we have seen the birth of new hypotheses regarding the control of gene expression; these hypotheses are focused on the role that RNA metabolism plays in creating protein variability. In fact, processes such as splicing, mRNA silencing, transport and localization of certain transcripts to sub cellular compartments, and processes to control RNA "quality" are all critical to ensure survival, development and maturation of a cell. If only one of these processes is altered, the physiology of the entire cell can be impaired. The results of post-translational control studies of gene expression have led to a new fascinating theory: the "RNA-operon", namely the coordination of trans-acting factors, which regulate the translation of multiple mRNAs in different pathways, allowing cells to respond rapidly to environmental cues (Keene and Lager 2005; Keene 2007). The fundamental components of the "operon" are the ribonucleoparticles (RNPs), complexes compose of multiple factors, such as RNA-binding proteins (RBPs), mRNAs, non-coding RNAs and other molecules including, for example, motor proteins (Keene 2007). The great heterogeneity of these particles, which may be composed by different proteins and mi/siRNAs, plus the presence of mRNA encoded for the same

protein in different RNPs localized in different cellular regions, have drastic effects on the regulation and translation of mRNAs, causing a very dynamic synthesis of proteins. This high variability in gene expression is the principal responsible for the rapidly cellular response to external and internal stimuli (Abdelmohsen, Pullmann et al. 2007; Keene 2007). Although the RNPs are composed by several proteins and molecules, the RNA-binding proteins have the most important role in the variability of gene expression: they are responsible to the maturation of pre-mRNA, they can bind different kinds of RNAs, including rRNAs, miRNAs and lncRNAs; moreover, the capacity of this proteins to mutually interact or with other proteins as the motor proteins permit the formation, the control and the mobility of the RNPs.

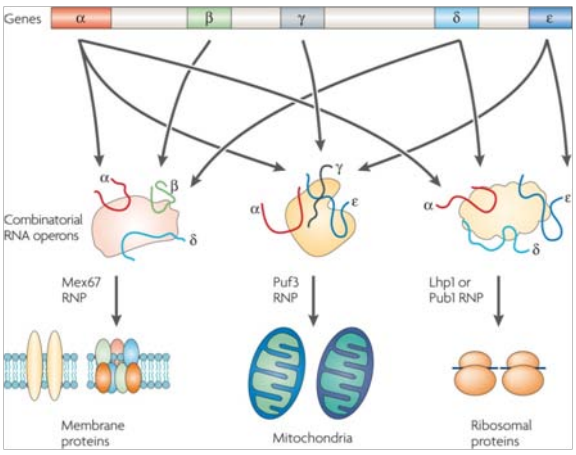

Figure 2 Formation and dynamics of ribonucleoprotein (RNP) complexes (Keene 2007)

1.1 THE RNA-BINDING PROTEINS

Due to the plethora of biological processes regulated by the RNA-binding proteins, these proteins must be able to recognize different RNA's structures, for example short sequences, secondary structures, RNA duplexes and many other structures (Sibley, Attig et al. 2012). This ability is given by specific structured domains known as RNA-binding domains (RBDs). More than ten different RBDs have been identified so far. Table 1 shows only a selected list of the most common RBDs. Each single domain recognizes a specific sequence or a defined structure of RNA. However, to guarantee the specific binding with their cargo mRNAs, several proteins contain two or more RBDs connected by a linker, also known as auxiliary domain, a short sequence that in most cases does not play a direct role in RNA binding (Lunde, Moore et al. 2007; Shazman and Mandel-Gutfreund 2008).

The auxiliar domains can be sequences located in other protein regions, in many case distant from the RBDs, and they have the capacity to promote RNA-binding activity or they can be used in protein-protein interaction. For example in the serine/arginine-rich (SR) splicing factor family (SRSF), the serine/arginine (SR) domain, which characterize this family, does not have any role in the recognition of RNA, but rather facilitates the recruitment of other spliceosomal components to pre-spliced RNA (Schaal and Maniatis 1999).

Domain	Topology	RNA-recognition surface	Protein–RNA interactions	Representative structures (PDB ID)
RRM	αβ	Surface of β-sheet	Interacts with about four nucleotides of ssRNA through stacking, electrostatics and hydrogen bonding	U1A N-terminal RRM[18] (1URN)
KH (type I and type II)	αβ	Hydrophobic cleft formed by variable loop between β2, β3 and GXXG loop. Type II: same as type I, except variable loop is between α2 and β2	Recognizes about four nucleotides of ssRNA through hydrophobic interactions between non-aromatic residues and the bases; sugar-phosphate backbone contacts from the GXXG loop, and hydrogen bonding to bases	Nova-1 KH3 (type I)[41] (1EC6), NusA (type II)[37] (2ASB)
dsRBD	αβ	Helix α1, N-terminal portion of helix α2, and loop between β1 and β2	Shape-specific recognition of the minor–major–minor groove pattern of dsRNA through contacts to the sugar-phosphate backbone; specific contacts from the N-terminal α-helix to RNA in some proteins	dsRBD3 from Staufen[51] (1EKZ)
ZnF-CCHH	αβ	Primarily residues in α-helices	Protein side chain contacts to bulged bases in loops and through electrostatic interactions between side chains and the RNA backbone	Fingers 4–6 of TFIIIA[56] (1UN6)
ZnF-CCCH	Little regular secondary structure	Aromatic side chains form hydrophobic binding pockets for bases that make direct hydrogen bonds to protein backbone	Stacking interactions between aromatic residues and bases create a kink in RNA that allows for the direct recognition of Watson–Crick edges of the bases by the protein backbone	Fingers 1 and 2 of TIS11d[57] (1RGO)
S1	β	Core formed by two β-strands with contributions from surrounding loops	Stacking interactions between bases and aromatic residues and hydrogen bonding to the bases	Ribonuclease II[121] (2IX1), exosome[99] (2NN6)
PAZ	αβ	Hydrophobic pocket formed by OB-like β-barrel and small αβ motif	Recognizes single-stranded 3′ overhangs of siRNA through stacking interactions and hydrogen bonds	PAZ[73] (1SI3), Argonaute[76] (1U04), Dicer[72] (2FFL)
PIWI	αβ	Highly conserved pocket, including a metal ion that is bound to the exposed C-terminal carboxylate	Recognizes the defining 5′ phosphate group in the siRNA guide strand with a highly conserved binding pocket that includes a metal ion	PIWI[75] (1YTU), Argonaute (1U04)[76]
TRAP	β	Edges of β-sheets between each of the 11 subunits that form the entire protein structure	Recognizes the GAG triplet through stacking interactions and hydrogen bonding to bases; limited contacts to the backbone	TRAP[122] (1C9S)
Pumilio	α	Two repeats combine to form binding pocket for individual bases; helix α2 provides specificity-determining residues	Binding pockets for bases provided by stacking interactions; specificity dictated by hydrogen bonds to the Watson–Crick face of a base by two amino acids in helix α2	Pumilio[84] (1M8Y)
SAM	α	Hydrophobic cavity between three helices surrounded by an electropositive region	Shape-dependent recognition of RNA stem–loop, mainly through interactions with the sugar-phosphate backbone and a single base in the loop	Vts1[123] (2ESE)

Table 1 **List of the most common RNA binding domains**. dsRBD, double-stranded RNA-binding domain; KH, K-homology; OB-like, oligonucleotide/oligosaccharide binding-like; PDB ID, Protein Data Bank identification; RRM, RNA-recognition motif; siRNA, small interfering RNA; ssRNA, single-stranded RNA; ZnF, zinc finger (Lunde, Moore et al. 2007)

RBPs must be controlled at transcriptional level, in order to guarantee an accurate control of gene expression. This idea sounds like the Latin quote:"*Quis custodiet ipsos custodes?*"[1] but, understanding the mechanisms regulating the expression of the RBPs as well as when and how these proteins are translated, is essential to figure out how these proteins control the RNA metabolism. In an article published in 2007, Janga and colleagues studied of mRNA stability, abundance and turn-over in the RNA-binding proteins of *Sacchoromyces cerevisiae* discovering that RBPs are indeed the most abundant proteins in the cell (Mittal, Roy et al. 2009). This abundance comes by a faster transcription and translation compared to other proteins non-RBPs. Moreover, the RBPs undergo a significant stabilization when compared to the half-life of other proteins. In contrast, the half-life of the corresponding mRNA is very short and the high level of transcripts is guaranteed from high transcription of the RBPs genes. This means that RBPs are not only the most common proteins into the cells, but also the

[1] Who guards the guards?

proteins with the high level of controls that occur at post-translational level: the guards control the guards (Mittal, Roy et al. 2009).

Although the post-translational control of RBPs is very important to maintain the cellular homeostasis, it cannot guarantee the functionality of proteins. The complexity of the interaction between RNAs and RBPs, the high number of RNAs which could be recognized by single RBPs, combined with the mutual interaction of these proteins in order to ensure the correct formation of specific RNPs, suggest the presence of an additional level of control besides the gene expression control. To guarantee these strict monitoring, the RNA-binding proteins could be controlled through post-translational modifications (PTMs) such as phosphorylation, methylation and SUMOylation. Many are the examples of the fine adjustment made through PTMs in several aspects of post-translational control. For example, cells can use SUMOylation of the heterogeneous nuclear ribonucleoprotein C and M (hnRNP C and M) to control the nucleo-cytoplasmic transport of mRNA (Vassileva and Matunis 2004). These results suggest that any change in RPBs availability may affect a vast number of transcripts with a consequently change in cellular physiology (Mittal, Roy et al. 2009).

Last but not least, due to their central role in gene expression, many genetic mutations affecting the RBPs can dramatically impair the organism survival. Many diseases have been recently correlated with mutations in RBPs. Some of these are summarize in Table 2 (Keene 2007).

Disease or syndrome	RNA-binding protein
Neurodegenerative diseases; POMA paraneoplastic neuropathies	hnRNP-P2; ELAV/HuB,C,D; NOVA1,2
Fragile X mental retardation	FMRP
Turner syndrome	Ribosomal proteins (RP)
Mitochondrial and metabolic disorders	mitRP; IRP1,2; PCBP1,2
Oculopharyngeal muscular dystrophy	PolyA-binding protein 2
Spinal muscular atrophy	SMN1,2
Myotonic dystrophy	CUG-BP/EDEN; CELF3,4,5,
α- and β-thalassaemia; cardiovascular disease	BRUNO; ELAV/Hu; hnRNP-L1; αCP1,2; ETR3
Cancer and genotoxic responses; congenital dyskeratosis	ELAV/Hu; EIF4E; CUG-BP; IMP1–3; RP; musashi; telomerase
Immunoregulatory disorders	TTP, TIA, TIAR, HuR

Table 2 Disease implications of RNA-binding proteins (Keene 2007)

1.2 THE hnRNP SUPER FAMILY

The complexity of the processes mediated by the RBPs, together with their structural complexity and regulation, prompted researchers to divide the RBPs in big families according to the structure and function of the RBDs (Chen and Varani 2005). One of the first families characterized has been the heterogeneous nuclear ribonucleoprotein (hnRNP). The name identifies those proteins that bind heterogeneous nuclear RNAs (hnRNAs), the historical name given to the transcripts produced by RNA polymerase II (Dreyfuss, Matunis et al. 1993).

The first studies aiming to isolate the hnRNPs were performed at biochemical level using sucrose density gradient (Krecic and Swanson 1999). Although this approach has been successfully used for other porpuses, it failed to isolate the hnRNP complexes. Only in 1984 Choi and Dreyfuss were able to isolate the first hnRNP C containing complex from Hela cell's nuclei through an immunoprecipitation assay (Figure 3). Proteins with a molecular weight ranging from 34 kDa to 43 kDa were isolated, and then identified as the hnRNP A1 and A2, B1 and B2 and hnRNP C1 and C2. In addition, the researchers isolated proteins ranging from 45 kDa to very high molecular mass, and these proteins were called hnRNP D-U (Choi and Dreyfuss 1984). From that moment other hnRNPs have been identified, such as the hnRNP-like RNA-binding factors which include CELF proteins, Fox, Nova and TDP-43. (Hallegger, Llorian et al. 2010; Busch and Hertel 2012)

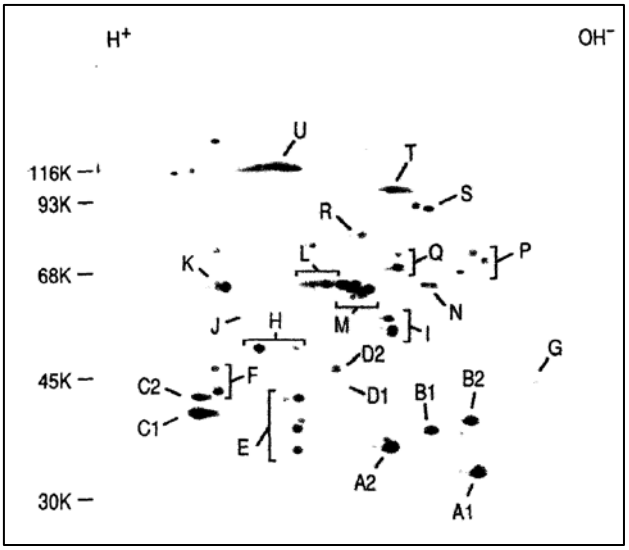

Figure 3 Protein composition of hnRNP complexes immunopurified with a monoclonal antibody, 4F4, to the C proteins. The hnRNP complexes were immunopurified from the nucleoplasm of [35S]methionine-labeled HeLa cells. The proteins were separated by non-equilibrium pH gradient gel electrophoresis (NEPHGE)in the first dimension and by SDS-PAGE in the second dimension, and visualized by fluorography (Dreyfuss, Matunis et al. 1993)

1.2.1 Properties of hnRNPs

The hnRNPs might exert different roles in the cell. They are involved principally in pre-mRNA splicing, mRNA transport, RNA editing and packaging, polyadenylation, silencing, shuttling and telomere biogenesis. Moreover, some hnRNPs like hnRNP C, hnRNP E/K, hnRNP U and AUF1 can bind DNA and are involved in DNA interactions and functions, including chromatin remodeling and packaging, DNA damage repair,

transcription and other functions. A short list of hnRNP and they functions is reported in Table 3 (Han, Tang et al. 2010; Pont, Sadri et al. 2012).

The main feature of the hnRNPs, that permits them to exert a high number of functions, is the presence of one or more RNA-binding domains. The most common domain present within this family is the RNA recognition motif (RRM). The RRM consists of 80-90 amino acids which form four-strands antiparallel β-sheets with two additional α-helices arranged in the order $\beta_1\alpha_1\beta_2\beta_3\alpha_2\beta_4$; these secondary structures form a barrel-like topology structure (Handa, Nureki et al. 1999; Antson 2000). Contacts between RRM domain and RNA are established by the consensus sequence, called RNP-1 and RNP-2, located in the β_3 and β_1 strands; each RNP consists in 4 aromatics amino acids, which associate with 2 bases of RNA allowing the

hnRNP	DNA interactions	RNA interactions	Protein interactions
A/B/D	Telomere maintenance Transcription DNA replication	Splicing Viral unspliced mRNA transport miRNA processing mRNA stability Translational regulation mRNA editing mRNA trafficking mRNA packaging	
C1–2	Chromatin remodelling Transcription	Splicing mRNA retention mRNA packaging Translational regulation Telomere biogenesis	
E/K	Transcription Chromatin remodelling Telomere biogenesis	Splicing Translational regulation mRNA stability	Signal transduction and integration
F/H		mRNA stability Splicing	Splicing
G	DNA repair Tumour suppressor Transcription factor	Splicing	
I/L	Transcription	Splicing mRNA export Translation regulation mRNA stability Polyadenylation	
M		Splicing Heat-shock response	Antigen receptor (only for the M4 isoform) Thyroglobulin receptor (only for the M4 isoform)
P	Transcription Genome stability	Splicing	Cell spreading and stress response Transcription
Q/R		Splicing RNA replication mRNA stability mRNA trafficking	
U	Chromatin organization DNA binding	RNA binding	Transcription

Table 3 **Short list of hnRNP** and their functions when interact with DNA, RNA or other proteins. For clarity, functions have been categorized based on the predominant nature of the hnRNP interaction, but it should be noted that these categories are not mutually exclusive (Han, Tang et al. 2010)

interaction between RNA and β-sheet surface (Birney, Kumar et al. 1993). Thus, the RRM can bind single-stranded nucleic acids with variable length, including ssDNA, in a non-sequence specific manner, with the consequence that several hnRNPs are associated with DNA metabolism (Birney, Kumar et al. 1993; Dreyfuss, Matunis et al. 1993; Maris, Dominguez et al. 2005; Han, Tang et al. 2010).

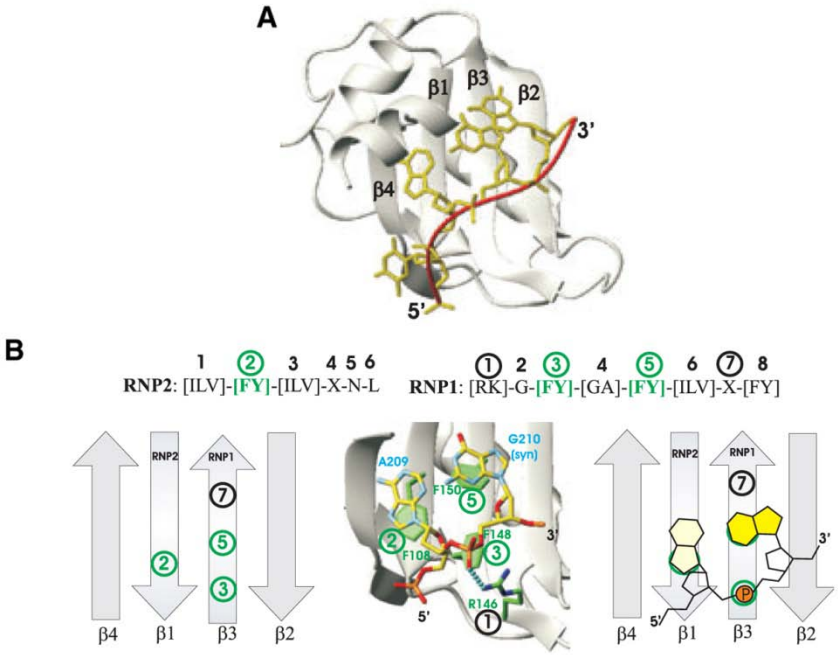

Figure 4 Structural representation arrangement of the RNA strand on the β-sheet of hnRNPA1–RRM (A). In (B) schematic representation of hnRNPA1 RRM 2 with the conserved RNP 1 and RNP 2 aromatic residue positions numbered according to each RNP sequence numbering. The conserved aromatic residues are highlighted by green circles (Maris, Dominguez et al. 2005)

The RRM motif is not the only domain present in the hnRNPs responsible for their interaction with nucleic acids, for example hnRNP E/K bind RNA via hnRNP KH (K homology) domain. The KH domain forms a $\beta_1\alpha_1\alpha_2\beta_2\beta'\alpha'$ structure that binds RNA or ssDNA between the β-sheet and the α–helices (Musco, Stier et al. 1996). Many others are the proteins which present a non classical RMM, for example, the proteins hnRNP F and H do not have the normal RRM, but they are composed of a qRRMs domain (quasi-RRMs), containing an extra β_3' loop (Dominguez, Fisette et al. 2010). The protein hnRNP I (also known as PTB) contains 4 non-canonical RRMs because these domains include unusual amino acids; in particular, in the RNPs of these RRM are absent the aromatic residues used by other RMM domains for non-specific contact with the RNA. Moreover the conserved glycine, present in the RNP-1 of classic RRMs, is substituted by amino acids with larger side chains in all RMM domains of PTB (Conte, Grune et al. 2000). Furthermore, hnRNP U binds RNA via a domain containing a glycine-rich region (Kiledjian and Dreyfuss 1992; Dreyfuss, Matunis et al. 1993; Han, Tang et al. 2010).

In addition to RRM, the hnRNPs have other auxiliary domains. One of the most common is the so called RGG box (arginine/glycine/glycine box), a sequence formed by several repeats of three amino acids. This domain is often involved in protein-protein interactions and might interact with RNA in a sequence-independent manner (Godin and Varani 2007). Differently from other RNA-binding domains and from other domains involved in protein-protein interaction, the connection between RGG boxes and other structures, formed by amino acids or nucleic acids, can be modulated by arginine methyl transferase enzymes (PRMTs), which can methylate the arginine guaridinum group (Dreyfuss, Matunis et al. 1993; Godin and Varani 2007; Han, Tang et al. 2010).

Others auxiliary domains are present in hnRNPs, and for many of these domains their function remains elusive. For example, a glycine-rich domain, which differs from

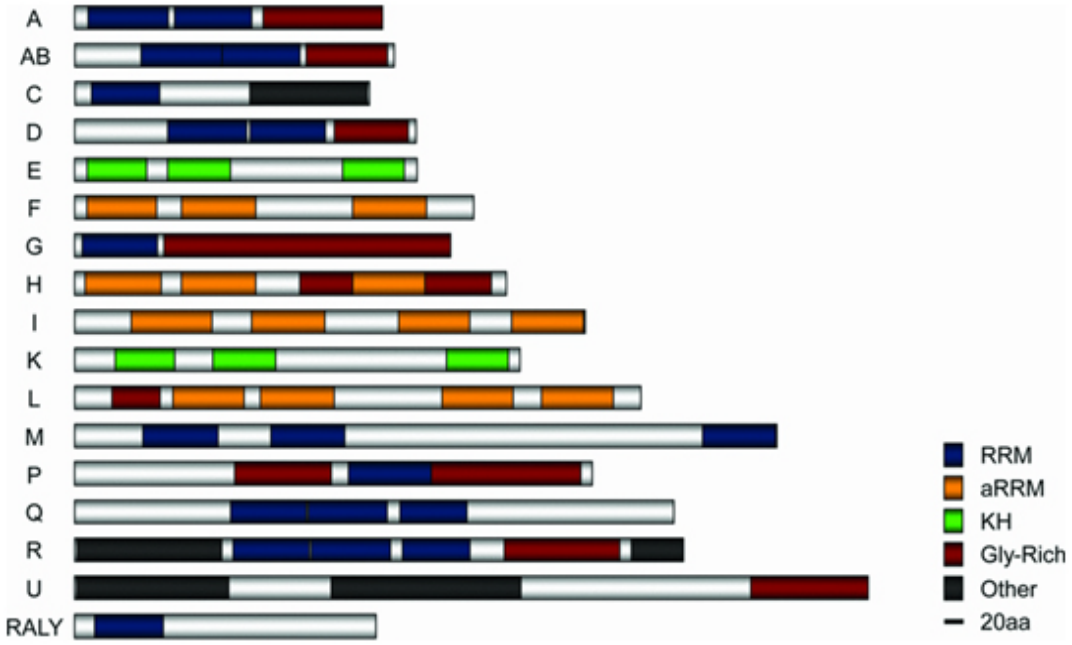

Figure 5 Schematic representation of RNA-binding domain in hnRNP structures. 'A' represents the hnRNP A proteins (A0, A1, A2/B1 and A3) that are structurally similar. Gly-Rich=RGG. (Han, Tang et al. 2010)

the canonicals RGG boxes, is present in hnRNP A1 proteins at their C-terminal region. This "pseudo-RGG" domain seems to mediate dimerization of hnRNP A1-A1. The hnRNP C contains a domain rich in acidic amino acids and a putative nucleotide triphosphates (NTP)-binding site whose function is not know yet (Dreyfuss, Matunis et al. 1993). In addition to these domains, a large number of hnRNPs bear one or more nuclear localization signals (NLS) as well as nuclear export signals (NES). Both domains allow the shuttling from nucleus to cytoplasm that is typical of many hnRNPs (Dingwall, Robbins et al. 1988; la Cour, Kiemer et al. 2004).

1.3 RALY: A NEW MEMBER OF hnRNPs

RALY, the RNA-binding protein Associated with Lethal Yellow mutation, also known as HNRPCL2 and P542, is considered a member of the hnRNP family because it shows a high similarity in amino acids sequence with hnRNP C. Moreover, RALY is very similar to other two hnRNPs: hnRNP CL1 and RALYL (RALY-Like) (Jiang, Guo et al. 1998; Busch and Hertel 2012). RALY is a protein of 306 amino acids (37 kDa) that is ubiquitously expressed. Two spliced isoforms of RALY (originally called RALY and P542) which differ for 16 amino acids immediately downstream the RBD, can be expressed in a tissue specific manner (Khrebtukova, Kuklin et al. 1999).

RALY is characterized by the presence of one RRM, very similar to hnRNP C RRM domain, at the N-terminal region, and one non-canonical RGG at the C-terminal. Several studies identified this particular RGG box as an auto antigenic epitope cross-reacting with the Epstein-Barr nuclear antigen 1 (EBNA1), a viral protein associated with Epstein-Barr virus (Vaughan, Valbracht et al. 1995); interesting, only the short isoform (P542) seems to have a role in this auto antigen response, but at the moment the real role of this particular domain remains elusive (Khrebtukova, Kuklin et al. 1999).

In mouse, the RALY gene is localized near the a*gouti* gene. The *agouti* gene (A) encodes for Agouti Signalling Peptide (APS), an endogenous antagonist of melatonin-1 receptor (MC1R). It is responsible for the coat in several animals. This gene is affected by several genetic mutations, including a deletion in the 5' region of *agouti* gene (A^y). The presence in homozygote of the a allele is responsible for the the dark black/brown pigment production, while the genotype a/A^y is responsible for yellow/red pigment in several animals such as cat, horse, sheep and mouse; the presence in homozygosis of mutant *agouti* A^y/A^y is responsible for the 'Yellow Lethal Mutation' pathology in mouse and Japanese quail: embryos with the double mutant alleles cannot finish the animal's development (Nadeau, Minvielle et al. 2008; Dreger, Parker et al. 2013).

The Lethal yellow mutation is a deletion of 170 kb in mouse and 90 kb in quail localized upstream the *agouti* allele. The deletion encompasses the coding region of RALY and of EIF2B (eukaryotic initiation factor 2B), with the consequence that *agouti*'s gene passes under control of *Raly* promoter's. The transcript derived from this mutation presents the 5'-UTR of *Raly*, the second, third and fourth exon of ASIP; this new protein is expressed ubiquitously, whereas RALY is no longer present in these animals (Nadeau, Minvielle et al. 2008). In 1993, Woychik and colleagues hypothesized the importance of RALY in the Lethal Yellow phenotype. Since the RBD of RALY shares 77% sequence identity with the RBD present in hnRNP C RBD, the researcher suggested that RALY, as hnRNP C, could bind and process specific mRNAs that are

important for the development of pre-implantation embryo. The authors concluded that in embryos with A^y allele in homozygosis these processes could not be performed causing the death of the embryo (Michaud, Bultman et al. 1993). In 2008, Mundy and colleagues proposed a different theory: they observed that in quail and mouse the deletion upstream *agouti* gene involves three genes, not only *Raly* and *agouti*, but also *EIF2B*, a gene that encodes for the subunit 2β of the eukaryotic translation initiation factor 2. Since this protein plays an important role in protein synthesis, they concluded that the lethality of the homozygous yellow condition might depend on the loss of function of this gene rather of RALY (Nadeau, Minvielle et al. 2008). Apart from these genetic studies concerning RALY, not much is known regarding the role that this RBP has within the cell.

In a recent article, RALY has been identified as a component of the spliceosome complex suggesting its possible involvement in RNA splicing (Jurica, Licklider et al. 2002). The data were confirmed in a second, independent article, reporting all proteins involved in Exon Junction Complex (EJC) (Singh, Kucukural et al. 2012). Both studies are very interesting, even if still preliminary and lacking any mechanistic analysis. Besides, no functional analysis proving any possible role of RALY in mRNA splicing has been shown.

In another article Lebel and colleagues demonstrate that RALY is up-regulated in adenocarcinoma cell lines (Tsofack, Garand et al. 2011). In human colon adenocarcinoma cell lines RALY, together with NONO/p54nrb, have been identified such as interactors of YB-1, a RNA-binding protein that is involved in splicing, transcription and translational regulation of specific mRNAs (Chen, Gherzi et al. 2000; Raffetseder, Frye et al. 2003). NONO is a DNA- and RNA-binding protein involved in several nuclear processes, including pre-mRNA splicing and double-strand break repair (Sewer, Nguyen et al. 2002; Bladen, Udayakumar et al. 2005). Indeed, YB-1 mediates pre-mRNA alternative splicing regulation, regulates the transcription of numerous genes and, like NONO, can play a role in the repairing nicks or breaks into double-stranded DNA (Raffetseder, Frye et al. 2003; Gaudreault, Guay et al. 2004). Moreover, YB-1 over-expression in different tumors has been related with the acquired resistance to specific tumor drugs (Ohga, Uchiumi et al. 1998; Schittek, Psenner et al. 2007). These considerations were supported by the observations that cells with both RALY and NONO up-regulated became more resistant to the effects of the drug oxaliplatin. In contrast, the depletion of RALY expression by RNAi sensitized colorectal cancer cell lines treated with the oxaliplatin without affecting the cell growth rate (Tsofack, Garand et al. 2011). The same results were obtained after down-regulation of

NONO and YB-1, demonstrating that the three proteins are functionally correlated. Interestingly, RALY transcript is over expressed in different cancer tissues and, this over-expression is associated with poor survival in ovarian, lung, bladder, brain and breast cancers as well as in multiple myelomas and melanomas (Tsofack, Garand et al. 2011). These data indicate a potential role of RALY in tumorigenesis that still requires further investigations and mechanistic analysis, but can be used as a starting point for our characterization.

RALY and other RNA-binding proteins, including members of the hnRNPs such as hnRNP H/F have been recently found also in the immunoprecipitate of RBFOX1/2. RBFOX1/2 is a RNA-binding protein that regulates alternative splicing events by binding to 5'-UGCAUGU-3' elements (Ponthier, Schluepen et al. 2006). This protein regulates alternative splicing of tissue-specific exons and of differentially spliced exons during erythropoiesis (Norris, Fan et al. 2002). Nevertheless, in contrast to hnRNP H that modulates the splicing activity of RBFOX1/2, RALY has no effects in this process because its misregulation does not impair alternative splicing of RBFOX1/2 mRNA targets (Sun, Zhang et al. 2012)

In conclusion, although there is evidence that RALY might play multiple roles in RNA metabolism, it’s remained poorly characterized in mammals and also its potential interactors remain still elusive.

2 - TOPIC OF MY PHD PROJECT

In an article under revision, Kiebler and colleagues characterized the interactome of 2 proteins involved in mRNA localization and translational control in neurons: Staufen2 (Stau2) and Barentsz (Btz or CASC3) (Härtel et al., under revision). Both proteins are molecular components of neuronal RNPs and are associated with mRNAs during transport into dendrites (Macchi, Kroening et al. 2003; Goetze, Tuebing et al. 2006). Interestingly, only one third of proteins interacting with STAU2 and CASC3 are common and this observation shows how heterogeneous and dynamics are the RNPs granules. In the above work, the researchers identified also RALY as a new interactor of Btz. Barentsz is a protein involved also in splicing and mRNA quality control: it is a core component of the exon junction complex (EJC), and remains bound to spliced mRNAs throughout all stages of mRNA metabolism thereby influencing downstream processes of gene expression. CASC3 is also a component of nonsense-mediated mRNA decay (NMD), plays a role in the stress granules formation and it is a component of the dendritic ribonucleoprotein particles in neurons (Macchi, Kroening et al. 2003; Palacios, Gatfield et al. 2004; Baguet, Degot et al. 2007; Chang, Imam et al. 2007). The interaction of RALY with components of transport RNPs, combined with little knowledge regarding RALY, led me to investigate the role of this protein within the cell and its possible implication in regulating the RNA metabolism.

I started with the characterization of the sub-cellular localization and expression patterns in different cell lines. Much of my work has been the characterization of the entire RALY interactome and the identification of new protein interactors (Paper 1, Appendix 7.1). At the same time, I continued RALY characterization, focusing my attention in the interaction between RALY and RNA. Using polyribosome profiling, I observed interactions between RALY and ribosomes. Interestingly, I found RALY enriched in those fractions containing polyribosomes and translating mRNAs.

Using a microarray analysis, I also investigated whether the loss of RALY by RNAi could affect the levels of specific mRNAs. These new results, in combination with the results on RALY's interactome, have allowed me to better understand the biological role of RALY. Last but not least, based on my microarray and proteomic data, I am currently studying the role of RALY in other cellular processes, such as the DNA damage repair and the cell proliferation.

Taken together, during my PhD I obtained interesting result regarding RALY and its role not only in post-transcriptional regulation, but also in DNA damage repair.

3 - RESULTS

3.1 PUBLICATION 1:

Proteome-Wide Characterization of the RNA-Binding Protein RALY-Interactome Using the in Vivo-Biotinylation-Pulldown-Quant (iBioPQ) Approach. (Tenzer, Moro et al. 2013)

All the results obtained whit the iBioPQ analysis are reported in the article entitled "Proteome-wide characterization of the RNA-binding protein RALY-interactome using the iBioPQ (in vivo-Biotinylation-Pulldown-Quant) approach" (Tenzer, Moro et al. 2013), where I share the first authorship with Dr. Stefan Tenzer (University of Mainz). We established a new approach using recombinant protein fused with the biotin acceptor peptide (BAP). This assay allowed me to obtain important results because I obtained and validate the RALY interactome. Using the list of interacting proteins derived from the mass spectrometry assay, I analyzed the gene ontology of these proteins and I obtained several attractive results that allowed me to speculate on the pathway where RALY is involved. Moreover, I could confirm the interaction between RALY and RNA, and the contribution of RNA in mediating some of the observed interactions.

I identified 143 proteins that interact with RALY, the majority of these involved in RNA metabolism, including splicing process. At the same time I treated the cell extract with RNase and then I performed the pull-down assay. Surprisingly, only for 18 proteins the interaction with RALY decreased in the absence of RNA. In contrast, the interactions between RALY and other 80 proteins, including several ribosomal proteins and proteins binding DNA, increased after RNase treatment. This is just a glimpse of the results that I obtained using this technique. All details (results and the discussion) can be found in the Publication 1 in Appendix 7.1.

My contribution in this paper consist in the creation of fusion protein RALY-BAP as well as the set up of the *in vivo* Biotinylation assay. All purification steps, including cloning and expression were done by myself. Moreover, I performed all experiments to validate the results obtained by the mass spectrometry. I performed all Western blots (Fig.5) as well as the immunofluorescence analysis (Fig.6). I did the treatments with RNase and DNase (Fig.6). I analyzed the list of RALY's interactors using the bioinformatics software DAVID (Fig.4) and then I started to clusterize the proteins in a network (Fig.3 A).

3.2 ADDITIONAL RESULTS

3.2.1 RALY localization

I started the characterization of RALY by assessing its intracellular localization in a more details. First, I determined the specificity of a commercially available antibody, in recognizing endogenous RALY. For this purpose I used the competition assay and the results are shown in Figure 6. In this experiment the antibody anti-RALY (Bethyl) was incubated in a solution containing the purified fusion protein GST-RALY (details are reported in Appendix 7.4). After 2 hours of incubation of the antibody with GST-RALY, the supernatant was used to decorate the Western blot. Figure 6 shows the detection of RALY using antibody not treated (control) compared to the detection performed using the solution after incubation with RALY-GST (competition). This result confirms the specificity of the antibody that I used during all my experiments.

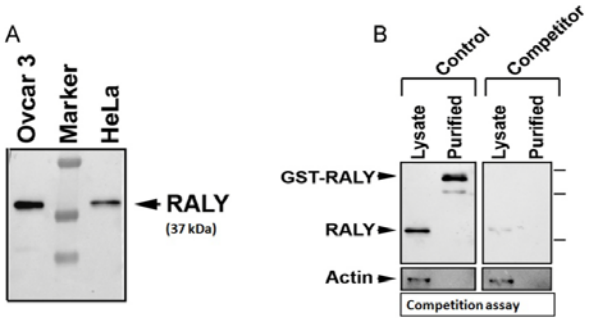

Figure 6: **Competition assay**. Panel A shows the western blot with commercial antibody anti-RALY in Ovcar3 and HeLa cell lines. Panel B shows the results of competition assay. It is possible to appreciate how in the blot detected with solution after competition no bands are present, while in the control the antibody recognized endogenous RALY and the fusion-protein GST-RALY.

I then performed an immunostaining analysis on HeLa cells. As expected, I observed a prominent nuclear accumulation of RALY in all cell types excluding the

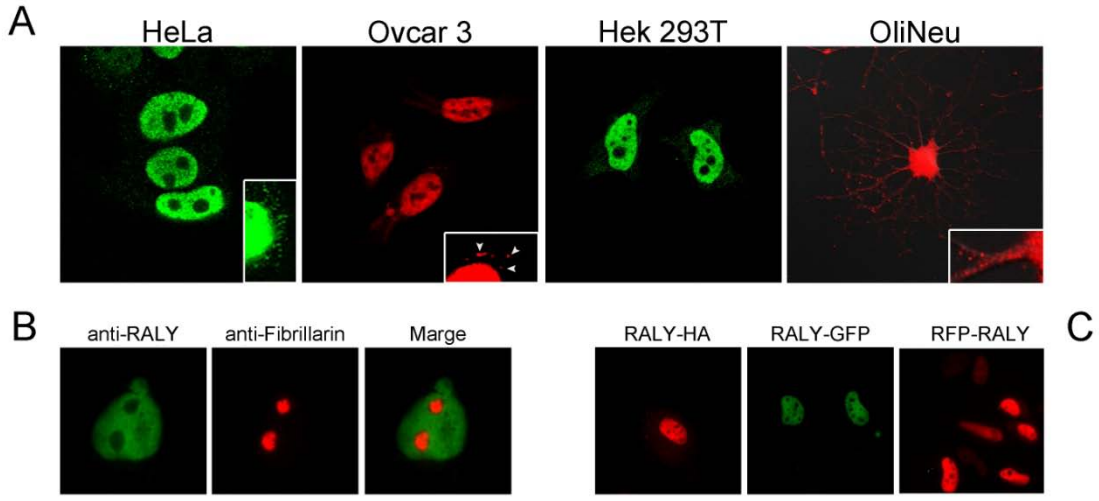

Figure 7: **RALY localization**. Panel A shows the nuclear localization of RALY in HeLa, Ovcar3, Hek293T and OliNeu cell lines. In the magnification is possible to appreciate the RALY's localization in the cytoplasm (white arrows indicate big RNPs). In panel B is observable the exclusion of RALY from the nucleoli, while in panel C is reported the pattern of 3 fusion proteins: RALY-HA, RALY-GFP and RFP-RALY. In all the conditions RALY has a nuclear localization.

nucleoli, as established after the co-staining with the nucleolar marker fibrillarin (Figure 7 B). Interestingly, several discrete particles, typical staining for RNPs, were also detected in the cytoplasm (Magnification in Figure 7 A). An identical nuclear and cytoplasmic localization was observed in the other cell types that I tested, including 293T cell lines, OVCAR3 and polarized cells such as oligodendrocytes, demonstrating that the pattern observed was not cell-specific (Figure 7 A). Especially in OliNeu cells, which are cells derived from the oligodendrocyte precursors, with morphology similar to normal oligodendrocyte (Jung, Kramer et al. 1995), the cytoplasmatic localization of RALY is more evident. RALY, as other RBP, localized in the conjunction between branches, but is detectable in little spots at the branching points of the processes of the cells (Figure 7 A). Furthermore, a similar localization pattern was observed in cells expressing RALY tagged with different marker, such as EGFP, RFP, HA (Figure 7 C) and others tag including BAP (Figure 1 in Publication 1).

To explain the nuclear localization of RALY, I performed a bioinformatics analysis in order to identify the specific domains responsible for the protein's pattern (Figure 21 in Discussion). As reported in the introduction, RALY possesses a RRM domain very similar to hnRNP C (77% of similarity) at the N-terminal, while in the C-terminal region is present a RGG box more different from the RGG boxes of other hnRNPs. In particular the RGG of RALY does not show arginine in the sequence, but it is composed by a stretch of 27 glycine interspersed from 4 serines and 1 alanine; the lack of arginine in the sequence suggests that this domain is not useful for the RNA binding. Moreover, the analysis reveals the presence of three putative Nuclear Localization Signals (NLSs) in the regions encompassing the amino acids 145-150, 153-159 and 219-225, while Nuclear Export Signal (NES) were not predicted. After having identified these domains, I characterized the putative NLSs using several mutants of RALY tagged with GFP.

The Figure 8 panel A shows the steps that allowed me to characterize the essential amino acids for the nuclear localization of RALY. I started observing the localization of the N-terminal region (containing the RRM domain), the C-terminal region (containing the predicted NLS), and the RALY-ΔG (the protein without the RGG box). As expected, only the N-terminal region also localized in the cytoplasm, while the other two deletions showed normal localization. These results demonstrate that the RRM is not responsible for the nuclear localization, and that the NLSs are located in the C-terminal region. Thus, I deleted the amino acids between the residue 145-159 (the first two putative NLSs) and the amino acids 219-225 (the third NLS). Moreover, the amino acids proline, lysine and arginine (the principal responsible for the nuclear localization), were

changed into a neutral amino acid alanine. Figure 8 panel B shows the resulting localization of RALY mutants. I indicated with the name “Mut1” the protein in which the amino acids proline and arginine within the first putative NLS (PVKPRV) were both mutated into alanine; in Mut2 two arginine amino acids within the second putative NLS (PLVRRVK) were both mutated into alanine; finally in Mut3 two lysine amino acids in the third NLS (PDGKKKG) have been changed into alanine. The data show that only the sequence between the aa 145 and aa150 (indicated as first NLS) are essential for nuclear import. This mutant shows a clear cytoplasmatic staining. Nuclear staining is still visible due to the passive diffusion of the protein into the nuclear compartment. Taken together, 3 potential NLSs were predicted by bioinformatics analysis. However, only one seems to be necessary and sufficient to import RALY into the nucleus. This

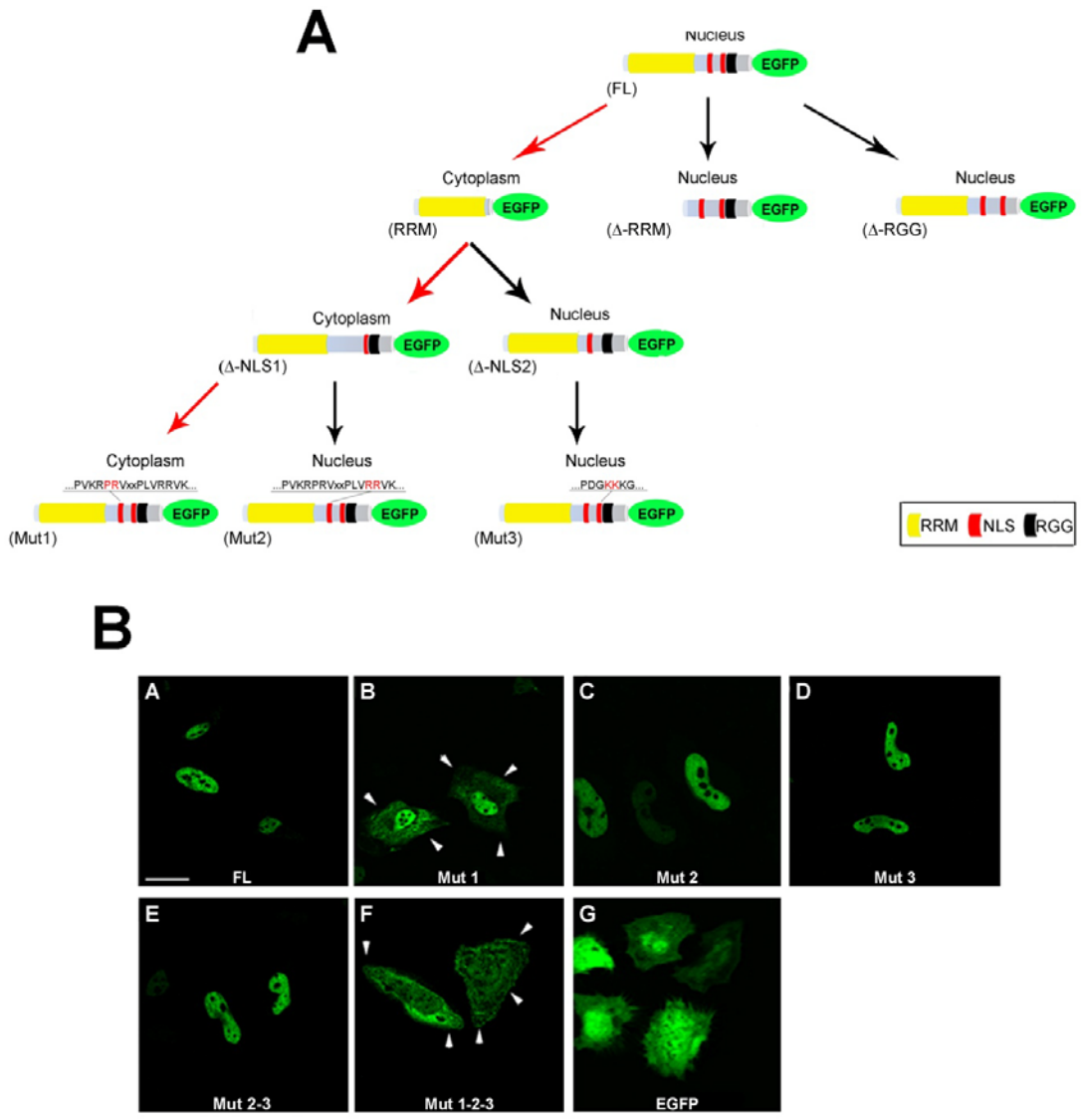

Figure 8: **NLS characterization**. Panel A reports the logical steps for the characterization of predicted NLSs. The point mutations ware performed as followed: first NLS (Mut1) = PVKRPRV → PVKRAAR; second NLS (Mut2) = PLVRRVK → PLVAAVK; third NLS (Mut3) = PDGKKKG → PDGAAKG. Panel B reports the photos, obtained at the confocal microscopy, for the RALY's mutants; the white arrows show the cytoplasmic accumulation of RALY with the first NLS mutated.

discovery opens an interesting question: could mutations in this sequence modify the behavior of the proteins to external and internal stimuli?

To answer to this question I observed the behavior of mutant RALY under oxidative stress induced by treatment with 0,5 mM Na-Arsenite. The cells reply to the oxidative stress accumulating few mRNAs in peculiar RNPs called stress granules (SGs). The SGs are composed by several RNA-binding proteins like Barentz and Pumilio 2 (Kedersha, Stoecklin et al. 2005; Vessey, Vaccani et al. 2006), but there is no evidence

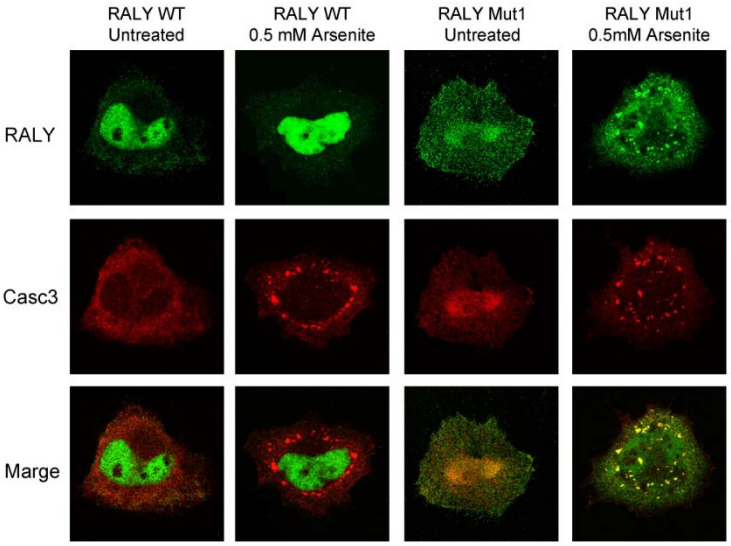

Figure 9: **oxidative stress**. It is showed the behaviour of RALY wild type and RALY with the first NLS mutated (RALY Mut1), either with GFP-tag, in normal conditions and after Arsenite treatment. In red is detected the protein CASC3 like marker of stress granules.

regarding the presence of RALY in these RNPs. Unexpectedly, the result reveals an accumulation of this mutant into stress granules, while the wild type protein does not show a similar accumulation under the same conditions (Figure 9). This result confirms the importance of the NLS for the nuclear localization of RALY, and at the same time the essentiality of this localization for the correct functioning of the protein.

Based on Kiebler's lab observation, I tested a possible involvement of RALY first in NMD and then in mRNA splicing. To investigate whether RALY is involved in NMD, I established a scientific collaboration with Dr. Niels Gehring at University of Cologne (Germany). Using an *in vitro* assay called tethered assay, we determined whether RALY could affect NMD. In this experiment, RALY and CASC3, known member of the NMD machinery, were tetherd to a reporter RNA that undergoes NMD due to the presence of a premature stop codon (Coller and Wickens 2002): when the complex is made, if the NMD is impaired, the reporter would not be degraded. As shown in Figure 10, the fusion protein RALY-tethered did not have any effect in the NMD. Although RALY interacts with CASC3, which is involved in NMD, my data suggest that RALY is not required for this process. I tried also to understand the possible role of RALY in the

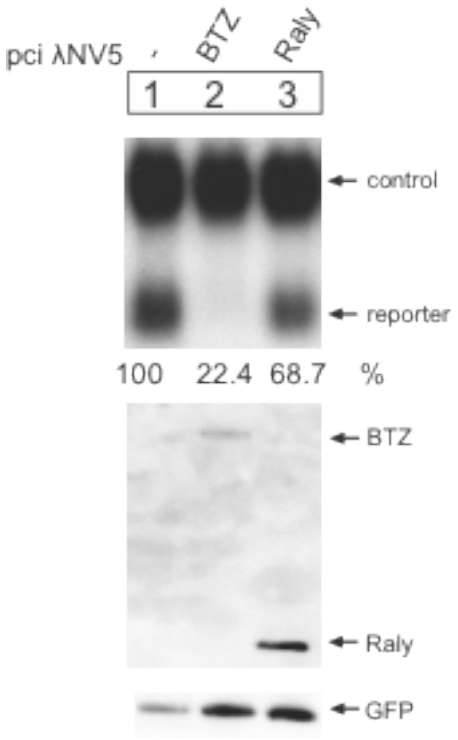

splicing using the pE1A minigene assay (Ricciardi, Kilstrup-Nielsen et al. 2009). My results did not show changes in splicing after miss expression of RALY.

Figure 10: **Tethered assay**. In the picture is reported the effect of tethered-RALY. It is possible to appreciate that the reporter's band is present after incubation with tethered-RALY, while it is disappeared after incubation with tethered-CASC3, used as control for the NMD process.

3.2.2 Polyribosome profiling

As shown in Figure 7 A I observed RALY granules in the cytoplasm. To understand the role of RALY in this behavior, I performed polyribosome profiles, on a sucrose gradient (Provenzani, Fronza et al. 2006). As shown in Figure 11, RALY is present in the low density fractions, indicated from the 4, 5 and 6, which represent the fractions co-sedimented with the subunits 40S, 60S and 80S of the ribosomes. Moreover, RALY was detected in fractions at higher molecular weight, from 9 to 11, fractions that are enriched in polyribosomes. Figure 11 shows how the pattern of RALY in the profiling is very similar to the pattern of ribosome proteins (e.g. RPL26), and it is different from the pattern exhibits by others RBPs, as Casc3, PABP and hnRNP A1. The first two proteins (Casc3 and PABP) are involved in several RNA processes, such as splicing, NMD and transport; besides, the polyribosome profiling for both the proteins show their presence in all the fractions from the 3, where the mRNA is in the cytoplasm but not associated with the polysomes, until the 13, the last fraction where the polysomes are still detected. In contrast, the protein hnRNP A1 is detected only in those fractions where mRNAs are not associated with ribosomes.

To assess the nature of RALY-ribosomes interaction, I repeated the gradient in the presence of puromycin, RNase and ETDA. The first two substances have effect prevalently in the polysome's formation. The puromycin decreases the capacity of the cell to assemble the polysomes; in the profile it is possible to observe an increase of fractions containing the 80S subunits, while the peaks with polysomes with high weight

disappear. RNase treatment has a similar effect causing an increase of the 80S as well as the disappearance of the polysomes. In contrast, EDTA, a chelating of bivalent ions, affects the ribosome's assembling by destabilizing and breaking the 80S subunits. Taken together, these results seem to confirm that RALY is strictly associated with ribosomes and translating mRNAs in an RNA-dependent manner. Is then RALY involved in ribosomal assembly and/or in rRNA metabolism?

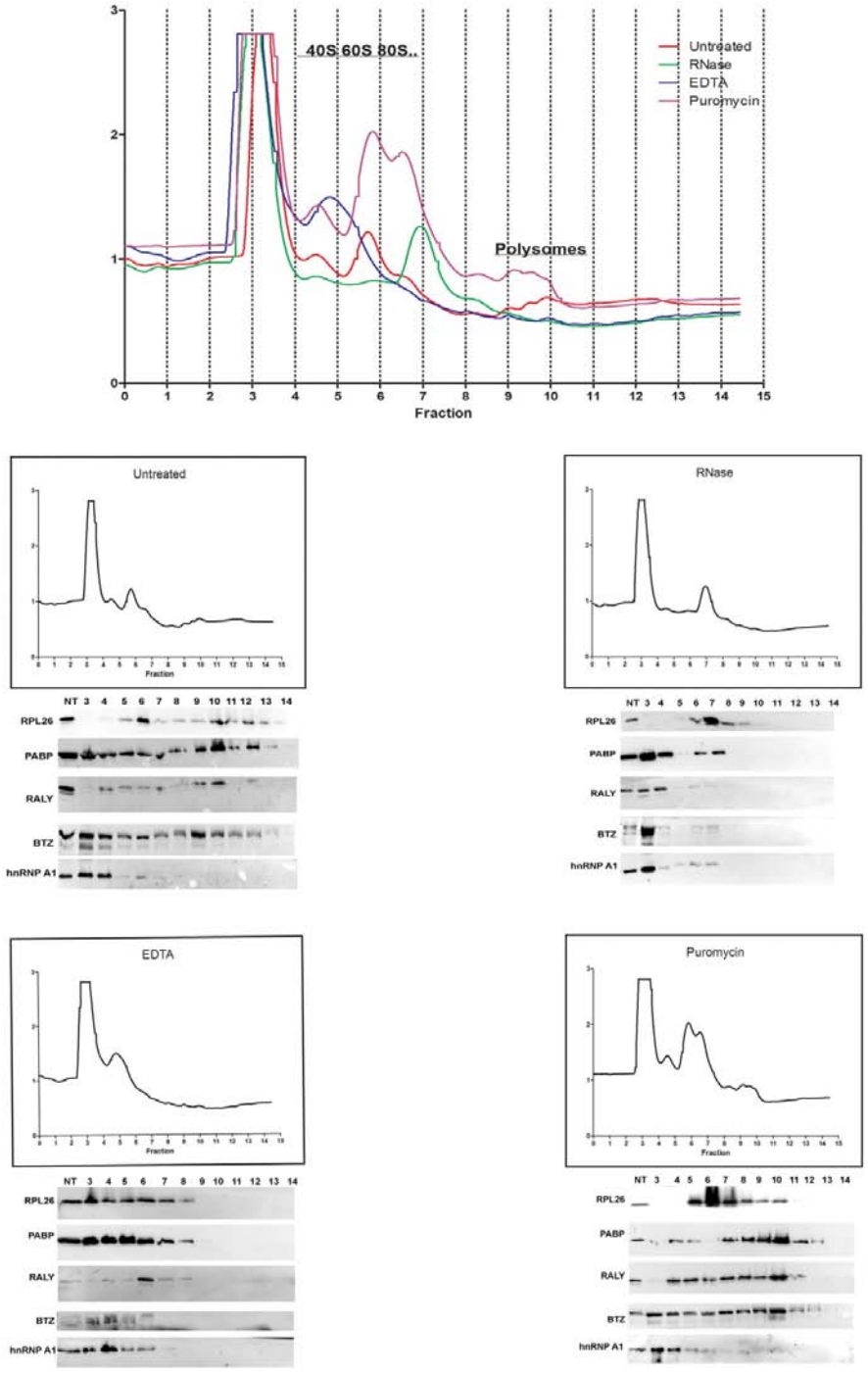

Figure 11: **The polyribosomes profiles.** The first graph shows the merge of the profiles in normal condition and after treatment. In red is represented the profile of untreated cells, while in green, blue and magenta the profile of cells treated with RNase, EDTA and puromycin respectively. Under the graph is showed the single polysome profiles and the western blot performed for every single fraction where RPL26, PABP, RALY, Barentz and hnRNP A1 are detected.

To investigate the potential role of RALY in ribosome assembly, I performed new polyribosomal profile in RALY down-regulated cells (Figure 12). As is possible to observe from the very preliminary results, the absence of RALY protein has not particular effects on polysomal profile, while it seems to produce an effect in the low fraction, with an increasing in absorbance not only in the fractions 40S and 60S, but also in the fraction where the RNA not associated with ribosomes is localized. In any case, these are only preliminary results that do not allow any speculations on the role of RALY in post-translational regulation.

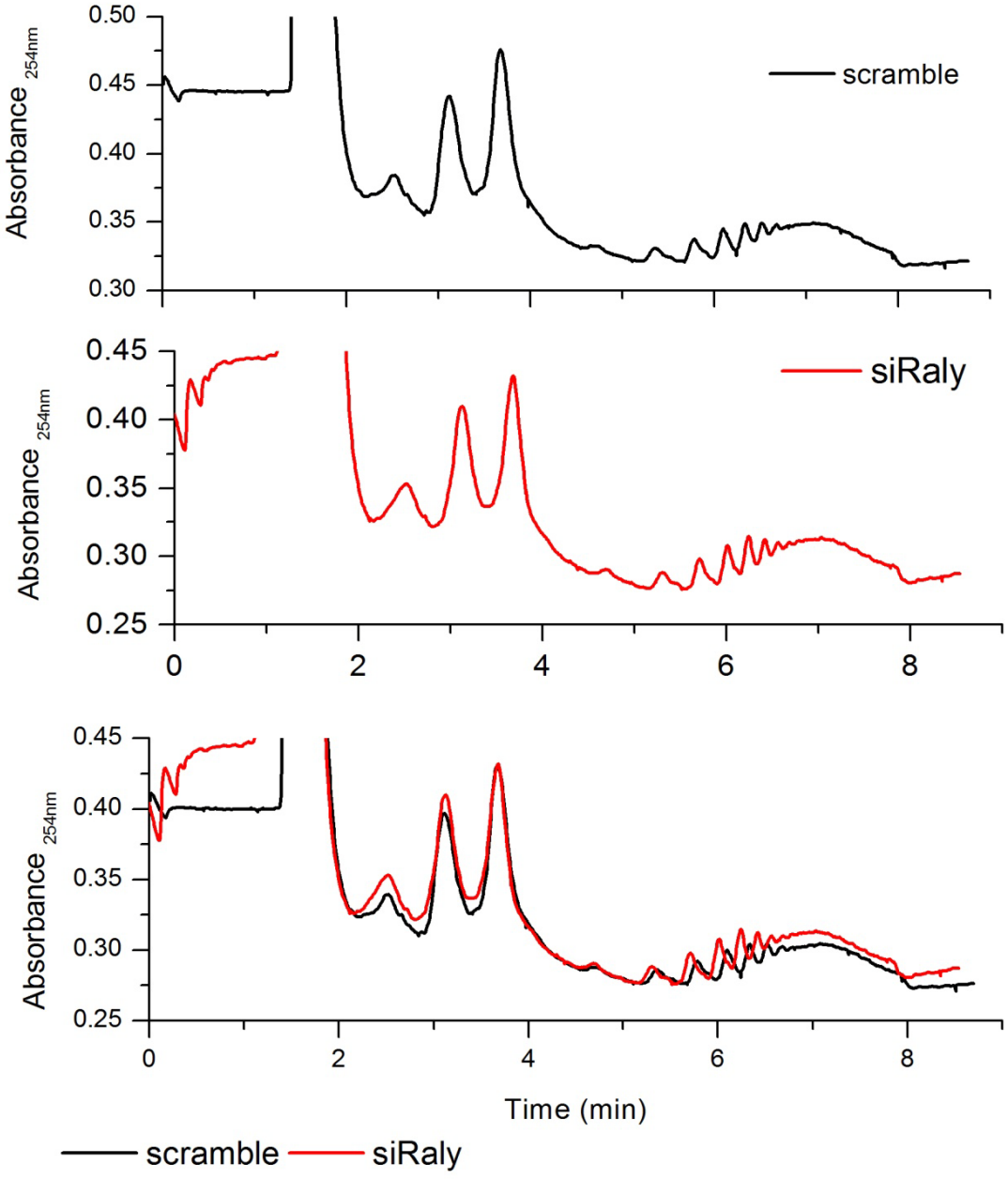

Figure 12: **Polysome after RALY silencing**. In the figure is showed the polyribosome profile for untreated cells (scramble, black curve), and for cells where RALY was silencing (red curve). The last graph shows the merge between the two profiles.

3.2.3 The microarray analysis

I performed microarray analysis to see total gene expression after silencing of RALY. At the beginning, I used the pSUPERIOR plasmids expressing short hairpin RNA (shRNA) to down-regulate RALY (Vessey, Vaccani et al. 2006). Unfortunately, I expressed three different plasmids but none of them yielded to a significant down-regulation of RALY. I then decided to use a commercial kit of siRNA distributed by Dharmacon, composed by a pool of four siRNAs specific for the mRNA of interest. This approach gave me good results, given that the silencing of RALY was approximately 100% (Figure 13). 3 days after transfection of siRNA, total RNA was purchased from HeLa, converted in cDNA and then in cRNA for the microarray assay. Probes were then ibridized on a chip purchase by Agilent of Whole Human Genome Microarray 44K (Agilent) specific for mature mRNA that provides a comprehensive coverage of genes and transcripts with the most up-to-date content (http://www.genomics.agilent.com/).

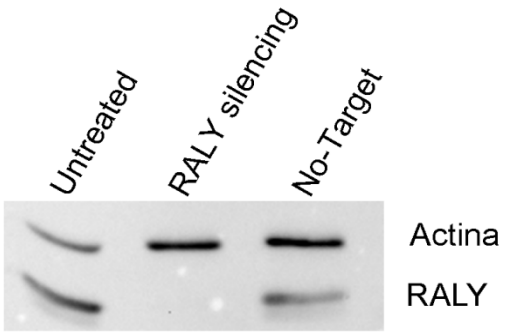

Figure 13 **RALY silencing**. The picture shows the RALY protein detection in untreated cells, cells transfected with siRNA for RALY (RALY silencing) and transfected with siRNA for no-target genes (sramble). The up band is the housekeeping gene Actin.

The results obtained from microarray analysis were processed with the appropriate programs Feature Extraction (Agilent) and Genespring (Agilent), to derive the information regarding gene fold-change. The results are shown in Appendix 7.3 containing the list of genes that increase or decrease their expression after silencing of RALY. From the entire list of more than 19000 probes, I focused my interest on about 1200 probes with a Fold-Change (FC) higher than 1.5; out of these 1226 probes with a significant FC after silencing, 709 are up-regulated, while 517 probes, including RALY, are down-regulated.

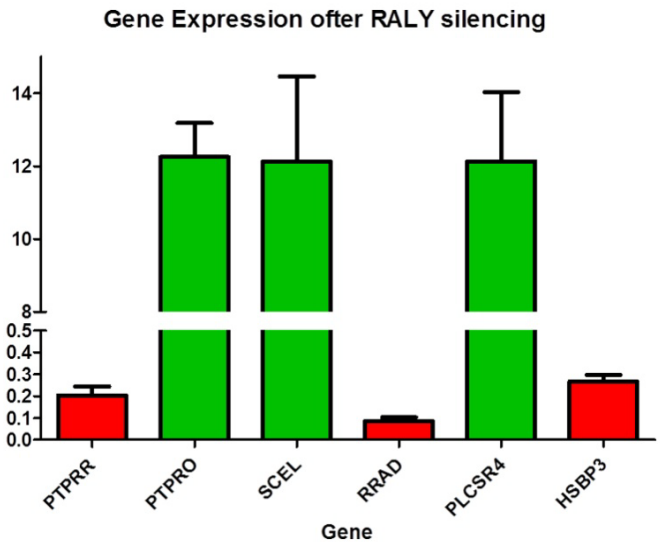

Figure 14: **Validation of microarray results**. The green bars identify the fold change of the up regulated genes from RALY silencing, while the red bars show the trend of down regulated genes after silencing of RALY. In order to expand the scale between 0 and 1 and could appreciate the FC, the Y axis has been splitted in two.

Before proceeding with further analysis, the microarray results were validated using real-time PRC: 6 genes, which showed the higher FC of the list (3 up and 3 down-regulated), were randomly chosen and amplified. The results are reported in Figure 15 and show how the three up-regulates genes (PTPRO, SCEL and PLSCR4, represented by the green bars) have a Fold Change higher than 1.5 also in the real-time assay, while the down-regulate genes (PRPRR, RRAD and HSBP3 indicate with the red bars) are under the threshold of 1 FC.

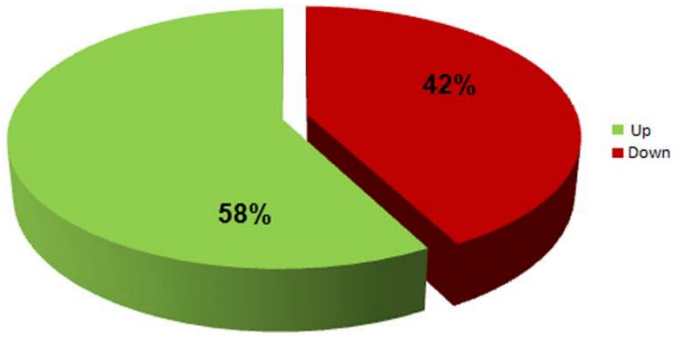

BP code	Term	PValue	Fold Enrichment	Bonferroni	Benjamini	FDR
GO:0006334	Nucleosome assembly	5,84E-08	5,94	1,29E-04	1,29E-04	1,02E-04
GO:0031497	Chromatin assembly	9,50E-08	5,73	2,10E-04	1,05E-04	1,65E-04
GO:0065004	Protein-DNA complex assembly	1,76E-07	5,48	3,89E-04	1,30E-04	3,06E-04
GO:0034728	Nucleosome organization	2,36E-07	5,36	5,22E-04	1,31E-04	4,11E-04
GO:0022610	Biological adhesion	1,19E-06	2,13	2,63E-03	5,26E-04	2,07E-03
GO:0048584	Positive regulation of response to stimulus	2,09E-06	3,17	4,60E-03	7,68E-04	3,63E-03
GO:0007155	Cell adhesion	2,76E-06	2,09	6,07E-03	8,69E-04	4,79E-03
GO:0006323	DNA packaging	4,74E-06	4,26	1,04E-02	1,31E-03	8,24E-03
GO:0002541	Activation of plasma proteins involved in acute inflammatory response	6,95E-06	7,25	1,52E-02	1,71E-03	1,21E-02
GO:0009611	Response to wounding	6,97E-06	2,23	1,53E-02	1,54E-03	1,21E-02

BP code	Term	PValue	Fold Enrichment	Bonferroni	Benjamini	FDR
GO:0006470	Protein amino acid dephosphorylation	7,64E-05	4,11	0,14	0,14	0,13
GO:0009725	Response to hormone stimulus	1,84E-04	2,52	0,30	0,16	0,31
GO:0016311	Dephosphorylation	3,06E-04	3,55	0,44	0,18	0,52
GO:0048771	Tissue remodeling	3,39E-04	6,00	0,48	0,15	0,58
GO:0009719	Response to endogenous stimulus	6,83E-04	2,28	0,73	0,23	1,16
GO:0042445	Hormone metabolic process	9,31E-04	3,96	0,83	0,26	1,58
GO:0010033	Response to organic substance	1,01E-03	1,86	0,86	0,24	1,72
GO:0042493	Response to drug	1,97E-03	2,72	0,98	0,38	3,31
GO:0010629	Negative regulation of gene expression	2,11E-03	2,00	0,98	0,36	3,54

Figure 15: **Microarray analysis**. The first graph shows the percentage of genes up and down regulated after RALY silencing in HeLa cells. Below the two tables show the first 10 terms of GeneOntology (Biological process) where the genes are involved (in the green table reported the results for up regulated genes, in red the results for down regulated genes)

Once confirmed the reliability of microarray assay, the list of genes with a significant fold-change were analyzed with the bioinformatics program DAVID (Huang da, Sherman et al. 2009) in order to obtain a clusterization of the identified genes based on the biological processes in which the genes are involved (Figure 14). The analysis revealed that the absence of RALY could affect genes involved in nucleosome assembly, aggregation, arrangement and bonding of the basic structure of eukaryotic chromatin composed by histones and DNA. I observed that these genes are implicated in processes such as chromatin assembly, exactly how reported from the analysis of the total genes; instead, the genes down expressed are involved not only in processes of phosphorylation/ dephosphorylation but also in processes that decrease the frequency, rate or extent of gene expression. The chromatin package and the

activation of specific kinases can be associated with a blocking of the cell cycle. Future investigations are needed to understand whether RALY is directly or indirectly associated with the cell cycle, though this hypothesis seems reasonable because RALY overexpression and high cell proliferation of several tumors has been recently reported (Tsofack, Garand et al. 2011).

3.2.4 DNA damage and repair

From the studies of interactome and microarray analysis it emerged that RALY is

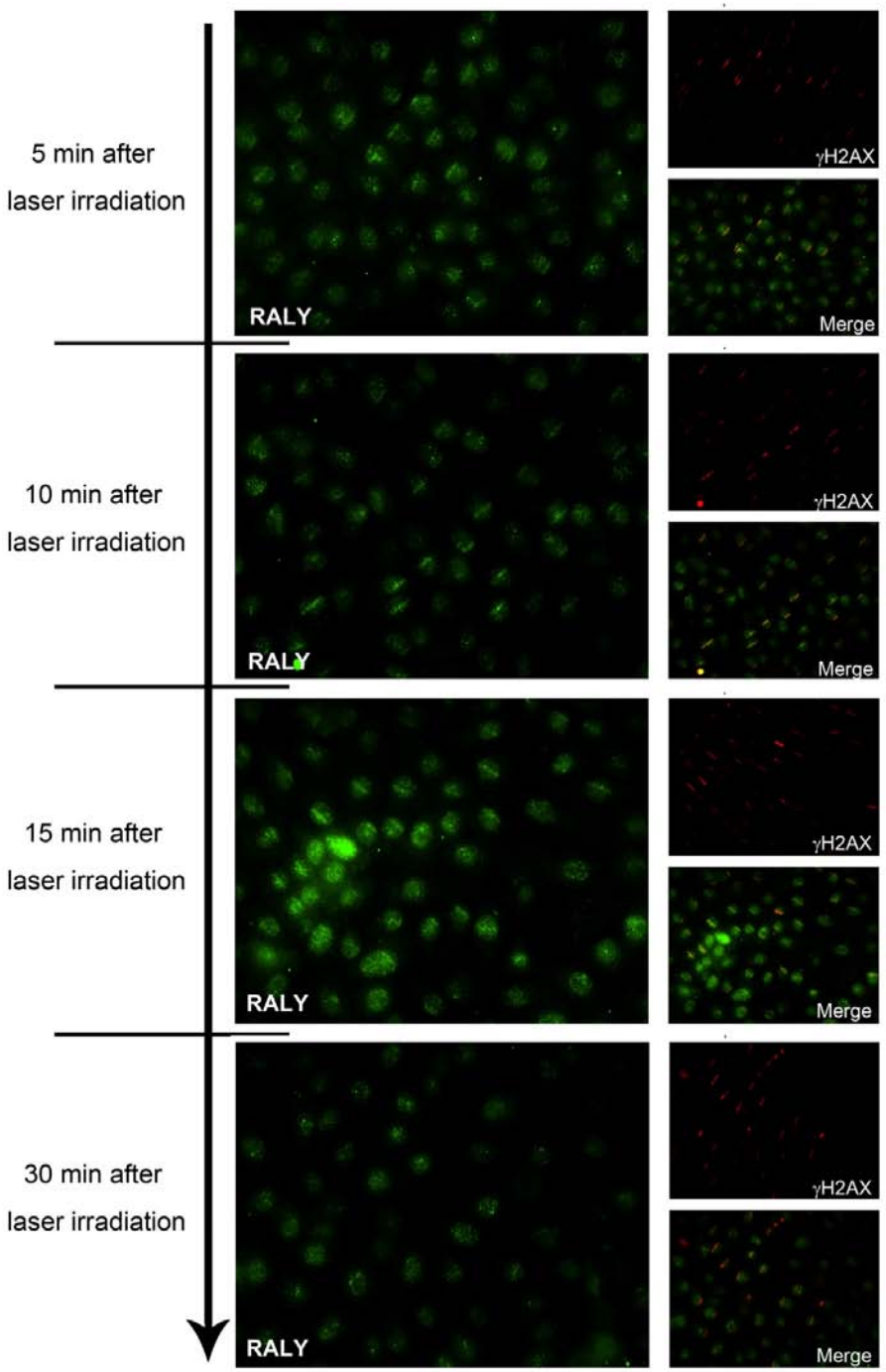

Figure 16: **Laser irradiation**. In the pictures is shown the pattern of RALY-GFP after 5, 10, 15 and 30 min from the laser irradiation. In red is detected the H2AX protein, which uses as report to identified the DNA double strand breaks sites

associated not only with proteins and mRNAs involved in RNA metabolism, but also with proteins involved in DNA metabolism. The interaction between RNPs and DNA is not new, and several articles reported that RNA binding proteins are involved in DNA damage repair as well as in chromatin's assembly (Adamson, Smogorzewska et al. 2012; Boucas, Riabinska et al. 2012; Polo, Blackford et al. 2012). The idea that RALY might be involved in DNA damage repair is confirmed by preliminary studies performed by Dr. Ferrari at the University of Zurich with whom I established a scientific collaboration. RALY-GFP was transfected in HeLa cells and after 24 hrs DNA damage was induced using laser irradiation laser. The laser irradiation causes DNA double-strand breaks (DBS). The localization of RALY-GFP was then analyzed at different time-points by fluorescence microscopy, as shown in Figure 16, and at very short time, less than 10 minutes after treatment, RALY localizes exactly to the break points, and disappearing after 30 minutes. After these preliminary results, experiments are in progress to confirm the involvement of RALY in the DNA damage repair.

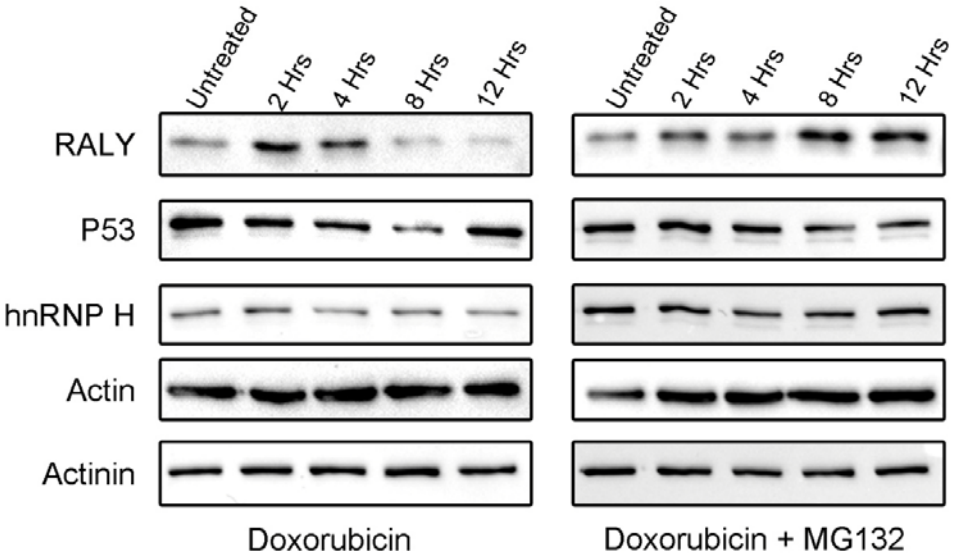

Figure 17: **Genotoxic stress**. The left picture shows the change in protein concentration of RALY against the concentration of p53 (positive control of genotoxic stress), hnRNP H (RALY's interactor involved in DNA damage response (Decorsiere, Cayrel et al. 2011)), Actin and Actinin at 0, 2 , 4, 8 and 12 hours after treatment with doxorubicin. The right picture shows the behaviour of the same protein in the same condition after proteosome inhibition through MG132.

I induced the DSB using Doxorubicin (Doxo), a drug that acts by inhibiting topoisomerase II (TopoII) causing DNA double-strand breaks (Pang, Qiao et al. 2013). The DNA double-strand breaks induce several changes in the expression and localization of few protein, for example the histone H2AX is phosphorylate and the protein is recruited in the DBS sites (Rogakou, Pilch et al. 1998). At the same time the DNA damage triggers the gene expression of proteins, including the well-know p53 and p21, both implicated in the genotoxic stress response. In order to investigate the behavior of RALY in this process in more details I observed changes of protein

concentration in MCF7 cells via Western blot assay and the pattern of RALY after DNA damage via confocal microscopy. I performed all these experiments on MCF7 cells because p53 is active in these cells, while the protein is not active in HeLa cells. I began the analyses by assessing the kinetics of RALY's expression at different time points (Figure 17). Cells were treated with Doxo for 1, 2, 4, 8, 12 hours and then lysated. Western blots were subsequently performed. While the concentration of p53 increases after 1 hour, the levels of RALY expression decreased after 4 hours and it disappeared almost completely after 8 hours. This behavior is common for other proteins involved in the DNA damage repairs such as EXO1. In human, EXO1 is expressed in two isoforms (hEXO1a and hEXO1b), both with a 5'->3' double-stranded DNA exonuclease activity. The isoform b is involved also in DNA mismatch repair (MMR) and it is rapidly degraded after single strand DNA damage induced by hydroxyurea (Schmutte, Sadoff et al. 2001; El-Shemerly, Janscak et al. 2005). To determine if RALY underwent degradation via proteaosome (ubiquitation dependent), the treatment with doxorubicin was conducted either in the presence or in the absence of the proteasome inhibitor MG132 (Figure 17). The presence of MG132 protected RALY from the degradation with a consequently accumulation of the protein. The observed down-regulation of the RALY protein is not correlated with a degradation of its corresponding mRNA. In fact using the real-time PCR I demonstrated that the levels of RALY mRNA in MCF7 cells did not change after 1, 2, 4, 6, 8 hours of doxorubicin treatment. In contrast p21, whose expression is stimulated by genotoxic stress (Ciribilli, Andreotti et al. 2010), increased its level of mRNA after treatment.

The data regarding the degradation of RALY, following genotoxic stress, obtained at biochemical levels were confirmed by confocal microscopy, and the results are reported in Figure 19. In this experiment I looked the pattern of RALY, p53 and γH2AX, after 4 and 16 hours of incubation with Doxorubicin. I used the pattern of the histone γH2AX to observe the localization of DNA damage, this protein is involved in DNA damage repair (DDR) and it accumulates in DNA damage sites. Moreover, I

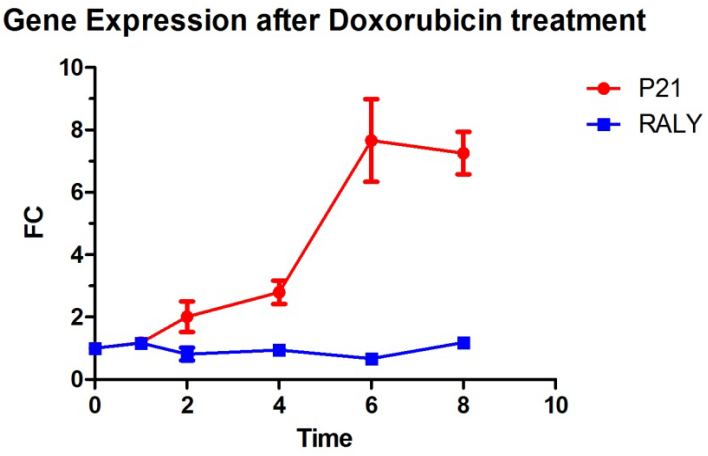

Figure 18: **mRNA stability after genotoxic stress**. The graph shows the trend of RALY's mRNA against the mRNA of the control protein p21.

observed the pattern after 16 hours of treatment because at this time there was the maximum expression of p53. The immunofluorescence assays were performed using only two antibodies together. By comparing the localization of RALY with p53 at T0 and T16 (Figure 19 C), it is possible to observe how the pattern of two proteins are opposite. As written before, the cells at T0 (not treated) have a nuclear presence of RALY, while p53 is almost completely absent in all the cells, except for sporadic spots within the cytoplasm. After 16 hours of treatment the situation was totally changed: p53 was very abundant and present only in the nucleus, whereas RALY was almost disappeared. In both cases the presence of γH2AX was not detectable. After 4 hours, instead, the γH2AX was well visible and the patterns of the two proteins were not the same in all the cells. At that time was possible to appreciate how the cells where protein γH2AX was more present, namely the cells under active DDR processes, presented also RALY in the nucleus, even if it was always less detectable. At the same time the expression of p53 is detectable in all the cells (Figure 19). These pictures seem to confirm the change in RALY expression during the DDR processes, but it is still not possible to understand whether this behavior is due to a direct involvement of the protein in the DDR, or is a cellular response to the DNA damage.

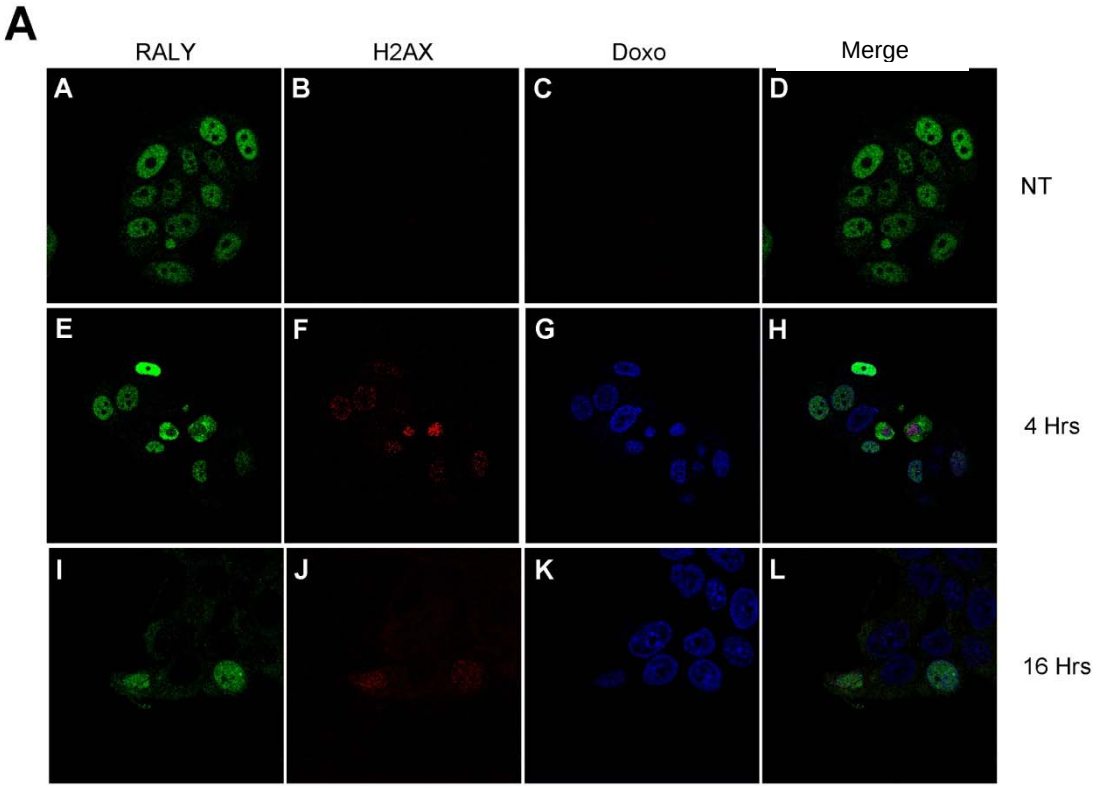

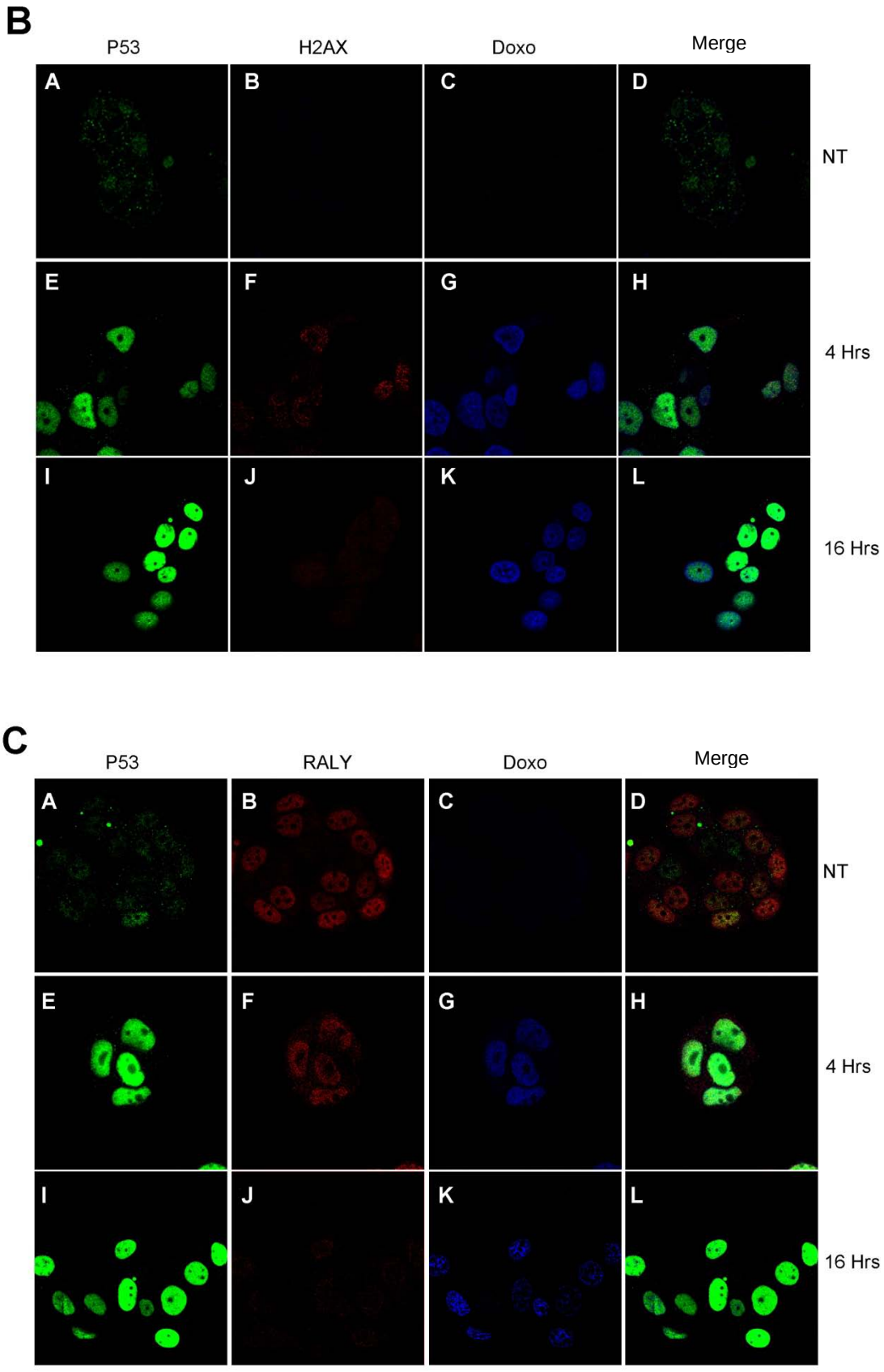

Figure 19: **RALY and p53 patterns after genotoxic stress**. Panel A shows the behavior of RALY (green) and H2AX (red) after 0, 4, 16 hours treatment with doxorubicin (blue). Same treatment is reported in panels B and C. Panel B show the trend of p53 (green) and H2AX (red), while panel C the trend of p53 (green) and RALY (red).

In any case, all the data, especially the results obtained from western blot, suggest that RALY undergoes post-translational modification. For this reason I started to investigate the possible PTMs affecting RALY via 2D SDS-PAGE; currently I have only preliminary results regarding the phosphorylation (Figure 20), further experiments are in progress.

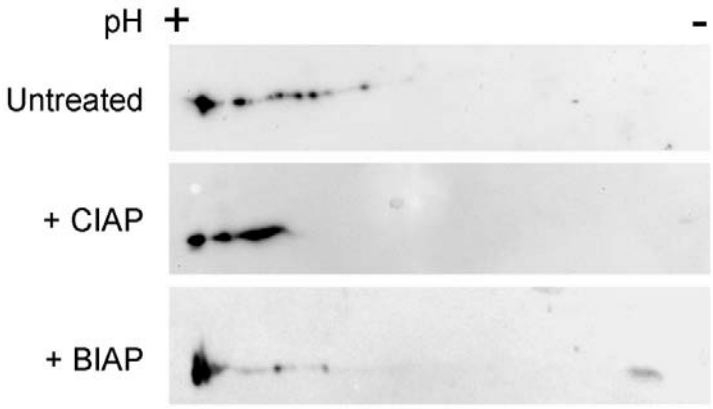

Figure 20: **2D electrophoresis**. The first picture shows the pattern of RALY under normal condition. It is possible to appreciate a series of spots that disappear after treatment with CIAP (Phosphatase, Alkaline from calf intestine) and BIAP (Phosphatase, Alkaline from bovine intestinal mucosa).

4 - DISCUSSION

RALY is an RNA-binding protein whose biological function in the mammalian cells was not evaluated yet. In humans, both *RALY* mRNA and protein are detected in several tissues (Khrebtukova, Kuklin et al. 1999), including the nervous system, kidney, liver, skeletal muscle, lung and pancreas (Macchi et al., unpublished). Interestingly, *RALY* mRNA is up-regulated in many tumor tissues (Yang, Ren et al. 2005; Tsofack, Garand et al. 2011), but the functional implications on cancer pathogenesis are currently unknown. Only few interaction partners of RALY protein have been described as components of RNA metabolism. RALY has been isolated from purified splicesome complex and from the EJC (Jurica, Licklider et al. 2002; Singh, Kucukural et al. 2012). However, a detailed picture of RALY interactome is still missing.

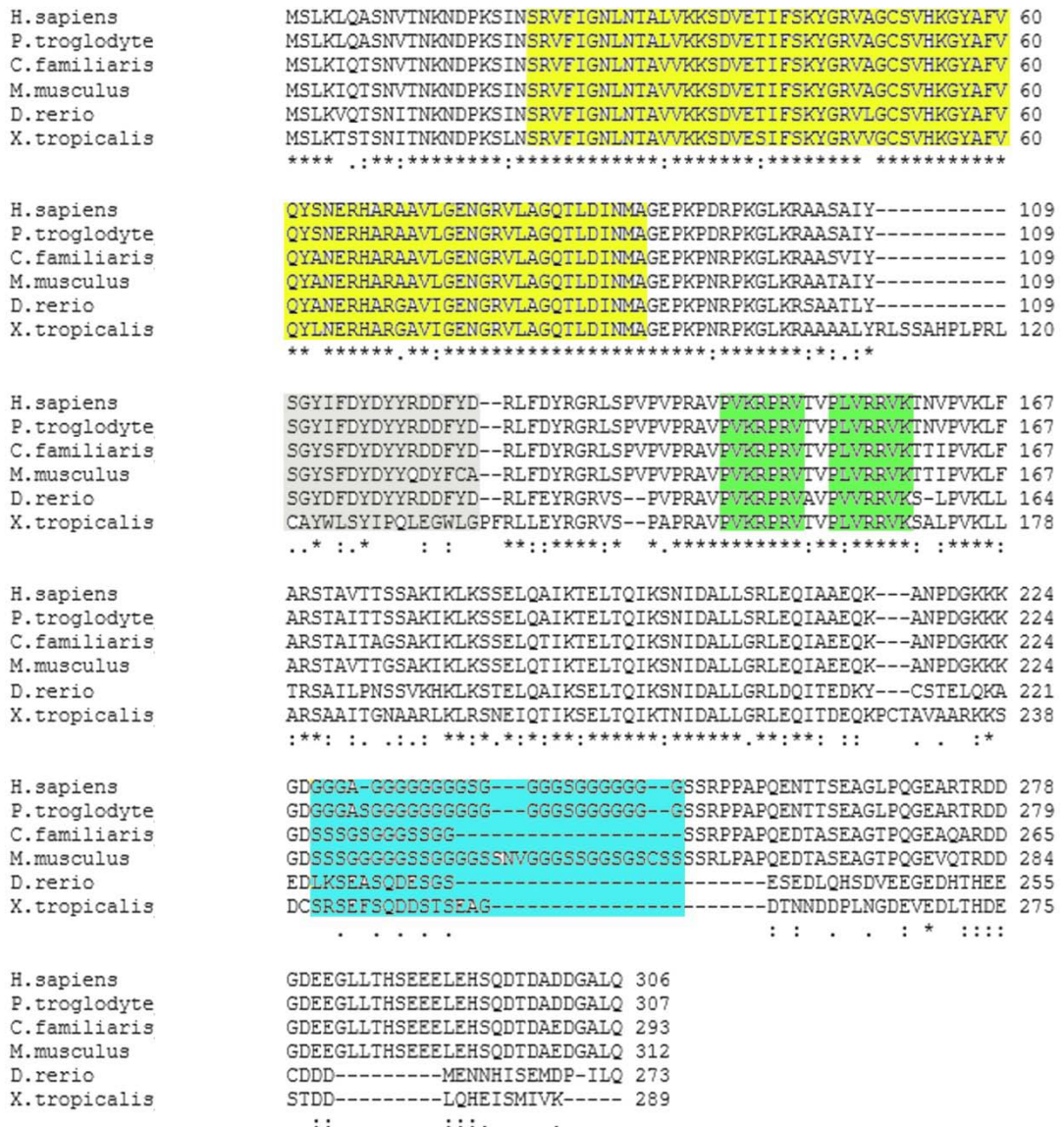

Figure 21 **RALY's alignment**. Sequence alignment of human RALY against chimpanzees, dog, mouse, zebrafish and Xenopus. In yellow is highlighted the RRM, in gray the splicing region, in green the NLS, and in blue the RGG box.

My studies concerning RALY started with a series of bioinformatics analysis, aiming at identifying peculiar domains. The human RNA-binding protein RALY shares 87% identity with the mouse homologue and it has 43% of amino acid identity with hnRNP C. This homology is higher within the N-terminal regions, which contain a predicted RNA-recognition motif (RRM). Low similarity has been found in the C-terminal region of RALY, where a sequence motif rich in glycine (GRR) is present. Even if its function is still unclear, it could be implicated in the protein-protein interaction, or the RGG domain could mediate the intracellular trafficking such as in hnRNP A2 and hnRNP H/F (Sun, Tang et al. 2003; Van Dusen, Yee et al. 2010). Actually, the RGG seems to be present only in primates. Comparison with mice's RGG shows that the two domains are very different: in mouse, the long stretch of glycine is interspersed by valine, serine and asparagines. In zebrafish and Xenopus RALY, the GRR domain is not present (Figure 21). Besides the RMM and RGG domains, three potential nuclear localization signals (NLS) were predicted by computer analysis. These RALY NLSs are conserved in many species, from human to zebrafish. Since no experiments regarding RALY localization had been performed, so far my first goal was to demonstrate the presence and activity of these predicted NLS in vivo. As reported in RESULTS 3.2.1 RALY localization (pg.16), RALY localizes in the nucleus and it is excluded from the nucleoli, but it can be detected in little spots within the cytoplasm. No NES have been identified: RALY distribution does not change after treatment with Leptomycin B (LMB), a compound that competes with the export factor CRM1 (Nishi, Yoshida et al. 1994).

A second unexpected result has been the localization of the RALY deprived of NLS. As expected, in normal condition this mutant is more present in the cytoplasm; moreover it can be detected in stress granules after oxidative stress, while RALY wild type could not localize in these particulars particles. An abnormal protein accumulation in SGs is a typical pattern of neurons affected by Amyotrophic lateral sclerosis (ALS); in this case the principals responsible for the disease are the proteins TDP-43 and FUS. Both are RNA binding proteins that present two RRM domains and one RGG sequence, moreover, studies demonstrated that mutations in these proteins may cause abnormal aggregation of the same proteins in SGs (Li, King et al. 2013). A mutation in RALY protein with a consequently cytoplasmatic accumulation has not been identified and for this there are not diseases associate with RALY mutation yet.

The major achievement of my research has been the identification of RALY interactome. Using gene ontology bioinformatics tools it is possible to cluster a record of genes/proteins and predict the biological processes (BP) in which they are involved. In my project I used several time this approach to obtain more useful information from

the interactome's results originating from the co-immunoprecipitation, as well as to identify possible pathways which are modified from the RALY absence, using the data derived from the microarray analysis.

Before doing that, it is necessary to have a “list” of genes/proteins, for example a record of possible interactors. In order to obtain this “list” of RALY’s interactors, my first approach was to perform a canonical experiment of immunoprecipitation (IP): using a specific antibody anti-RALY I planned to isolate my protein from a cells lysate and to identify the proteins which co-immunoprecipitated with RALY. Unfortunately, this approach did not give reproducible results, the material obtained after coIP was variable and the background noise was very high. To overcome these drawbacks, I decided to use a fusion protein to increase the efficiency of immunoprecipitation. However, the most common tagged I tested (e.g. HA, FLAG, myc) did not immunoprecipitate tagged-RALY in an efficient way. I decided to setup the immunoprecipitation using a BAP-tagged RALY that can be biotinylated *in vivo*. *In-vivo* Biotinylation followed by a pulldown assay was previously used to isolate mRNAs associated with the RNA-binding protein PABP (Penalva and Keene 2004). A similar approach has been recently applied to elucidate the FoxP3’s interactome, leading to the identification of 361 FoxP3 interacting proteins, underlining its potential to identify protein interaction partners (Rudra, deRoos et al. 2012). However, this technique has not been integrated into a label-free quantitative proteomics workflow until now. The integration between i*n-vivo* Biotinylation and label-free quantitative proteomics workflow increases the amount of purified protein and, at the same time, it decreases the number of unspecific interactors identified via mass spectrometry (all the details of this technique are reported in Appendix 7.1 (Tenzer, Moro et al. 2013). In this way I obtained a list of specific interactors of RALY that allowed me to start a deeper bioinformatics analysis.

In spite of the good results that I obtained with coIP and mass spectrometry analysis, I would like to spend a few words concerning the limitation of my analysis. The knowledge of the protein's interactome is essential for its characterization: the identification of possible protein complexes where the protein is involved could help to understand the role of the protein into the cells; nevertheless, this information might bring to inconclusive results. All current techniques of PPI (protein-protein interaction) show several advantages and disadvantages: for this reason, before to choosing one or another technique it is better to analyze pros and contras. The coIP of an endogenous protein is a very effective technique to isolate a protein in its native state and at its native concentration; moreover, the protein's transfection allows to mutate

specific sites in order to understand the role of these sites in the protein's interactions. At the same time the coIP shows several disadvantages, especially concerning the biological role; indeed, the mixing of compartments during cell's lyses and the protein purification brings an interaction between proteins which might not be specific. In addition, the interaction between the protein of interest and other proteins could be very transient, and during the coIP process is possible that weak interactions are lost. Last but not least, coIP does not indicate whether interaction between two proteins is direct or mediated by other proteins or substances as RNA (Orchard, Salwinski et al. 2007). To obtain this information is necessary to integrate the coIP analysis with other methods such as X-ray crystallography; unfortunately, also the X-ray crystallography technique shows several limitations: the first is that to perform a good experiment of X-ray is necessary a large amounts of purified proteins for the analysis; furthermore, this technique is very expensive and very low-throughput. For these reasons a wonderful resource for the PPI analysis is represented by interaction databases. These databases collect data and annotation from more researchers and articles with the aim at combining data derived from multiple techniques in order to obtain the most realistic representation of protein-protein interaction.

In my work I use the IntAct database and the free software Cytoscape in order to try to produce useful information from the long list of RALY's interactors obtained from the mass spectrometry analysis. In the 1929 the writer Frigyes Karinthy proposed the theory of the “Six degrees of separation”: everything and everyone is six or fewer steps away from any other person in the world. A similar idea is the basis of my speculation: the 80% of proteins into the cells are connected, directly or indirectly. For this reason is plausible to think that all the proteins that I found from mass spectrometry are connected to each other in a direct way, or through other cellular components such as RNA, but not via interaction mediated by proteins which are not in the coIP list. To investigate this hypothesis, my approach has been to create a big network starting from data of published PPI, where my source nodes were established RALY's interactors; from this very big and complicate network, I isolated the proteins found in the mass spectrometry list and I examined if all these proteins were connected (Figure 22). Unexpected, only 68 out of 143 proteins (the 47,5 %) are associated each others, and the majority of these proteins are components of mRNA metabolism, especially RNA splicing; these data confirm the analysis of GeneOntology presented in the article.

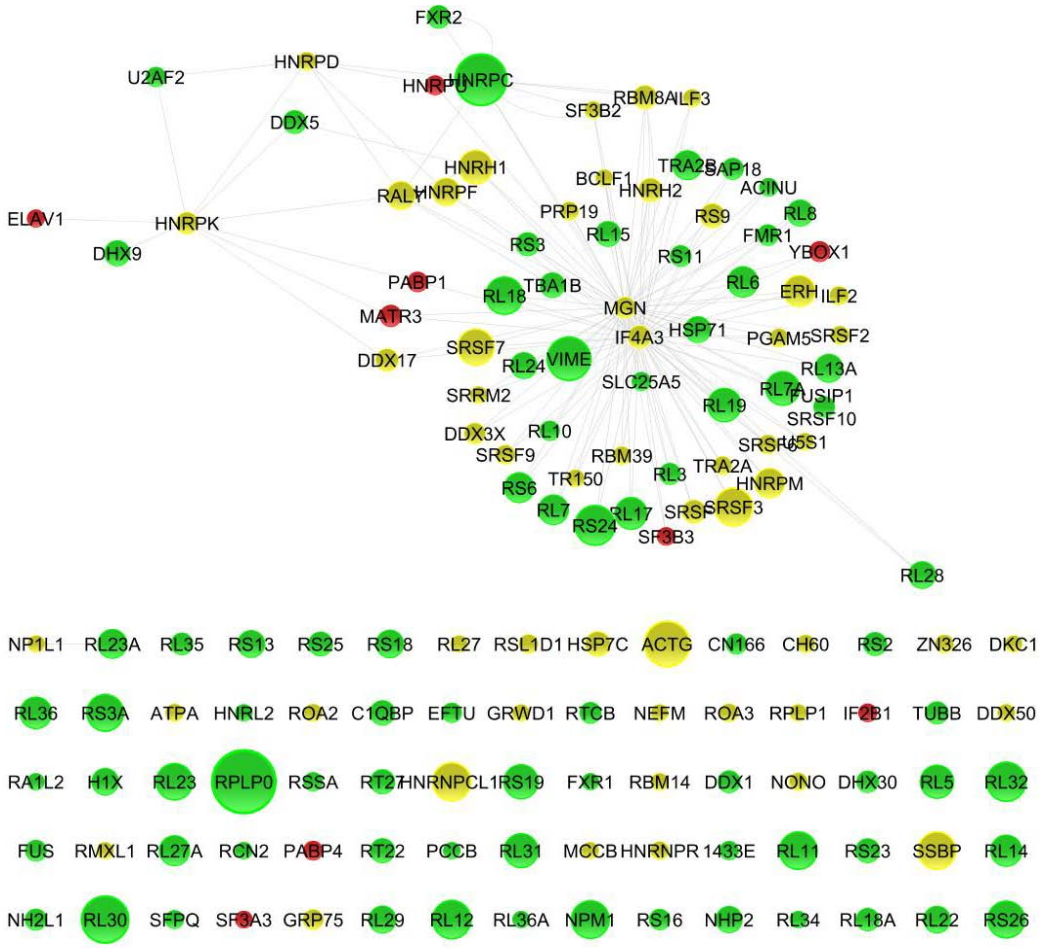

Figure 22: **RALY's network**. The figure show the protein-protein interactions known for the RALY's interactors derived from mass spectrometry. The not connecting proteins are interactors of RALY which are not associated with other interactors. The nodes represent the proteins and are colored are reported in the article (Tenzer, Moro et al. 2013), while the size depend from the max score in according with the results reported in the same publication

Relatively to the remaining proteins (the 52,5% of the total), although many of these are involved in RNA metabolism, in the interactome of these proteins there are not proteins identified through my coIP experiment. Many are the possible interpretations for this unforeseen result: the first possibility is that the complete interactome of these proteins is also unknown, and for this reason the program does not find interaction between these proteins and other interactors of RALY; the second chance is the indirect interaction: in this case the interaction between RALY and the protein is mediated by RNA, DNA or other substances. Since the majority of these proteins are involved in the RNA metabolism (according to the GeneOntology analysis) almost all these proteins would be expected to disappear after RNase treatment. On the contrary, the interaction between RALY and the proteins increase after that treatment. The last hypothesis for this result is that RALY interacts with the mRNA of these proteins but not with the proteins themselves, and the interaction resulting from mass spectrometry is probably due to the interaction between RALY and mRNA during all the translational processes. If this hypothesis was correct, the interaction between

the two proteins would be not properly mediated by RNA, but rather through the ribosome. This fascinating hypothesis could find a first confirmation in the high number of ribosomal's proteins associated with RALY; nevertheless, to have more evidence, it will be necessary to investigate which RNAs are bound by RALY, together with the interaction between RALY and the complete ribosome.

4.1 RNA INTERACTION

With the idea to investigate the interaction between RALY and the ribosome, in order to understand the role of the RALY into the cell, my interest has shifted to identify the interaction between RALY and RNA. I decided to follow three different ways of investigation to observe RALY's localization in the polyribosome profiling assay; to identify the RNAs bound to RALY using the RNAseq analysis; finally, to observe changes in gene expression of the cells after RALY silencing. The first and third approach gave me positive results but, unfortunately, the RNAseq analysis is still in progress due to technical problems, similar to the problems encountered during the co-immunoprecipitation assay.

Although the results arising from RNAseq analysis could better elucidate my previous hypothesis, the results from the polyribosome profiling have interesting perspectives. As shown in RESULTS 3.2.2 Polyribosome profiling, the localization of RALY is not the typical pattern shown by other RBPs; indeed, it seems more similar to the pattern shown by the ribosomal proteins. In particular RALY does not locate in the fraction lacking ribosomal subunits, like the fraction three, where PABP and hnRNP A1 are detectable. This result could be another brick in the wall of the previous hypothesis: RALY is not present in the "ribosome free" fraction, this could indicate a direct association between RALY and the ribosome. The consequence of the association between RALY and some proteins depends on the transcription of these proteins in the ribosome. This theory is also far from being clarified, but some small steps in this direction have been done, and I can conclude that probably the interaction between RALY and some of its interactors is a “false positive”, or better is an interaction “under construction”, namely an association between RALY and a protein through the mRNA and the ribosome.

Regarding the results derived from the microarray assay, I cannot comment further, because the analysis is also ongoing, and what I showed is only the preliminary result; even if RALY silencing seems to push the cells towards a block of proliferation, with a chromatin assembly, before understanding if RALY plays a role in cell proliferation. It is necessary to make several further experiments; at the moment I can conclude only

observing that the loss of RALY protein induces an increase, in terms of gene expression, of proteins involved in DNA metabolism.

All the results obtained using microarray and mass spectrometry, besides to confirming the implication of RALY in the regulation of gene expression, have shown the possible role of this protein also in DNA metabolism. For this reason I checked the possible implications of RALY in DNA damage repair. As described above, the preliminary results obtained after the treatment with doxorubicin, a drug which produces double strand breaks of DNA, seem to be promising. Nevertheless, these results do not elucidate if RALY is directly involved in the DDR or else it has only a "support" role in this processes. In addition could be interesting to observe the post-translational modification of RALY in this situation; indeed, some other RBPs can be recruited in the DNA damage repair process through phosphorylation via ATM/Chk2 pathway (Boucas, Riabinska et al. 2012). Moreover, the understanding of PTMs affecting RALY can elucidate how this protein could take part in different processes which involve different substrates such as RNA and DNA, and this is a matter of my current investigation.

5 - OUTLOOK

In this project, I characterized the RNA-binding protein RALY. The existence of RALY is known from many years, the first study concerning the gene encoding this protein dates back to 1995, but no research regarding the biological role of RALY within cells has been done so far. Although many questions still remain regarding the biological role(s) of RALY, my results have opened several lines of investigation.

During my PhD, I elucidated several aspects of RALY protein, from the intracellular pattern to the interactome, and my results gave weight to the speculation that the interaction between RALY and its interactors could be mediated by other proteins or complexes. In this sense the identification of ribosomal complex components in the RALY interactome, together with the association between RALY and the ribosomal subunits, could support the speculation. Taken together, these results permit the hypothesis of a possible active role of RALY in the translation of mRNA encoding for a protein involved in a pathway not correlate with RNA metabolism. This idea could elucidate because RALY interacts with protein involved in processes like DNA metabolism. However, this is just an interesting hypothesis and requires many additional studies for it to be confirmed. For this reason I started to investigate which RNAs are bound by RALY, and awaiting for data coming from RNA-seq analysis, the microarray assay gave me preliminary hints regarding which genes are up and down-regulated by RALY.

The absence of RALY seems to stimulate the packing of chromatin through histone activation, while there is down-regulation of proteins involved in the processes of dephosphorylation, such as several member of the PTPR family (the entire list of genes is reported in Appendix 7.3). There is likely to be a direct correlation between these processes and a block cell proliferation, and RALY could be an important player in these processes. This second observation could explain the high concentration of RALY in cancer cell lines, and the lethal response that the deletion of RALY gene has in mice and quails. Moreover, RALY silencing, as result of DNA damage, could be associated with the block of cell proliferation more than DNA damage repair. Unfortunately, there is no evidence supporting this hypothesis, but currently my experiments are moving towards this direction. In order to confirm the role of RALY in cell proliferation I have started to observe how the RALY silencing could modified the cellular behavior using microarray and FACS assay.

For this second hypothesis the identification of the post-translational modifications (PTMs) affecting this protein would also be a useful, and in RALY I observed the

presence of 6 phosphorylation sites. The identification and characterization of PTMs are important in the characterization of proteins: indeed, several proteins change their behavior depending on their post-translational modification. Over the past few years many studies have shown how PTMs influence protein-protein interaction and consequently complex assemblies such as stress granules. For example, the phosphorylation of eIF2α following heat shock or oxidative stress induces the eIF2α protein to accumulate in SGs (Kedersha, Chen et al. 2002; Xie and Denman 2011). There are many other examples of the effects of PTMs on protein function: in my case, the identification of post-translational modifications may be useful for confirming the role of RALY in cell proliferation, as these modifications may explain how external signals can activate or deactivate RALY within the cell.

It will be interesting to investigate the role of RALY in post mitotic cells such as neuronal cells. These cells represent a good model for studies concerning RBPs for two principal reasons: first, they are polarized cell, with clear defined subcellular compartments (e.g. dendrites, cell body, axons) with the capability to quickly respond to external stimuli; second, the response does not necessary involve the whole cell, but can be localized to specific compartments (e.g. synapses). The RBPs are necessary for several aspects of the neuronal activity, (Kiebler and Bassell 2006; Vessey, Schoderboeck et al. 2010), including the myelin formation in oligodendrocytes, another example of highly polarized cell type (White, Gonsior et al. 2012). Moreover, as mentioned in the Introduction, the local translation of mRNA independently regulates the expression of specific genes in different region and allowing for a fast synthesis of new proteins, (Dahm, Kiebler et al. 2007). Last, but not least, mutations in neuronal RBPs is responsible for several neurological diseases, such as Amyotrophic lateral sclerosis (ALS), or the dystrophia myotonica (Ramaswami, Taylor et al. 2013).

Although RALY has been originally identified as an interactor of Barentsz, its function in the neurons is still completely unknown. In my studies I have identified many interactors of RALY which play important role in neurons, among these, eIF4A3 (Giorgi, Yeo et al. 2007), TUBB5 (Breuss, Heng et al. 2012), and hnRNP A2/B1 (Liang, Shi et al. 2011). Also FMR1, FXR1 and FXR2 have been identified in RALY-containing complex: these three proteins are paralogs and are involved in Fragile X mental retardation syndrome, the most common form of hereditary mental retardation (Zhang, O'Connor et al. 1995). Again, no studies have been performed to elucidate the biological significance of RALY interaction with proteins involved in Fragile X disease.

Taken together, future experiments will be mandatory to analyze RALY in the nervous system.

All my preliminary results reveal that further investigation is needed; moreover, many other questions have been raised that need answering. I started to address these questions, but at the moment I can conclude that characterization of RALY is only the first step necessary in identifying its role within cells. Unfortunately, I did not have the time to investigate all these questions, and in this thesis I focused particularly on protein localization, proteomic analysis and gene ontology, which gave the most significant results that I have obtained during this period. Besides I attempted to explain my hypothesis regarding the role of RALY, in order to demonstrate that the study of RBPs are essential for understanding the complexity of cell life.

6 - BIBLIOGRAPHY

Abdelmohsen, K., R. Pullmann, Jr., et al. (2007). "Phosphorylation of HuR by Chk2 regulates SIRT1 expression." Mol Cell 25(4): 543-557.

Adamson, B., A. Smogorzewska, et al. (2012). "A genome-wide homologous recombination screen identifies the RNA-binding protein RBMX as a component of the DNA-damage response." Nat Cell Biol 14(3): 318-328.

Antson, A. A. (2000). "Single-stranded-RNA binding proteins." Curr Opin Struct Biol 10(1): 87-94.

Baguet, A., S. Degot, et al. (2007). "The exon-junction-complex-component metastatic lymph node 51 functions in stress-granule assembly." J Cell Sci 120(Pt 16): 2774-2784.

Birney, E., S. Kumar, et al. (1993). "Analysis of the RNA-recognition motif and RS and RGG domains: conservation in metazoan pre-mRNA splicing factors." Nucleic Acids Res 21(25): 5803-5816.

Bladen, C. L., D. Udayakumar, et al. (2005). "Identification of the polypyrimidine tract binding protein-associated splicing factor.p54(nrb) complex as a candidate DNA double-strand break rejoining factor." J Biol Chem 280(7): 5205-5210.

Boucas, J., A. Riabinska, et al. (2012). "Posttranscriptional regulation of gene expression-adding another layer of complexity to the DNA damage response." Front Genet 3: 159.

Breuss, M., J. I. Heng, et al. (2012). "Mutations in the beta-tubulin gene TUBB5 cause microcephaly with structural brain abnormalities." Cell Rep 2(6): 1554-1562.

Busch, A. and K. J. Hertel (2012). "Evolution of SR protein and hnRNP splicing regulatory factors." Wiley Interdiscip Rev RNA 3(1): 1-12.

Chang, Y. F., J. S. Imam, et al. (2007). "The nonsense-mediated decay RNA surveillance pathway." Annu Rev Biochem 76: 51-74.

Chen, C. Y., R. Gherzi, et al. (2000). "Nucleolin and YB-1 are required for JNK-mediated interleukin-2 mRNA stabilization during T-cell activation." Genes Dev 14(10): 1236-1248.

Chen, Y. and G. Varani (2005). "Protein families and RNA recognition." FEBS J 272(9): 2088-2097.

Choi, Y. D. and G. Dreyfuss (1984). "Isolation of the heterogeneous nuclear RNA-ribonucleoprotein complex (hnRNP): a unique supramolecular assembly." Proc Natl Acad Sci U S A 81(23): 7471-7475.

Ciribilli, Y., V. Andreotti, et al. (2010). "The coordinated p53 and estrogen receptor cis-regulation at an FLT1 promoter SNP is specific to genotoxic stress and estrogenic compound." PLoS One 5(4): e10236.

Coller, J. and M. Wickens (2002). "Tethered function assays using 3' untranslated regions." Methods 26(2): 142-150.

Conte, M. R., T. Grune, et al. (2000). "Structure of tandem RNA recognition motifs from polypyrimidine tract binding protein reveals novel features of the RRM fold." EMBO J 19(12): 3132-3141.

Dahm, R., M. Kiebler, et al. (2007). "RNA localisation in the nervous system." Semin Cell Dev Biol 18(2): 216-223.

Decorsiere, A., A. Cayrel, et al. (2011). "Essential role for the interaction between hnRNP H/F and a G quadruplex in maintaining p53 pre-mRNA 3'-end processing and function during DNA damage." Genes Dev 25(3): 220-225.

Dingwall, C., J. Robbins, et al. (1988). "The nucleoplasmin nuclear location sequence is larger and more complex than that of SV-40 large T antigen." J Cell Biol 107(3): 841-849.

Dominguez, C., J. F. Fisette, et al. (2010). "Structural basis of G-tract recognition and encaging by hnRNP F quasi-RRMs." Nat Struct Mol Biol 17(7): 853-861.

Dreger, D. L., H. G. Parker, et al. (2013). "Identification of a Mutation that Is Associated with the Saddle Tan and Black-and-Tan Phenotypes in Basset Hounds and Pembroke Welsh Corgis." J Hered 104(3): 399-406.

Dreyfuss, G., M. J. Matunis, et al. (1993). "hnRNP proteins and the biogenesis of mRNA." Annu Rev Biochem 62: 289-321.

El-Shemerly, M., P. Janscak, et al. (2005). "Degradation of human exonuclease 1b upon DNA synthesis inhibition." Cancer Res 65(9): 3604-3609.

Gaudreault, I., D. Guay, et al. (2004). "YB-1 promotes strand separation in vitro of duplex DNA containing either mispaired bases or cisplatin modifications, exhibits endonucleolytic activities and binds several DNA repair proteins." Nucleic Acids Res 32(1): 316-327.

Giorgi, C., G. W. Yeo, et al. (2007). "The EJC factor eIF4AIII modulates synaptic strength and neuronal protein expression." Cell 130(1): 179-191.

Godin, K. S. and G. Varani (2007). "How arginine-rich domains coordinate mRNA maturation events." RNA Biol 4(2): 69-75.

Goetze, B., F. Tuebing, et al. (2006). "The brain-specific double-stranded RNA-binding protein Staufen2 is required for dendritic spine morphogenesis." J Cell Biol 172(2): 221-231.

Hallegger, M., M. Llorian, et al. (2010). "Alternative splicing: global insights." FEBS J 277(4): 856-866.

Han, S. P., Y. H. Tang, et al. (2010). "Functional diversity of the hnRNPs: past, present and perspectives." Biochem J 430(3): 379-392.

Handa, N., O. Nureki, et al. (1999). "Structural basis for recognition of the tra mRNA precursor by the Sex-lethal protein." Nature 398(6728): 579-585.

Huang da, W., B. T. Sherman, et al. (2009). "Systematic and integrative analysis of large gene lists using DAVID bioinformatics resources." Nat Protoc 4(1): 44-57.

Jiang, W., X. Guo, et al. (1998). "Four distinct regions in the auxiliary domain of heterogeneous nuclear ribonucleoprotein C-related proteins." Biochim Biophys Acta 1399(2-3): 229-233.

Jung, M., E. Kramer, et al. (1995). "Lines of murine oligodendroglial precursor cells immortalized by an activated neu tyrosine kinase show distinct degrees of interaction with axons in vitro and in vivo." Eur J Neurosci 7(6): 1245-1265.

Jurica, M. S., L. J. Licklider, et al. (2002). "Purification and characterization of native spliceosomes suitable for three-dimensional structural analysis." RNA 8(4): 426-439.

Kedersha, N., S. Chen, et al. (2002). "Evidence that ternary complex (eIF2-GTP-tRNA(i)(Met))-deficient preinitiation complexes are core constituents of mammalian stress granules." Mol Biol Cell 13(1): 195-210.

Kedersha, N., G. Stoecklin, et al. (2005). "Stress granules and processing bodies are dynamically linked sites of mRNP remodeling." J Cell Biol 169(6): 871-884.

Keene, J. D. (2007). "RNA regulons: coordination of post-transcriptional events." Nat Rev Genet 8(7): 533-543.

Keene, J. D. and P. J. Lager (2005). "Post-transcriptional operons and regulons co-ordinating gene expression." Chromosome Res 13(3): 327-337.

Khrebtukova, I., A. Kuklin, et al. (1999). "Alternative processing of the human and mouse raly genes(1)." Biochim Biophys Acta 1447(1): 107-112.

Kiebler, M. A. and G. J. Bassell (2006). "Neuronal RNA granules: movers and makers." Neuron 51(6): 685-690.

Kiledjian, M. and G. Dreyfuss (1992). "Primary structure and binding activity of the hnRNP U protein: binding RNA through RGG box." EMBO J 11(7): 2655-2664.

Krecic, A. M. and M. S. Swanson (1999). "hnRNP complexes: composition, structure, and function." Curr Opin Cell Biol 11(3): 363-371.

la Cour, T., L. Kiemer, et al. (2004). "Analysis and prediction of leucine-rich nuclear export signals." Protein Eng Des Sel 17(6): 527-536.

Li, Y. R., O. D. King, et al. (2013). "Stress granules as crucibles of ALS pathogenesis." JCB.

Liang, Y., S. L. Shi, et al. (2011). "The localization of hnRNP A2/B1 in nuclear matrix and the aberrant expression during the RA-induced differentiation of human neuroblastoma SK-N-SH cells." J Cell Biochem 112(7): 1722-1729.

Lunde, B. M., C. Moore, et al. (2007). "RNA-binding proteins: modular design for efficient function." Nat Rev Mol Cell Biol 8(6): 479-490.

Macchi, P., S. Kroening, et al. (2003). "Barentsz, a new component of the Staufen-containing ribonucleoprotein particles in mammalian cells, interacts with Staufen in an RNA-dependent manner." J Neurosci 23(13): 5778-5788.

Maris, C., C. Dominguez, et al. (2005). "The RNA recognition motif, a plastic RNA-binding platform to regulate post-transcriptional gene expression." FEBS J 272(9): 2118-2131.

Michaud, E. J., S. J. Bultman, et al. (1993). "The embryonic lethality of homozygous lethal yellow mice (Ay/Ay) is associated with the disruption of a novel RNA-binding protein." Genes Dev 7(7A): 1203-1213.

Mittal, N., N. Roy, et al. (2009). "Dissecting the expression dynamics of RNA-binding proteins in posttranscriptional regulatory networks." Proc Natl Acad Sci U S A 106(48): 20300-20305.

Musco, G., G. Stier, et al. (1996). "Three-dimensional structure and stability of the KH domain: molecular insights into the fragile X syndrome." Cell 85(2): 237-245.

Nadeau, N. J., F. Minvielle, et al. (2008). "Characterization of Japanese quail yellow as a genomic deletion upstream of the avian homolog of the mammalian ASIP (agouti) gene." Genetics 178(2): 777-786.

Nishi, K., M. Yoshida, et al. (1994). "Leptomycin B targets a regulatory cascade of crm1, a fission yeast nuclear protein, involved in control of higher order chromosome structure and gene expression." J Biol Chem 269(9): 6320-6324.

Norris, J. D., D. Fan, et al. (2002). "A negative coregulator for the human ER." Mol Endocrinol 16(3): 459-468.

Ohga, T., T. Uchiumi, et al. (1998). "Direct involvement of the Y-box binding protein YB-1 in genotoxic stress-induced activation of the human multidrug resistance 1 gene." J Biol Chem 273(11): 5997-6000.

Orchard, S., L. Salwinski, et al. (2007). "The minimum information required for reporting a molecular interaction experiment (MIMIx)." Nat Biotechnol 25(8): 894-898.

Palacios, I. M., D. Gatfield, et al. (2004). "An eIF4AIII-containing complex required for mRNA localization and nonsense-mediated mRNA decay." Nature 427(6976): 753-757.

Pang, B., X. Qiao, et al. (2013). "Drug-induced histone eviction from open chromatin contributes to the chemotherapeutic effects of doxorubicin." Nat Commun 4: 1908.

Penalva, L. O. and J. D. Keene (2004). "Biotinylated tags for recovery and characterization of ribonucleoprotein complexes." Biotechniques 37(4): 604, 606, 608-610.

Petris, G., L. Vecchi, et al. (2011). "Efficient detection of proteins retro-translocated from the ER to the cytosol by in vivo biotinylation." PLoS One 6(8): e23712.

Polo, S. E., A. N. Blackford, et al. (2012). "Regulation of DNA-end resection by hnRNPU-like proteins promotes DNA double-strand break signaling and repair." Mol Cell 45(4): 505-516.

Pont, A. R., N. Sadri, et al. (2012). "mRNA decay factor AUF1 maintains normal aging, telomere maintenance, and suppression of senescence by activation of telomerase transcription." Mol Cell 47(1): 5-15.

Ponthier, J. L., C. Schluepen, et al. (2006). "Fox-2 splicing factor binds to a conserved intron motif to promote inclusion of protein 4.1R alternative exon 16." J Biol Chem 281(18): 12468-12474.

Provenzani, A., R. Fronza, et al. (2006). "Global alterations in mRNA polysomal recruitment in a cell model of colorectal cancer progression to metastasis." Carcinogenesis 27(7): 1323-1333.

Raffetseder, U., B. Frye, et al. (2003). "Splicing factor SRp30c interaction with Y-box protein-1 confers nuclear YB-1 shuttling and alternative splice site selection." J Biol Chem 278(20): 18241-18248.

Ramaswami, M., J. P. Taylor, et al. (2013). "Altered ribostasis: RNA-protein granules in degenerative disorders." Cell 154(4): 727-736.

Ricciardi, S., C. Kilstrup-Nielsen, et al. (2009). "CDKL5 influences RNA splicing activity by its association to the nuclear speckle molecular machinery." Hum Mol Genet 18(23): 4590-4602.

Rogakou, E. P., D. R. Pilch, et al. (1998). "DNA double-stranded breaks induce histone H2AX phosphorylation on serine 139." J Biol Chem 273(10): 5858-5868.

Rudra, D., P. deRoos, et al. (2012). "Transcription factor Foxp3 and its protein partners form a complex regulatory network." Nat Immunol 13(10): 1010-1019.

Schaal, T. D. and T. Maniatis (1999). "Multiple distinct splicing enhancers in the protein-coding sequences of a constitutively spliced pre-mRNA." Mol Cell Biol 19(1): 261-273.

Schittek, B., K. Psenner, et al. (2007). "The increased expression of Y box-binding protein 1 in melanoma stimulates proliferation and tumor invasion, antagonizes apoptosis and enhances chemoresistance." Int J Cancer 120(10): 2110-2118.

Schmutte, C., M. M. Sadoff, et al. (2001). "The interaction of DNA mismatch repair proteins with human exonuclease I." J Biol Chem 276(35): 33011-33018.

Sewer, M. B., V. Q. Nguyen, et al. (2002). "Transcriptional activation of human CYP17 in H295R adrenocortical cells depends on complex formation among p54(nrb)/NonO, protein-associated splicing factor, and SF-1, a complex that also participates in repression of transcription." Endocrinology 143(4): 1280-1290.

Shazman, S. and Y. Mandel-Gutfreund (2008). "Classifying RNA-binding proteins based on electrostatic properties." PLoS Comput Biol 4(8): e1000146.

Sibley, C. R., J. Attig, et al. (2012). "The greatest catch: big game fishing for mRNA-bound proteins." Genome Biol 13(7): 163.

Singh, G., A. Kucukural, et al. (2012). "The cellular EJC interactome reveals higher-order mRNP structure and an EJC-SR protein nexus." Cell 151(4): 750-764.

Sun, K. H., S. J. Tang, et al. (2003). "Autoantibodies to dsDNA cross-react with the arginine-glycine-rich domain of heterogeneous nuclear ribonucleoprotein A2 (hnRNP A2) and promote methylation of hnRNP A2." Rheumatology (Oxford) 42(1): 154-161.

Sun, S., Z. Zhang, et al. (2012). "Mechanisms of activation and repression by the alternative splicing factors RBFOX1/2." RNA 18(2): 274-283.

Tamburini, S., A. Ballarini, et al. (2013). "Comparison of quantitative PCR and flow cytometry as cellular viability methods to study bacterial membrane permeabilization following supercritical CO2 treatment." Microbiology 159(Pt 6): 1056-1066.

Tenzer, S., A. Moro, et al. (2013). "Proteome-Wide Characterization of the RNA-Binding Protein RALY-Interactome Using the in Vivo-Biotinylation-Pulldown-Quant (iBioPQ) Approach." J Proteome Res.

Tsofack, S. P., C. Garand, et al. (2011). "NONO and RALY proteins are required for YB-1 oxaliplatin induced resistance in colon adenocarcinoma cell lines." Mol Cancer 10: 145.

Van Dusen, C. M., L. Yee, et al. (2010). "A glycine-rich domain of hnRNP H/F promotes nucleocytoplasmic shuttling and nuclear import through an interaction with transportin 1." Mol Cell Biol 30(10): 2552-2562.

Vassileva, M. T. and M. J. Matunis (2004). "SUMO modification of heterogeneous nuclear ribonucleoproteins." Mol Cell Biol 24(9): 3623-3632.

Vaughan, J. H., J. R. Valbracht, et al. (1995). "Epstein-Barr virus-induced autoimmune responses. I. Immunoglobulin M autoantibodies to proteins mimicking and not mimicking Epstein-Barr virus nuclear antigen-1." J Clin Invest 95(3): 1306-1315.

Vessey, J. P., L. Schoderboeck, et al. (2010). "Mammalian Pumilio 2 regulates dendrite morphogenesis and synaptic function." Proc Natl Acad Sci U S A 107(7): 3222-3227.

Vessey, J. P., A. Vaccani, et al. (2006). "Dendritic localization of the translational repressor Pumilio 2 and its contribution to dendritic stress granules." J Neurosci 26(24): 6496-6508.

Vidalino, L., L. Monti, et al. (2012). "Intracellular trafficking of RNASET2, a novel component of P-bodies." Biol Cell 104(1): 13-21.

White, R., C. Gonsior, et al. (2012). "Heterogeneous nuclear ribonucleoprotein (hnRNP) F is a novel component of oligodendroglial RNA transport granules contributing to regulation of myelin basic protein (MBP) synthesis." J Biol Chem 287(3): 1742-1754.

Xie, W. and R. B. Denman (2011). "Protein methylation and stress granules: posttranslational remodeler or innocent bystander?" Mol Biol Int 2011: 137459.

Yang, X. Y., C. P. Ren, et al. (2005). "Identification of differentially expressed genes in metastatic and non-metastatic nasopharyngeal carcinoma cells by suppression subtractive hybridization." Cell Oncol 27(4): 215-223.

Zhang, Y., J. P. O'Connor, et al. (1995). "The fragile X mental retardation syndrome protein interacts with novel homologs FXR1 and FXR2." EMBO J 14(21): 5358-5366.

7 - APPENDIX

7.1 PUBLICATION

During my PhD project has been the characterization of a new RNA binding protein, called RALY, in mammalian cells. During this project, I focused my investigation on the identification of protein interactors of RALY. I used a technique called iBioPQ (in vivo-Biotinylation-Pulldown-Quant) in collaboration with Dr. Stefan Tenzer. We identified more than 140 new interactors and our data have been shown in an article published on *Journal of Proteome Research*, where I am the shared first author.

Journal of proteome research

Article

pubs.acs.org/jpr

Proteome-Wide Characterization of the RNA-Binding Protein RALY-Interactome Using the in Vivo-Biotinylation-Pulldown-Quant (iBioPQ) Approach

Stefan Tenzer,[#,†] Albertomaria Moro,[#,‡] Jörg Kuharev,[†] Ashwanth Christopher Francis,[§] Laura Vidalino,[‡] Alessandro Provenzani,[¶] and Paolo Macchi*[,‡]

[†]Institute for Immunology, University Medical Center of the Johannes Gutenberg-University Mainz, Langenbeckstrasse 1, 55131 Mainz, Germany

[‡]Laboratory of Molecular and Cellular Neurobiology, CIBIO-Centre for Integrative Biology, University of Trento, via Delle Regole 101, 38060, Mattarello, Trento, Italy

[§]Laboratory of Molecular Virology, CIBIO-Centre for Integrative Biology, University of Trento, Trento, Italy

[¶]Laboratory of Genomic Screening, Centre for Integrative Biology, University of Trento, Trento, Italy

Supporting Information

ABSTRACT: RALY is a member of the heterogeneous nuclear ribonucleoproteins, a family of RNA-binding proteins generally involved in many processes of mRNA metabolism. No quantitative proteomic analysis of RALY-containing ribonucleoparticles (RNPs) has been performed so far, and the biological role of RALY remains elusive. Here, we present a workflow for the characterization of RALY's interaction partners, termed iBioPQ, that involves in vivo biotinylation of biotin acceptor peptide (BAP)-fused protein in the presence of the prokaryotic biotin holoenzyme synthetase of BirA so that it can be purified using streptavidin-coated magnetic beads, circumventing the need for specific antibodies and providing efficient pulldowns. Protein eluates were subjected to tryptic digestion and identified using data-independent acquisition on an ion-mobility enabled high-resolution nanoUPLC-QTOF system. Using label-free quantification, we identified 143 proteins displaying at least 2-fold difference in pulldown compared to controls. Gene Ontology overrepresentation analysis revealed an enrichment of proteins involved in mRNA metabolism and translational control. Among the most abundant interacting proteins, we confirmed RNA-dependent interactions of RALY with MATR3, PABP1 and ELAVL1. Comparative analysis of pulldowns after RNase treatment revealed a protein−protein interaction of RALY with eIF4AIII, FMRP, and hnRNP-C. Our data show that RALY-containing RNPs are much more heterogeneous than previously hypothesized.

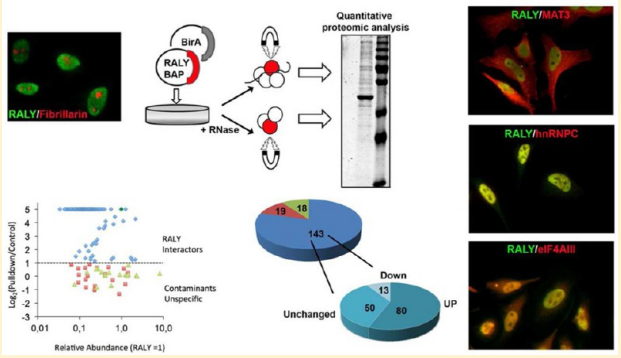

KEYWORDS: *proteomics, biotinylation, protein−protein interactions RALY, heterogeneous nuclear ribonucleoproteins, RNA-binding proteins*

INTRODUCTION

The heterogeneous nuclear ribonucleoproteins (hnRNPs) is a family consisting of more than 20 RNA-binding proteins, which exert several roles in the RNA metabolism, such as splicing, mRNA stability and nuclear export in many different cell types.[1−5] Some hnRNPs are also known to recruit regulatory proteins associated with molecular pathways related to DNA metabolism and DNA damage repair.[6] Although the hnRNPs are the most abundant nuclear proteins, some of them shuttle between the nucleus and the cytoplasm where they can remain associated to the cognate mRNA during its transport, subcellular localization and subsequent translation.[7−11] Generally, hnRNPs are characterized by the presence of one or two RNA-binding motifs (RRMs), whose consensus sequence can vary among the members of the family.[3,12]

RALY, also known as hnRNP C-related protein, is a member of the hnRNP family that was initially identified as an autoantigen cross-reacting with the Epstein−Barr nuclear antigen 1 (EBNA1), a viral protein associated with Epstein−Barr virus.[13] Subsequent studies associated a genomic deletion of Raly with the lethal yellow mutation, being the *Raly* gene locus near to the locus A^y in this mouse.[14,15] In human colon adenocarcinoma cell line, RALY together with NONO/p54nrb[16] have been identified as interactors of YB-1, an

Received: March 4, 2013
Published: April 24, 2013

RNA-binding protein that is involved in splicing, transcription and translational regulation of specific mRNAs.[17] Importantly, YB-1 overexpression in different tumors has been related with the secondary acquired resistance to specific drugs.[18,19] Interestingly, RALY transcript is overexpressed in different cancer tissues, and this correlates with a poor outcome of the disease.[17] Depletion of RALY expression by RNAi sensitizes colorectal cancer cell lines treated with the platinum analogue oxaliplatin without affecting the cell growth rate,[17] indicating a potential role of RALY in tumorigenesis that still requires further investigations and mechanistic analysis. RALY was previously identified in spliceosomal complexes, suggesting its possible involvement in RNA splicing.[20] RALY and other RNA-binding proteins, including members of the hnRNPs such as hnRNPH/F, were also found in the immunoprecipitates for RBFOX1/2.[21] RBFOX1/2 are members of a protein family that regulates alternative splicing in a tissue-specific manner.[22,23] Nevertheless, in contrast to hnRNPH that modulates the splicing activity of RBFOX1/2, RALY has no effects in this process and its misregulation does not impair alternative splicing of RBFOX1/2 mRNA targets.[21] Although there is evidence that RALY might have multiple roles in RNA metabolism, RALY remains poorly characterized in mammals and the list of its potential protein interactors is still elusive. Because of the difficulty to obtain efficient immunoprecipitating antibodies, the molecular composition of RALY-containing ribonucleoprotein (RNP) complexes is still unknown.

In recent years, mass spectrometric analysis has become the method of choice for the identification of protein interaction partners from affinity purified material.[24] Latest developments in mass spectrometry instrumentation facilitate the identification of higher numbers of proteins from limited amounts of sample.[25] However, while this enables the identification of not only core interacting proteins but also weaker interaction partners, increasing numbers of contaminating or nonspecifically binding proteins are being identified. This sometimes obscures the interpretation of identified potential interactors and their biological functions.[26] To reduce the problem of unspecific binding, highly specific affinity purification methods, including tandem affinity purification, have been developed (for excellent reviews, see refs 27 and 28) to isolate target proteins and their associated binding partners. In the past years, several methods have been described for linking quantitative affinity purification methods to mass spectrometric identification (q-AP-MS) based on SILAC[26] or label-free approaches,[29] enabling not only the identification, but also the relative quantification of proteins in pulldowns and controls, to identify unspecifically binding proteins. In vivo biotinylation-based pulldown has been initially developed to identify site-specific protein modifications[30] and the single-step purification of transcription factors.[31] Furthermore, the same approach has been recently applied to elucidate the FoxP3 interactome, identifying 361 FoxP3 interacting proteins,[32] underlining its potential to identify protein interaction partners. However, this technique has not yet been integrated into a label-free quantitative proteomics workflow.

In this study, we applied the iBioPQ approach to identify RALY-associated proteins to learn about the molecular mechanisms underlying the cellular function of RALY. By combining efficient streptavidin-based pulldown of in vivo biotinylated RALY with subsequent ion-mobility enhanced, data-independent-acquisition-based label-free quantitative proteomic analysis of pulldowns, we identified 143 protein components of RALY protein complexes that were either exclusively detected in pulldowns or >2-fold enriched compared to controls. Among these, MATR3, PABP1 and ELAVL1, proteins involved in mRNA metabolism and translational control, were among the most abundant interacting proteins. Moreover, we found that eIF4AIII, FMRP, and hnRNP-C associate with RALY via protein−protein interactions. Our data show that RALY-containing RNPs are much more heterogeneous than previously thought and that RALY might have pleiotropic effects on RNA metabolism and translation.

MATERIALS AND METHODS

Cell Cultures and Expression Constructs

293T and HeLa cells were grown in DMEM supplemented with 10% FCS, at 37 °C and 5% CO_2 atmosphere. Cell lines were transfected using the TransIT transfection reagent (Mirus, Bio LLC) according to the manufacturer's protocol. RT-PCR was performed on total RNA isolated from cells using the TRIzol reagent (Invitrogen). Human RALY cDNA was amplified with the Phusion High-Fidelity DNA polymerase (New England BioLabs) and then cloned in the pEGFP-N1 vector (Clontech). BAP-tagged Raly was created using two complementary primers: 5′-ccgggtggcctgaacgacatcttcgaggctcagaaaatcgaatggcacgaataa and 5′-ggccttattcgtgccattcgattttctgagcctcgaagatgtcgttcaggccaccc. The underlined sequence encodes the BAP peptide (GLNDIFEAQKIEWHE).[30] The primers were annealed and cloned in frame to RALY cDNA in the pEGFP-N1 vector lacking the EGFP-coding sequence. The construct to express RALY lacking the glycine-rich region (RALY-ΔGRR) was created using the site-directed mutagenesis kit (Finnzymes, Thermo Scientific) according to the manufacturer's protocol with the following primers: 5′-gagaacacaacttctgaggcaggc and 5′-ctgctccaagcggctcagcagggc.

Pulldown Assay

The purification of RALY-BAP was performed using streptavidin-conjugated beads (Invitrogen). Briefly, 293T cells grown on 10 cm Petri dishes were transfected with RALY-BAP and Bir(A) constructs. After 30 h the cells were lysed with NEHN lysis buffer [20 mM HEPES pH 7.5, 300 mM NaCl, 0.5% NP-40, 20% glycerol, 1 mM EDTA, phosphatase and protease inhibitors (Roche)] and incubated for 30 min in ice. 40 μL of beads were then added to 1 mg of protein extract and incubated overnight at 4 °C under rotation. The beads were washed five times with NEHN buffer and incubated for 20 min at room temperature in 40 μL of elution buffer [7 M urea, 2 M thiourea, 2% CHAPS, 20 mM Tris-HCl pH 8]. For RNase treatment, cell extracts were treated either with RNase A (100 μg/mL) for 15 min or with DNase (10 U) for 30 min at 37 °C, before the incubation with beads. For Western blot analysis, 10 μL of purified samples were separated by 12% SDS-PAGE and blotted onto nitrocellulose (Schleicher & Schuell) as previously described.[33] The following primary antibodies were used: rabbit polyclonal anti-PABPC, rabbit polyclonal anti-FMRP, rabbit polyclonal anti-eIF4AIII and mouse monoclonal anti-ELAVL1 (all provided by Abcam); rabbit polyclonal anti-hnRNP-C (Millipore); rabbit polyclonal anti-Matrin3 and rabbit polyclonal anti-PRP19 (GeneTex); anti-YB1 (Santa Cruz); mouse monoclonal anti-Mago and mouse monoclonal anti-Histone H1FX (Abnova); rabbit polyclonal anti-RL7a and rabbit polyclonal antibeta Tubulin (Cell Signaling); rabbit polyclonal anti-APP (Sigma). The following secondary antibodies were

dx.doi.org/10.1021/pr400193j | J. Proteome Res. 2013, 12, 2869−2884

used: horse radish peroxidise (HRP)-conjugated goat antimouse and antirabbit antibodies (1:5.000, Santa Cruz Biotechnology). To identify biotinylated RALY-BAP, the membrane was decorated with the rabbit polyclonal anti-RALY antibody (1:5.000; Bethyl). The membrane was then stripped and incubated for 45 min with an HRP-conjugated antistreptavidin (1:10.000; Pierce). All Western blots were analyzed with the ChemiDoc XRS+ System (Bio-Rad).

Immunocytochemistry and Fluorescence Microscopy

Cells grown on coverslips were washed in prewarmed 1xPBS and then fixed in 4% PFA for 15 min at room temperature. Immunocytochemistry was carried out as previously described[33] using the primary antibodies listed above. To detect RALY-biotinylated, cells were incubated with Alexa-488 labeled avidin (Invitrogen) for 1 h. Alexa 594- and Alexa 488-coupled goat antimouse and antirabbit IgG antibodies (Molecular Probes) were used as secondary antibodies. Microscopy analysis was performed using the Zeiss Observer Z.1 microscope implemented with the Zeiss ApoTome device. Pictures were acquired using AxioVision imaging software package (Zeiss) and assembled with Adobe Photoshop CS3. Images were not modified other than adjustments of levels, brightness and magnification.

Protein Digestion

Two biological replicates of pulldown and control samples were prepared and processed for LC−MS analysis in parallel. All samples were then analyzed in triplicate by nanoUPLC. Proteins were digested using a modified FASP method.[34] Briefly, eluted protein was loaded on the filter, and detergents were removed by washing three times with buffer containing 8 M urea. The proteins were then reduced using DTT and alkylated using iodoacetamide. The excess reagent was quenched by addition of DTT and washed through the filters. Buffer was exchanged by washing with 50 mM NH_4HCO_3 and proteins digested overnight by trypsin (Trypsin Gold, Promega) in with an enzyme to protein ratio of 1:50. After overnight digestion, peptides were recovered by centrifugation and two additional washes using 50 mM NH_4HCO_3. Flowthroughs were combined, lyophilized and redissolved in 20 μL 0.1% formic acid by sonication. The resulting tryptic digest solutions were diluted with aqueous 0.1% v/v formic acid to a concentration of 200 ng/μL and spiked with 25 fmol/μL of enolase 1 (*Saccharomyces cerevisiae*) tryptic digest standard (Waters Corporation).

UPLC−MS Configuration

Nanoscale LC separation of tryptic peptides was performed with a nanoAcquity system (Waters Corporation) equipped with a BEH C18 1.7 μm, 75 μm × 150 mm analytical reversed-phase column (Waters Corporation) in direct injection mode as described before.[35] 0.2 μL of sample (40 ng of total protein) was injected per technical replicate. Mobile phase A was water containing 0.1% v/v formic acid, while mobile phase B was ACN containing 0.1% v/v formic acid. Peptides were separated with a gradient of 3−40% mobile phase B over 120 min at a flow rate of 300 nL/minute, followed by a 10-min column rinse with 90% of mobile phase B. The columns were re-equilibrated at initial conditions for 15 min. The analytical column temperature was maintained at 55 °C. The lock mass compound, [Glu^1]-Fibrinopeptide B (100 fmol/μL), was delivered by the auxiliary pump of the LC system at 300 nL/minute to the reference sprayer of the NanoLockSpray source of the mass spectrometer.

Mass spectrometric analysis of tryptic peptides was performed using a Synapt G2-S mass spectrometer (Waters Corporation, Manchester, U.K.). For all measurements, the mass spectrometer was operated in v-mode with a typical resolution of at least 25 000 fwhm (full width half-maximum). All analyses were performed in positive mode ESI. The time-of-flight analyzer of the mass spectrometer was externally calibrated with a NaI mixture from m/z 50 to 1990. The data were postacquisition lock mass corrected using the doubly charged monoisotopic ion of [Glu^1]-Fibrinopeptide B. The reference sprayer was sampled with a frequency of 30 s. Accurate mass LC−MS data were collected in data-independent modes of analysis[36,37] in combination with online ion mobility separations.[38] For ion mobility separation, a wave height of 40 V was applied. Traveling wave velocity was ramped from 800 to 500 m/s over the full IMS cycle. The spectral acquisition time in each mode was 0.7 s with a 0.05-s interscan delay. In low energy MS mode, data were collected at constant collision energy of 4 eV. In elevated energy MS mode, the collision energy was ramped from 25 to 55 eV during each 0.7-s integration. One cycle of low and elevated energy data was acquired every 1.5 s. The radio frequency (RF) amplitude applied to the quadrupole mass analyzer was adjusted such that ions from m/z 350 to 2000 were efficiently transmitted, ensuring that any ions observed in the LC−MS data less than m/z 350 were known to arise from dissociations in the collision cell. All samples were analyzed in triplicate.

Data Processing and Protein Identification

Continuum LC−MS data were processed and searched using ProteinLynx GlobalSERVER version 2.5.2 (Waters Corporation). The resulting peptide and protein identifications were evaluated by the software using statistical models as described.[36] Protein identifications were assigned by searching the human taxon of the UniProtKB/SwissProt database (release 2012_01) supplemented with known possible contaminants and standard proteins (porcine trypsin, yeast enolase, BirA, streptavidin) using the precursor and fragmentation data afforded by the LC−MS acquisition method as reported.[36] The search parameter values for each precursor and associated fragment ions were automatically set by the software using the measured mass error obtained from processing the raw continuum data. Peptide identifications were restricted to tryptic peptides with no more than one missed cleavage. Carbamidomethyl cysteine was set as fixed modification, and oxidized methionine, protein N-acetylation, and deamidation of asparagine and glutamine were searched as variable modifications. Database search was performed allowing a maximal mass deviation of 3 ppm for precursor ions and 10 ppm for fragment ions. For a valid protein identification, the following criteria had to be met: at least 2 peptides were detected with together at least 7 fragments. All reported peptide identifications provided by the IDENTITY^E-algorithm are correct with >95% probability as described.[36] The initial false positive rate for protein identification was set to 3% on the basis of a search of a 5× randomized database, which was generated automatically using PLGS2.5.2 by randomizing the sequence of each entry. By using replication rate of identification as a filter, the false positive rate is further reduced to <0.1%. Additional data processing including retention time alignment, normalization, isoform/homology and replicate filtering, as well as final TOP3-

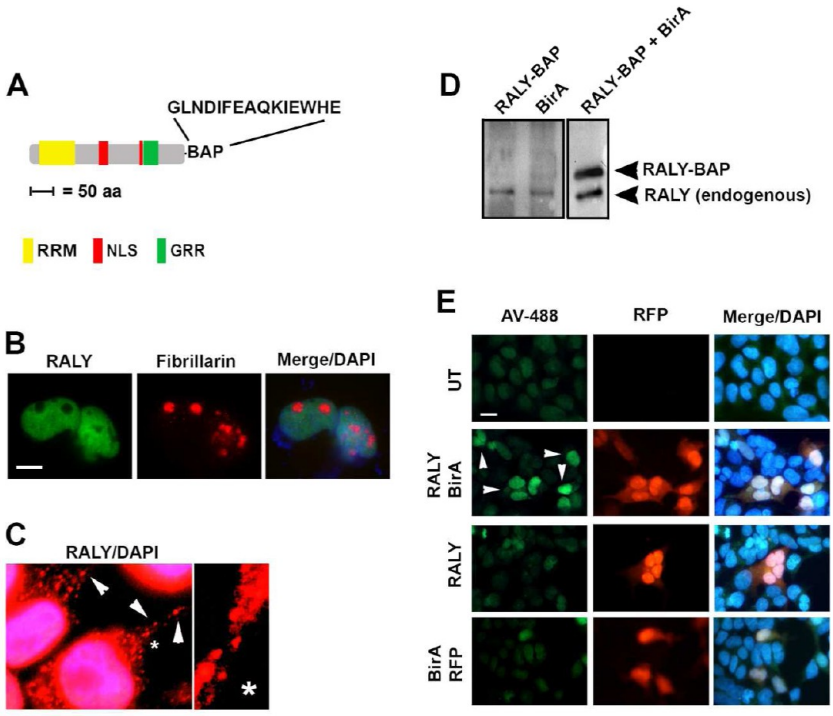

Figure 1. (A) Domain structure of human RALY (accession UniProt: Q9UKM9). Predicted domains are indicated by different colors. The RNA-recognition domain (RRM, amino acids 20−89) and a glycine rich region (GRR, amino acids 227−251) are present at the N- and C-terminal region, respectively. Moreover, two putative NLS (in red, amino acids 145−158 and 218−224, respectively) are predicted. The 15-amino acids sequence of the biotin acceptor peptide (BirA) added to the C-terminal region of RALY is indicated. See also Figure S1A (Supporting Information) for the detailed sequence. (B) Intracellular localization of RALY protein in 293T cells. Dual visualization of endogenous RALY (green) and the nucleolar marker fibrillarin (red). RALY localizes in the nuclei but not in the nucleoli. The nuclei are stained with DAPI. Scale bar = 5 μm. (C) RALY is detected in the cytoplasm. 293T cells were fixed and stained with a polyclonal antibody anti-RALY. Discrete RALY particles, indicated by arrowheads, are distributed throughout the cytoplasm and at the periphery of the cell. Inset: enlarged view of the area indicated by the asterisk. (D) In vivo biotinylation of RALY. Lysates of transfected 293T cells were prepared as described in Materials and Methods, and the Western blot was decorated with an anti-RALY antibody together with an antistreptavidin antibody that recognizes the biotinylated form of RALY. Biotinylation leads to the shift of RALY-BAP that migrates at a higher molecular weight. In contrast, only the endogenous RALY at 37 kDa is detected in 293T cells transfected with only RALY-BAP or BirA alone, indicating that endogenous biotinylation does not occur in the absence of BirA and RALY-BAP coexpression. Biotinylation of RALY can be detected by a HRP-conjugated antistreptavidin. (E) Intracellular localization of biotinylated RALY. Biotinylated RALY shows a remarkably similar localization with endogenous RALY in the nucleus of 293T cells. 293T cells coexpressing RALY-BAP and BirA were fixed and stained with alexa-488 conjugated antistreptavidin (AV-488). Construct expressing the red fluorescence protein (RFP) was used as marker for cotransfection. Biotinylated RALY protein mainly accumulates within the nucleus as the endogenous demonstrating that biotinylation does not change RALY subcellular localization. In contrast, no signal of AV-488 is detected in cells expressing only RALY-BAP or BirA. UT, untransfected cells. Scale bar = 10 μm.

based label-free quantification[39,40] was performed using the ISOQuant software pipeline as described previously.[35]

Bioinformatics and Statistical Analysis

Hierarchal clustering analysis was performed on the basis of absolute label-free protein quantification results provided by ISOQuant using dedicated R scripts in R2.14.0 execution environment.[35] Additional data processing was performed using DAVID (http: david.abcc.ncifcrf.gov).[41,42] Subcellular localizations of RALY interacting proteins were predicted using WoLF-PSORT, TargetP and SubLoc Servers. Transmembrane helices were predicted using Phobius, TMHMM, TMPred and Scampi.[38,43,44] For experiments stating *p*-values, a paired Student's *t* test was performed as described,[35] assuming significance at $p < 0.05$.

RESULTS

Our goal was to isolate RALY-containing RNPs from cellular extracts to decipher their molecular composition. The human RNA-binding protein RALY sequence contains a predicted RNA-recognition motif (RRM) at the N-terminal region (Figure 1A and Figure S1A, Supporting Information). A sequence motif rich in glycine (GRR), whose function is still unclear, is present at the C-terminal region.[45] Moreover, two potential nuclear localization signals (NLS) were predicted by computer analysis, but their activity still remains uninvestigated in vivo. To gain information about the role of RALY in mammals, we determined its distribution within the cell by immunostaining. RALY showed a prominent nuclear accumulation, but it was excluded from the nucleoli as shown after the costaining with the nucleolar marker fibrillarin (Figure 1B). Similar localization pattern was observed in HeLa cells expressing RALY tagged with EGFP (data not shown). In addition, several discrete particles, typical staining for ribonucleoparticle (RNP) complexes, were also detected in the cytoplasm at the cell periphery (Figure 1C). An identical nuclear and cytoplasmic localization was observed in other cell types, including 293T cell lines, OVCAR3 and polarized cells such as oligodendrocytes (data not shown), demonstrating that the pattern observed was not cell-specific. To biotinylate RALY in vivo, 15 amino acids of the biotin acceptor peptide (BirA)

dx.doi.org/10.1021/pr400193j | J. Proteome Res. 2013, 12, 2869−2884

were added to the C-terminal region of RALY full length (Figure 1A). The resulting construct was then coexpressed in 293T cells together with BirA, a bacterial protein−biotin ligase.[46] We then proceeded to determine whether RALY was efficiently biotinylated in vivo. As expected, the antibody detected in untransfected cells a band at 37 kDa corresponding to the endogenously expressed RALY protein (Figure 1D, UT). Another band, shifted at the higher molecular weight, corresponding to biotinylated RALY (RALY-BAP), was detected by Western blot when cells expressed RALY-BAP together with BirA (Figure 1D). In contrast, no shifted band was observed when only RALY-BAP or BirA were expressed (Figure 1D). The localization of the endogenous RALY protein was also compared with the exogenously expressed BAP-tagged RALY. 293T cells coexpressing RALY-BAP together with the red fluorescent protein (RFP) were stained with the alexa 488-conjugated antistreptavidin antibody (AV-488) (Figure 1E). In untreated cells, a diffuse signal of AV-488 was observed (Figure 1E, UT). In contrast, a significant nuclear staining was detected only in those cells expressing RALY-BAP in the presence of BirA (Figure 1E, second row). As expected no nuclear staining was observed in cells expressing each single plasmid (Figure 1E, third and fourth row). All patterns analyzed were remarkably similar, indicating that the biotinylated protein behaves like the endogenous counterpart. Taken together, these data excluded the possibility that the position of the added tag influenced the intracellular localization of the resulting recombinant protein.

Having characterized the localization pattern of the endogenous as well as of the recombinant BAP-tagged RALY, we determined the protein composition of RALY-containing RNP complexes. The schematic outline of the purification procedure used in this study is shown in Figure S1B (Supporting Information). Cell extracts were prepared from 293T cells expressing RALY-BAP together with BirA. 293T cells expressing either RALY-BAP alone or BirA alone served as negative controls. The efficiency of biotinylation was verified by binding tagged RALY in crude cell extracts to streptavidin-coupled paramagnetic Dynabeads. Western blot analysis of the material eluted from the beads showed that tagged RALY protein was enriched in the pulldown (Figure 2A). In contrast, no RALY was detected in the pulldown in the absence of BirA (Figure 2A). The purified extracts were separated using SDS-PAGE and stained (Figure 2B). Silver staining of the gel loaded with purified RALY-BAP showed several bands that were not present in control cell lysates. To distinguish between RNA-dependent or -independent interactions, the cell lysate was incubated with RNase in order to disassemble RNP-complexes,[47] prior to incubation with streptavidin-beads. We observed an enrichment of specific bands after treatment with RNase compared to control treated lysate (Figure 2B). Taken together, these data show that RALY can be efficiently biotinylated and purified as RNP-complexes from cell extracts.

After the isolation of the pull-down samples treated either with or without RNase and control pulldowns from singly (either RALY-BAP, or BirA) transfected cells, eluted proteins were digested with trypsin. Tryptic peptides were separated by nanoUPLC directly coupled to a Synapt G2-S mass spectrometer operated in ion-mobility-enhanced data-independent acquisition mode. Overall, we were able to identify and quantify >220 proteins at <1% FDR (Table S1, Supporting Information). Table 1 shows the list of the 143 proteins that we found to be specifically associated with RALY (see also Figure 3A); of these, 113 were detectable only in pulldowns from

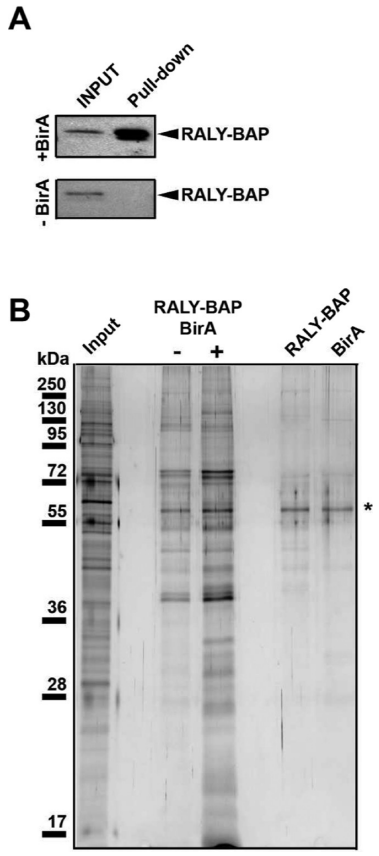

Figure 2. (A) Purification of RALY-tagged protein monitored by Western blot. 293T cells coexpressing RALY-BAP and BirA were washed and treated as described in Materials and Methods. As shown in the upper panel, RALY can be efficiently purified and enriched in the eluate. The Western blot was incubated with the HRP-conjugated antistreptavidin antibody. The lower panel shows that no purified RALY-BAP is detected in the flow through in the absence of BirA expression. Since no biotinylation of recombinant RALY occurs in the absence of BirA, the Western blot was decorated with the anti-RALY antibody. (B) Preparative purification of RALY from 293 T cell extract. The silver-stained 12% SDS-PAGE shows that the protein eluates from 293T cells expressing either RALY-BAP together with BirA, RALY-BAP or BirA. Cell lysate was prepared as described in Materials and Methods and incubated with (+) or without (−) RNase before the purification with streptavidin-coated beads (see also Figure S1B, Supporting Information). Input represents 10% of the loaded whole cells extract used for the pulldown experiments.

double-transfected cells, and another 30 proteins were found to be at least 2-fold more abundant compared to controls. The high proportion of proteins detected only in the pulldown samples confirmed the high specificity of the iBioPQ approach. Additionally, using TOP3-based absolute quantification, we determined the molar ratios of highest abundant interactors (Figure 3C). The most abundant interactors were HNRH1, MATR3 and HNRPF, which were present at approximately equimolar amounts.

Among identified putative RALY-interacting proteins, we confirmed the presence of NONO that has been recently identified as an interactor of YB1-containing complex together with RALY.[17] In addition, some members of the hnRNP family such as hnRNP C1/2, hnRNP F, hnRNP K, hnRNP L, hnRNP M and hnRNP U were also identified. The biological roles of these molecules, which exert a plethora of roles in RNA metabolism, have been covered by several excellent re-

dx.doi.org/10.1021/pr400193j | J. Proteome Res. 2013, 12, 2869−2884

Table 1. Identification of RALY Binding Proteins Identified by iBioPQ[a]

UniProt						
accession	ID	gene name	description	max score	reported peptides	RNase treatment
P62258	1433E	YWHAE	14-3-3 protein epsilon	2128.87	5	
Q9UKV3	ACINU	ACIN1	Apoptotic chromatin condensation inducer in the nucleus	1653.10	11	++
P63261	ACTG	ACTG1	Actin cytoplasmic 2	29066.54	13	
P05141	ADT2	SLC25A5	ADP ATP translocase 2	2064.63	4	
P25705	ATPA	ATP5A1	ATP synthase subunit alpha mitochondrial	1197.64	5	
Q9NYF8	BCLF1	BCLAF1	Bcl 2 associated transcription factor 1	507.21	3	
Q07021	C1QBP	C1QBP	Complement component 1 Q subcomponent binding protein mitochondrial	8074.07	5	++
P10809	CH60	HSPD1	60 kDa heat shock protein mitochondrial	1350.57	5	
Q9Y224	CN166	C14orf166	UPF0568 protein C14orf166	3827.05	4	++
Q92499	DDX1	DDX1	ATP dependent RNA helicase DDX1	5459.53	15	++
Q92841	DDX17	DDX17	Probable ATP dependent RNA helicase DDX17	5711.10	12	
O00571	DDX3X	DDX3X	ATP dependent RNA helicase DDX3X	4329.04	13	++
P17844	DDX5	DDX5	Probable ATP dependent RNA helicase DDX5	6412.09	12	++
Q9BQ39	DDX50	DDX50	ATP dependent RNA helicase DDX50	679.87	5	
Q7L2E3	DHX30	DHX30	Putative ATP dependent RNA helicase DHX30	5046.24	23	++
Q08211	DHX9	DHX9	ATP dependent RNA helicase A	8697.80	30	++
O60832	DKC1	DKC1	H ACA ribonucleoprotein complex subunit 4	2895.81	6	++
P49411	EFTU	TUFM	Elongation factor Tu mitochondrial	2949.42	5	++
Q15717	ELAV1	ELAVL1	ELAV like protein 1	785.05	3	−−
P84090	ERH	ERH	Enhancer of rudimentary homologue	14686.37	3	
Q06787	FMR1	FMR1	Fragile X mental retardation protein 1	4229.49	7	++
P35637	FUS	FUS	RNA binding protein FUS	4455.03	3	++
P51114	FXR1	FXR1	Fragile X mental retardation syndrome related protein 1	2484.20	7	++
P51116	FXR2	FXR2	Fragile X mental retardation syndrome related protein 2	6090.89	12	++
P38646	GRP75	HSPA9	Stress 70 protein mitochondrial	3703.39	10	
Q9BQ67	GRWD1	GRWD1	Glutamate rich WD repeat containing protein 1	915.48	2	++
Q92522	H1X	H1FX	Histone H1x	10130.50	3	++
O60812	HNRCL	HNRNPCL1	Heterogeneous nuclear ribonucleoprotein C like 1	21886.77	12	++
P31943	HNRH1	HNRNPH1	Heterogeneous nuclear ribonucleoprotein H	17205.07	12	
P55795	HNRH2	HNRNPH2	Heterogeneous nuclear ribonucleoprotein H2	6796.38	7	
Q1KMD3	HNRL2	HNRNPUL2	Heterogeneous nuclear ribonucleoprotein U like protein 2	267.02	2	
P07910	HNRPC	HNRNPC	Heterogeneous nuclear ribonucleoproteins C1 C2	35024.63	21	
Q14103	HNRPD	HNRNPD	Heterogeneous nuclear ribonucleoprotein D0	1608.73	3	
P52597	HNRPF	HNRNPF	Heterogeneous nuclear ribonucleoprotein F	10977.72	6	
P61978	HNRPK	HNRNPK	Heterogeneous nuclear ribonucleoprotein K	5036.54	8	
P52272	HNRPM	HNRNPM	Heterogeneous nuclear ribonucleoprotein M	13139.34	28	
O43390	HNRPR	HNRNPR	Heterogeneous nuclear ribonucleoprotein R	1554.47	4	−−
Q00839	HNRPU	HNRNPU	Heterogeneous nuclear ribonucleoprotein U	2608.45	9	−−
P08107	HSP71	HSPA1A	Heat shock 70 kDa protein 1A 1B	9345.12	16	
P11142	HSP7C	HSPA8	Heat shock cognate 71 kDa protein	8124.75	14	
Q9NZI8	IF2B1	IGF2BP1	Insulin like growth factor 2 mRNA binding protein 1	1481.40	4	−−
P38919	IF4A3	EIF4A3	Eukaryotic initiation factor 4A III	5958.01	9	
Q12905	ILF2	ILF2	Interleukin enhancer binding factor 2	1891.69	6	
Q12906	ILF3	ILF3	Interleukin enhancer binding factor 3	984.24	10	
P43243	MATR3	MATR3	Matrin 3	4921.41	11	−−
Q9HCC0	MCCB	MCCC2	Methylcrotonoyl CoA carboxylase beta chain mitochondrial	29783.84	20	−−
P61326	MGN	MAGOH	Protein mago nashi homologue	4326.43	2	
P07197	NFM	NEFM	Neurofilament medium polypeptide	1185.35	4	−−
P55769	NH2L1	NHP2L1	NHP2 like protein 1	4685.52	2	++
Q9NX24	NHP2	NHP2	H ACA ribonucleoprotein complex subunit 2	9793.06	3	++
Q15233	NONO	NONO	Non-POU domain containing octamer binding protein	1258.06	3	
P55209	NP1L1	NAP1L1	Nucleosome assembly protein 1 like 1	2623.78	2	++
P06748	NPM	NPM1	Nucleophosmin	21390.75	9	++
P11940	PABP1	PABPC1	Polyadenylate binding protein 1	3219.85	9	−−
Q13310	PABP4	PABPC4	Polyadenylate binding protein 4	2380.50	7	−−
P05166	PCCB	PCCB	Propionyl CoA carboxylase beta chain mitochondrial	20069.40	19	−−
Q96HS1	PGAM5	PGAM5	Serine threonine protein phosphatase PGAM5 mitochondrial	1921.23	4	
Q9UMS4	PRP19	PRPF19	Pre mRNA processing factor 19	1847.87	6	

dx.doi.org/10.1021/pr400193j | J. Proteome Res. 2013, 12, 2869−2884

Table 1. continued

UniProt						
accession	ID	gene name	description	max score	reported peptides	RNase treatment
Q32P51	RA1L2	HNRNPA1L2	Heterogeneous nuclear ribonucleoprotein A1 like 2	1509.86	2	++
Q9UKM9	RALY	RALY	RNA binding protein Raly	11463.77	14	
Q96PK6	RBM14	RBM14	RNA binding protein 14	604.41	3	
Q14498	RBM39	RBM39	RNA binding protein 39	1360.36	2	
Q9Y5S9	RBM8A	RBM8A	RNA binding protein 8A	6745.83	2	
Q14257	RCN2	RCN2	Reticulocalbin 2	8969.04	7	++
P27635	RL10	RPL10	60S ribosomal protein L10	3048.30	4	++
P62913	RL11	RPL11	60S ribosomal protein L11	21121.41	5	++
P30050	RL12	RPL12	60S ribosomal protein L12	22004.44	5	++
P40429	RL13A	RPL13A	60S ribosomal protein L13a	11425.01	5	++
P50914	RL14	RPL14	60S ribosomal protein L14	14799.98	3	++
P61313	RL15	RPL15	60S ribosomal protein L15	8458.17	4	++
P18621	RL17	RPL17	60S ribosomal protein L17	15467.44	5	++
Q07020	RL18	RPL18	60S ribosomal protein L18	20979.24	5	++
Q02543	RL18A	RPL18A	60S ribosomal protein L18a	5997.83	2	++
P84098	RL19	RPL19	60S ribosomal protein L19	17165.41	3	++
O76021	RL1D1	RSL1D1	Ribosomal L1 domain containing protein 1	2315.82	7	++
P35268	RL22	RPL22	60S ribosomal protein L22	10237.77	2	++
P62829	RL23	RPL23	60S ribosomal protein L23	20098.35	6	++
P62750	RL23A	RPL23A	60S ribosomal protein L23a	12431.37	5	++
P83731	RL24	RPL24	60S ribosomal protein L24	9559.97	4	++
P61353	RL27	RPL27	60S ribosomal protein L27	9041.97	4	++
P46776	RL27A	RPL27A	60S ribosomal protein L27a	13679.50	4	++
P46779	RL28	RPL28	60S ribosomal protein L28	10318.82	5	++
P47914	RL29	RPL29	60S ribosomal protein L29	10583.58	2	++
P39023	RL3	RPL3	60S ribosomal protein L3	4713.76	9	++
P62888	RL30	RPL30	60S ribosomal protein L30	30626.38	6	++
P62899	RL31	RPL31	60S ribosomal protein L31	17685.82	4	++
P62910	RL32	RPL32	60S ribosomal protein L32	22785.35	5	++
P49207	RL34	RPL34	60S ribosomal protein L34	11664.61	4	++
P42766	RL35	RPL35	60S ribosomal protein L35	5370.88	2	++
Q9Y3U8	RL36	RPL36	60S ribosomal protein L36	15226.67	3	++
P83881	RL36A	RPL36A	60S ribosomal protein L36a	5518.44	2	++
P46777	RL5	RPL5	60S ribosomal protein L5	16832.74	12	++
Q02878	RL6	RPL6	60S ribosomal protein L6	13973.62	10	++
P18124	RL7	RPL7	60S ribosomal protein L7	13322.13	9	++
P62424	RL7A	RPL7A	60S ribosomal protein L7a	17385.37	9	++
P62917	RL8	RPL8	60S ribosomal protein L8	9561.39	5	++
P05388	RLA0	RPLP0	60S acidic ribosomal protein P0	47057.78	12	++
P05386	RLA1	RPLP1	60S acidic ribosomal protein P1	71871.37	2	++
Q96E39	RMXL1	RBMXL1	RNA binding motif protein X linked like 1	3873.01	2	
P22626	ROA2	HNRNPA2B1	Heterogeneous nuclear ribonucleoproteins A2 B1	916.63	3	
P51991	ROA3	HNRNPA3	Heterogeneous nuclear ribonucleoprotein A3	1465.80	4	
P62280	RS11	RPS11	40S ribosomal protein S11	4369.03	4	++
P62277	RS13	RPS13	40S ribosomal protein S13	10457.01	3	++
P62249	RS16	RPS16	40S ribosomal protein S16	4115.29	2	++
P62269	RS18	RPS18	40S ribosomal protein S18	11165.43	5	++
P39019	RS19	RPS19	40S ribosomal protein S19	17796.30	6	++
P15880	RS2	RPS2	40S ribosomal protein S2	6647.55	5	++
P62266	RS23	RPS23	40S ribosomal protein S23	7508.04	3	++
P62847	RS24	RPS24	40S ribosomal protein S24	23479.49	2	++
P62851	RS25	RPS25	40S ribosomal protein S25	7363.56	3	++
P62854	RS26	RPS26	40S ribosomal protein S26	20581.14	3	++
P23396	RS3	RPS3	40S ribosomal protein S3	6653.01	7	++
P61247	RS3A	RPS3A	40S ribosomal protein S3a	20345.70	13	++
P62753	RS6	RPS6	40S ribosomal protein S6	13377.20	5	++
P46781	RS9	RPS9	40S ribosomal protein S9	7676.78	6	
P08865	RSSA	RPSA	40S ribosomal protein SA	2139.39	2	++
P82650	RT22	MRPS22	28S ribosomal protein S22 mitochondrial	7739.10	8	++

dx.doi.org/10.1021/pr400193j | J. Proteome Res. 2013, 12, 2869−2884

Table 1. continued

UniProt						
accession	ID	gene name	description	max score	reported peptides	RNase treatment
Q92552	RT27	MRPS27	28S ribosomal protein S27 mitochondrial	7870.53	8	++
Q9Y3I0	RTCB	C22orf28	tRNA splicing ligase RtcB homologue	4433.22	9	++
O00422	SAP18	SAP18	Histone deacetylase complex subunit SAP18	4780.17	2	++
Q12874	SF3A3	SF3A3	Splicing factor 3A subunit 3	517.52	2	−−
Q13435	SF3B2	SF3B2	Splicing factor 3B subunit 2	634.29	3	
Q15393	SF3B3	SF3B3	Splicing factor 3B subunit 3	1355.61	8	−−
P23246	SFPQ	SFPQ	Splicing factor proline and glutamine rich	1780.61	4	++
Q9UQ35	SRRM2	SRRM2	Serine arginine repetitive matrix protein 2	342.98	8	
O75494	SRS10	SRSF10	Serine arginine rich splicing factor 10	4308.84	3	
Q07955	SRSF1	SRSF1	Serine arginine rich splicing factor 1	6424.17	5	
Q01130	SRSF2	SRSF2	Serine arginine rich splicing factor 2	1564.12	3	
P84103	SRSF3	SRSF3	Serine arginine rich splicing factor 3	21695.02	5	
Q13247	SRSF6	SRSF6	Serine arginine rich splicing factor 6	2556.39	4	
Q16629	SRSF7	SRSF7	Serine arginine rich splicing factor 7	19836.63	6	
Q13242	SRSF9	SRSF9	Serine arginine rich splicing factor 9	2428.25	3	
Q04837	SSBP	SSBP1	Single stranded DNA binding protein mitochondrial	21125.56	5	
P68363	TBA1B	TUBA1B	Tubulin alpha 1B chain	8048.62	7	++
P07437	TBB5	TUBB	Tubulin beta chain	5734.63	8	++
Q9Y2W1	TR150	THRAP3	Thyroid hormone receptor associated protein 3	985.35	6	
Q13595	TRA2A	TRA2A	Transformer 2 protein homologue alpha	1780.67	4	
P62995	TRA2B	TRA2B	Transformer 2 protein homologue beta	12611.33	6	++
P26368	U2AF2	U2AF2	Splicing factor U2AF 65 kDa subunit	3166.23	6	++
Q15029	U5S1	EFTUD2	116 kDa U5 small nuclear ribonucleoprotein component	554.99	7	
P08670	VIME	VIM	Vimentin	27065.79	30	
P67809	YBOX1	YBX1	Nuclease sensitive element binding protein 1	3634.61	2	−−
Q5BKZ1	ZN326	ZNF326	DBIRD complex subunit ZNF326	1592.55	3	

[a]Proteins listed were either detected specifically in pulldowns from doubly transfected cells or showed at least 2.8-fold enrichment compared to controls. The effect of RNAse treatment on the relative amount of each protein is indicated; (++)/(−−) indicates >2-fold effects. The Max Score refers to the maximum identification score provided by PLGS (ProteinLynx Global Server) across all technical and biological replicates for the respective protein.

views.[3,48−50] Moreover, several ribosomal proteins were also enriched in RALY-purified protein complex (Figure 3A). To gain insight into the various functions of the identified proteins, we performed gene ontology (GO) term analysis using DAVID. Statistically significant over represented ontologies of RALY-interacting proteins were grouped into 26 categories, mostly involved in RNA metabolism, including mRNA, rRNA and ncRNA processing, RNA stability, transport and translational control (Figure 4). Some categories comprised factors involved in ribosomal assembly, rRNA stability and posttranscriptional regulation. We then analyzed any changes in the molecular composition of RALY-containing complex upon treatment with RNase. Altogether, we observed significantly increased association of 80 proteins with RALY after RNase treatment (Table 1, Figure 3C). Among these proteins, we found factors involved in noncoding RNA (ncRNA) and rRNA processes, ribosome biogenesis, translation and translation elongation (Table 1 and Figure 4, green bars). In contrast, only 13 proteins mainly involved in RNA stability and splicing were decreased after the same treatment, suggesting that RALY might act as a bridge to link other protein complexes bound to the same mRNA. (Table 1 and Figure 4, red bars). Finally, 50 proteins remained unchanged (i.e., observed change was less than 2-fold), suggesting that their interactions with RALY were not affected by the presence (or absence) of intact RNA (Table 1 and Figure 4, yellow bars).

Next, we confirmed specific interaction of selected identified candidate proteins with RALY by Western blot analysis: Matrin3 (MAT3),[51] PABP1, eIF4AIII,[52−54] the human homologue of Drosophila mago nashi protein (Magoh),[55] the Y-box binding protein 1 (YB-1),[56] PRP19,[57,58] ELAVL1,[59,60] the ribosomal protein L7a, the histone H1 and the fragile X mental retardation protein (FMRP).[61−63] Western blot analysis confirmed the interactions of RALY with PABP, ELAVL1 and MAT3. As predicted, the interactions were mediated by an intact RNA (Figure 5A). Low but detectable amounts of Magoh protein and PRP19 were also detected in RALY pulldown, and their associations remained unchanged after treatment with RNase. In contrast, the disassembly of the RNPs complexes by RNase increases the association of RALY with FMRP, eIF4AIII and hnRNP C, respectively (Figure 5A). To our surprise, we did not observe any pulldown of YB-1 with RALY as recently described by another group.[17] Moreover, neither histone H1 nor RL7a were detected in RALY pulldown. To demonstrate the specificity of the observed interactions, two proteins not identified by mass spectrometry, namely the amyloid beta precursor protein (APP) and beta tubulin, were used as negative controls. In this case, no copurification of beta tubulin and APP proteins with RALY were observed (Figure 5B). Some proteins associated with RALY identified by iBioPQ, for example, the histone H1, hnRNP C and PRP19, are known to interact either directly or indirectly also with the DNA. To determine whether DNA could mediate the interactions of RALY with these molecules, cell lysates were treated with DNaseI before purification (Figure 5C). As Figure 5C shows,

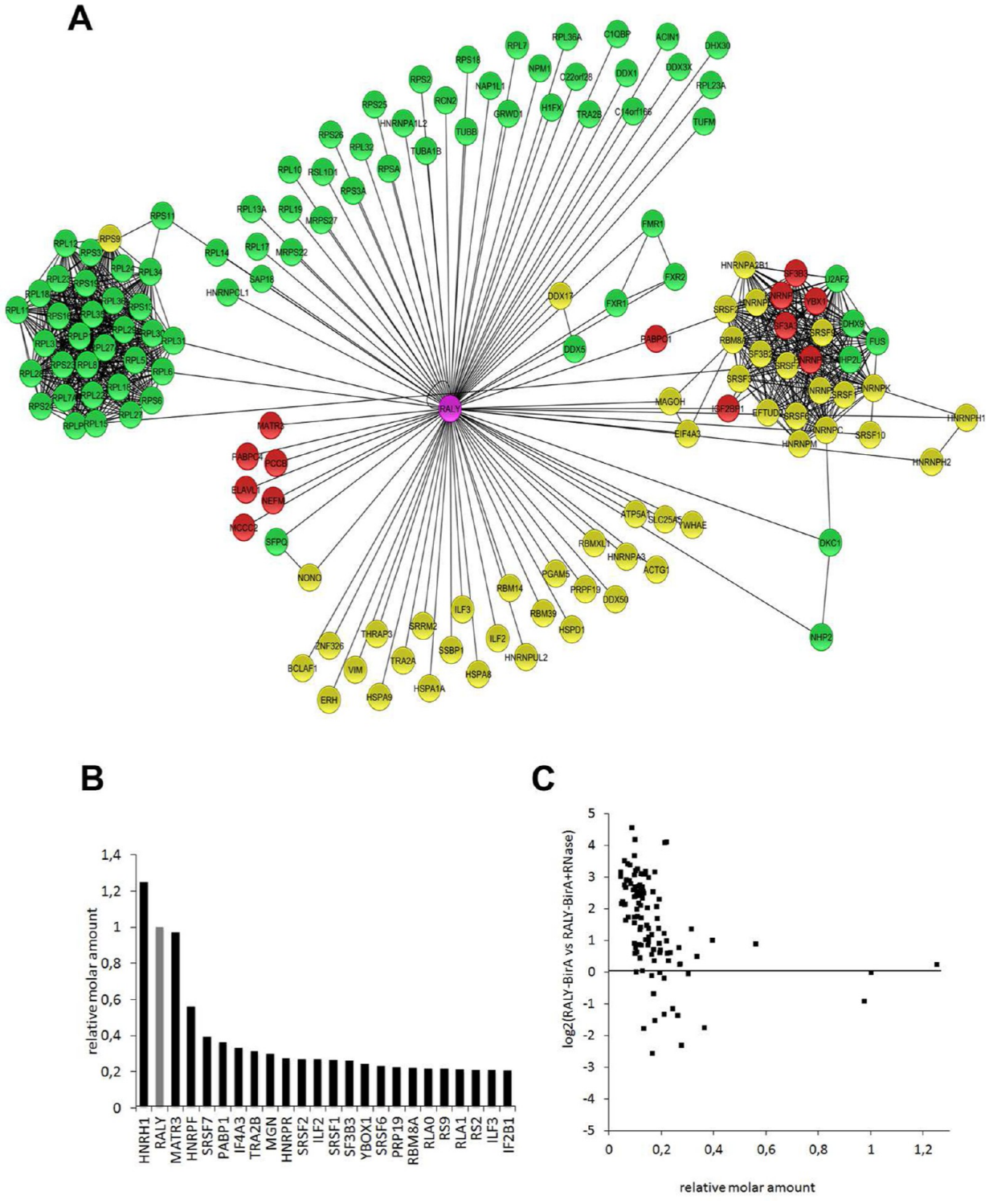

Figure 3. (A) Schematic network of RALY-interacting proteins identified by iBioPQ using Cytoscape program. Proteins that decrease or increase in RALY pull-down after RNase treatment are indicated in red and green colors, respectively. Black lines represent the interactions between RALY and its associated partners. RALY was linked with only a few proteins belonging to the major group of interactors. Proteins that remain unchanged after RNase treatment are depicted in yellow. The relationships among the different proteins were determined by using the String program (http://string-db.org/) with high confidence (score 0.7). (B) Relative molar amounts (normalized to RALY) of highest abundance interacting proteins as quantified using the TOP3 approach. (C) Quantitative analysis of the effects of RNase treatment on interacting proteins. The logarithmic change in relative amounts induced by RNase treatment was plotted vs the relative molar amount of the respective protein.

the treatment did not affect their association with RALY, demonstrating that the interaction does not require DNA.

Having verified the interaction of RALY with selected partners identified by mass spectrometry, we determined whether our findings were consistent with their subcellular localization in 293T cells. We have established that RALY is mainly nuclear with a discrete cytoplasmic distribution. As expected, RALY showed an almost identical distribution pattern

dx.doi.org/10.1021/pr400193j | J. Proteome Res. 2013, 12, 2869−2884

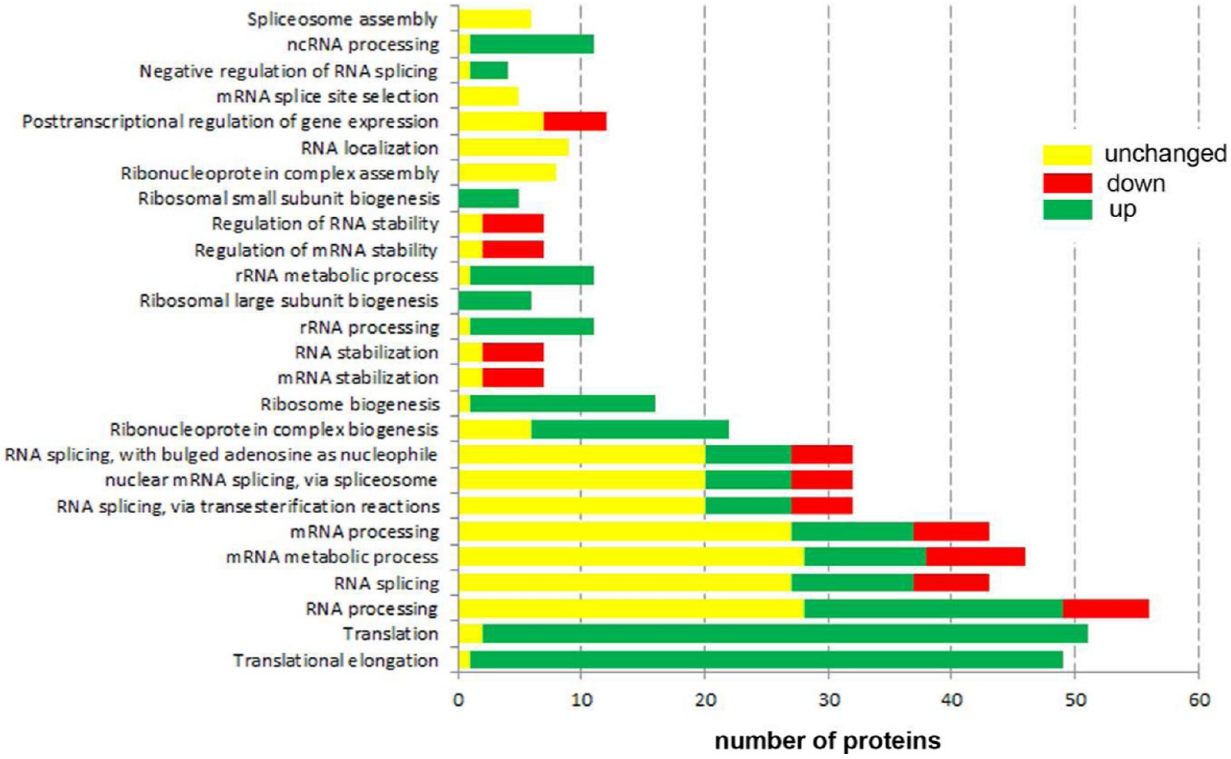

Figure 4. Functional annotation of RALY-associated proteins identified using analysis of GO term enrichment of the "biological process" category by DAVID. GO terms ranked according to the number of counts are plotted. All associations are significant ($p < 0.01$ after Bonferroni correction). Each bar represents the number of RALY's interactors involved in 26 different biological processes. The amount of proteins that decrease, increase, or remain unchanged (i.e., display less than 2-fold change) in RALY pull-down after RNase treatment is depicted as in Figure 3A.

with hnRNP-C and ELAVL1 in the nuclear compartment (Figure 6A). The elongation initiation factor eIF4AIII is part of the exon-junction-complex (EJC),[64] but also component of the nonsense-mediated mRNA decay (NMD) machinery, was also identified in RALY pulldown upon treatment with RNase. As previously described, eIF4AIII was detected in the nucleoplasm and in the nuclear speckles, subnuclear domains containing pre-mRNA processing factors and noncoding RNAs that are involved in multiple steps of gene expression, including transcription, pre-mRNA processing and mRNA transport.[53,65,66] Although RALY is not particularly enriched in the nuclear speckles, a colocalization with eIF4AIII was observed in the nucleoplasm (Figure 6A). PRP19 belongs to a complex that has a well-established and conserved function in mRNA splicing.[67] As for eIF4AIII, PRP19 localized to nucleoplasm and to dot-like structures that resemble nuclear speckles. RALY colocalization within the cell nucleus is similarly observed, although its signal is more diffuse throughout the nucleoplasm (Figure 6A). We also observed colocalization of RALY with MATR3. MATR3 was found both in the cytoplasm and in the nucleus as part of the nuclear matrix, excluding the nucleoli (Figure 6A). PABP showed a predominant cytoplasmic localization, and the immunostaining analysis did not reveal a significant colocalization with RALY in the nuclear compartment. However, subset of PABP particles showed colocalization with RALY in the cytoplasm at higher exposure (Figure 6B). Since PABP resides in the nuclear compartment, we cannot exclude that RALY might transiently interact with PABP also in this compartment. Taken together, these results show that RALY is in the same complex with the above-mentioned proteins, in vitro as well as in vivo.

In contrast to RALY, most hnRNPs contain repeats of Arg-Gly-Gly tripeptides domain and/or additional glycine-rich or proline-rich domains that seem to promote protein−protein interactions.[3,68] We asked whether the peculiar glycine-rich domain (GRR) that RALY harbors at the C-terminal region was required for the interactions with the newly identified interactors (Figures S1A and S2B, Supporting Information). Thus, we performed pull down using extracts from cells that expressed RALY-BAP lacking the GRR (RALY-ΔGRR). We first determined the subcellular localization of RALY-ΔGRR by tagging the deleted protein with EGFP. The deleted form was not degraded when exogenously expressed by the cells. As for the full length, RALY lacking the glycine rich region localized in the nucleus but not in the nucleoli (Figure 6C). Moreover, RALY-ΔGRR still retained its RNA-binding activity (data not shown). These results demonstrate that the GRR domain is not necessary to target RALY to the nuclear compartment. To determine whether the GRR domain could modulate protein−protein interactions, 293T cells were transfected with the plasmid expressing BAP-tagged RALY-ΔGRR with or without BirA. Cell lysates were then treated with RNase or untreated, and the purified extracts were analyzed by Western blot (Figure 6D). The majority of the RNA-mediated interactions were unaffected by the absence of the GRR domain. Proteins such as PABP as well as MATR3 were copurified, and their interactions with RALY were still sensitive to RNase treatment, demonstrating that the lack of the GRR domain did not affect both RNA-dependent and independent interaction of RALY with newly identified interactors (Figure 6D, + RNase). We then tested for the presence of ELAVL1. Interestingly, ELAVL1 was not copurified with RALY-ΔGRR, suggesting that the GRR

dx.doi.org/10.1021/pr400193j | J. Proteome Res. 2013, 12, 2869−2884

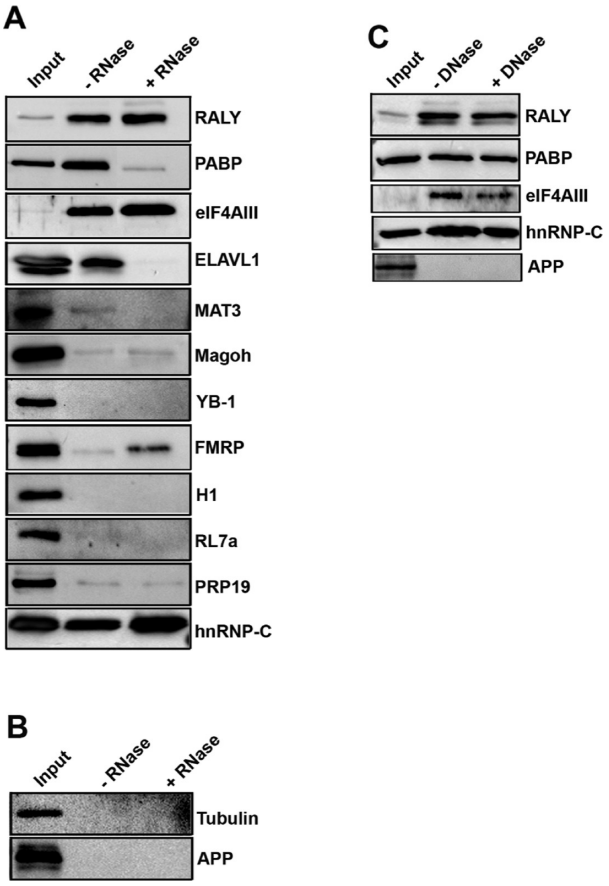

Figure 5. Pulldown of selected proteins with RALY. (A) Human 293T cells were transfected with plasmids expressing RALY-BAP and BirA. The purified eluates were analyzed by immunoblotting with the indicated antibodies. First lane: loaded whole cell extract (Input). Second lane represents the pulldown performed in the absence of RNase (-RNase). The third lane shows the pulldown performed in the presence of ribonucleases A (+RNase). Treatment with RNase enhanced the association of proteins such as eIF4AIIII, Magoh, hnRNP-CFMRP with RALY suggesting for protein−protein-based interactions. Interestingly, RALY can interact with itself in the absence of RNA. In contrast, RNA is required for the interaction of RALY with PABP, ELAVL1 and MAT3. No interaction is observed with RL7a and YB-1. (B) Western blot showing a control pulldown. Pull down of RALY does not involve either tubulin or APP. (C) Cell lysate was treated with DNase before purification, and the precipitated complexes were blotted with the indicate antibodies. In contrast to RNA, DNA does not mediate the interaction of RALY with the indicated proteins. APP was used as a negative control.

domain is required for the interaction with ELAVL1 even in the presence of RNA (Figure 6D).

■ DISCUSSION

The current work describes the identification of novel protein interactors of the RNA-binding protein RALY by an in vivo-biotinylation pulldown-quantitative approach. The RNA-binding protein RALY, previously known as hnRNP C like-protein, contains a RNA-recognition motif similar to hnRNP C and two predicted NLS (Figure S2A, Supporting Information). Human RALY shares 87% identity with the mouse homologue, and the major differences are located within the C-terminal region (Figure S2A, Supporting Information). Moreover, RALY shares 43% amino acid identity with hnRNP C, and in contrast to hnRNP C and to other hnRNPs, RALY contains a peculiar domain composed by a long stretch of glycine repeats (GRR) (Figure S2B, Supporting Information). The functional role of the GRR domain is unclear. Shorter glycine-rich repeats present in hnRNP A2 and hnRNP H/F seem to mediate their general intracellular trafficking.[69,70] When expressed in mammalian cell lines, however, the intracellular localization of GFP-tagged RALY-ΔGRR was unchanged, and the protein still accumulated within the nucleus but not in the nucleoli. Although the subcellular localization as well as the RNA-binding activity of RALY was not altered by the absence of the GRR domain, the dynamics might be impaired. Could the GRR domain mediate protein−protein interactions? Pulldowns performed using RALY-ΔGRR assessed that the glycine-rich repeats is not required for the protein−protein interactions of RALY with some of the newly identified interactors (Figure 6D). However, the RNA-dependent interaction of ELAVL1 with RALY-ΔGRR was abolished, suggesting that the GRR domain might promote the recruitment of ELAVL1 and RALY to the RNA.

RALY has been found in complexes with molecules involved in RNA metabolism, but its biological role in the mammalian cells has not been thoroughly evaluated. In human, both *RALY* mRNA and protein are detected in several tissues,[71] including the nervous system, kidney, liver, skeletal muscle, lung and pancreas. Interestingly, *RALY* mRNA is upregulated in many tumor tissues, even if associated functional implications are currently unknown.[17,72] Although the modulation of RALY expression has been observed in different tumors, the role of RALY in tumorigenesis is a matter of ongoing investigation. While few interaction partners of RALY have been already described, a complete picture of the RALY interactome is lacking as no quantitative proteomic analysis of RALY RNP-complexes have been published so far. We isolated RALY complexes from cell cultures in order to identify possible molecular pathways in which RALY could be involved and gain information regarding its functions. Unfortunately, any attempt to immunoprecipitate RALY using various antibodies was unsuccessful or not efficient (data not shown). One explanation might rely on the observation that RALY, as many other RNA-binding proteins, is a constituent of large RNP-complexes, making it poorly accessible to the antibodies thereby hampering their immunoprecipitation under native conditions. To overcome this limitation, we expressed BAP-tagged RALY to purify RALY-containing complexes. Cotransfection with BirA leads to in vivo biotinylation of RALY, facilitating highly specific interaction of the in vivo biotinylated RALY with streptavidin-coated beads. A similar approach has been previously used to isolate mRNAs associated with the RNA-binding protein PABP.[73] Using cells transfected with untagged proteins and cells without BirA ligase, negative controls are readily available, rendering our method inexpensive, sensitive, and reliable. The strong interaction between biotin and streptavidin as well as the specificity of Bir(A) enzyme have several benefits: it increases the amount of purified protein, and in the same time, it decreases the number of unspecific interactors. Moreover, this approach minimizes the dissociation of weak interactions and thus maximizes the sensitivity of the approach and the yield of transient molecular interactors. These aspects are essential to reduce unspecifically bound proteins that would be falsely classified as potentially interacting proteins during subsequent mass spectrometric analysis. However, a major problem of mass spectrometric identification of potential interaction partners, even when using a high affinity pulldown and sensitive instrumentation, remains to distinguish interactors from

dx.doi.org/10.1021/pr400193j | J. Proteome Res. 2013, 12, 2869−2884

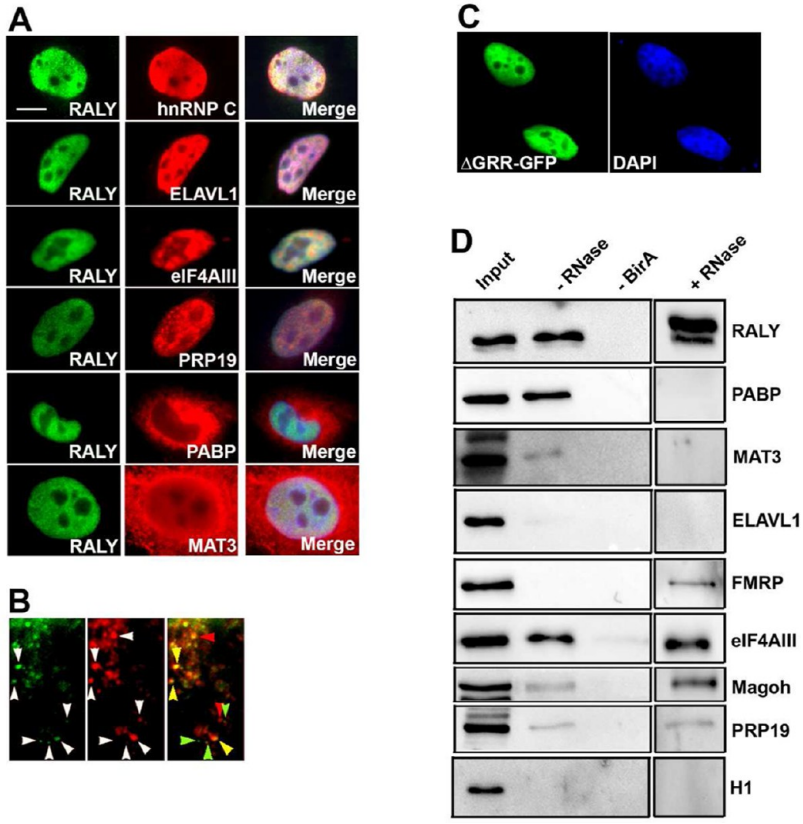

Figure 6. (A) Immunofluorescence microscopy of 293T cells showing colocalization of RALY (green) with the indicated proteins (in red). Scale bar = 5 μm. (B) High magnification image showing colocalization of RALY (green) and PABP (red) in the cytoplasm. Cells were fixed and stained as described in Materials and Methods. Particles colocalizing are indicated by yellow arrowheads. (C) Subcellular localization of deleted RALY in HeLa cells. EGFP-tagged RALY lacking the GRR domain still localizes in the nucleus except nucleoli. Scale bar = 5 μm. (D) GRR domain is not required for protein−protein interactions. Human 293T cells were transfected with plasmids expressing BAP-tagged RALY-ΔGRR with BirA. Control purification of 293T cells expressing BAP-tagged RALY-ΔGRR without BirA was done in parallel as a negative control. The purified eluates were separated on a 12% SDS-PAGE gel and analyzed by immunoblotting with the indicated antibodies.

proteins that bind unspecifically to the pulldown material. In the iBioPQ approach, parallel processing of pulldown and controls and subsequent label-free quantification by LC−MS^E allows to pinpoint potential interactors on the basis of their relative protein abundance ratio between pulldown and control samples, therefore increasing the specificity of interaction partner identification.

For mass spectrometric identification of interacting proteins, we applied an ion-mobility enhanced data-independent acquisition approach,[36−38] which was previously used to quantify the composition of the myelin proteome.[44] In contrast to data-dependent acquisition (DDA), data-independent acquisition provides high technical reproducibility due to avoiding the stochastic nature of the peptide selection process. For example, in one previous study applying DDA, only 35−60% overlap of identified peptides was observed between technical replicates.[74] In contrast, we observed >90% overlap between both technical and biological replicates on protein level (see Figure S3, Supporting Information), thereby underlining the reproducibility of our approach. Additionally, no proteins were uniquely detected in control samples, which confirms the low unspecific background of our approach. Requiring candidates to be identified in both analyzed biological replicates provided additional stringency of the workflow.

Taken together, the iBioPQ approach allowed us to identify and quantify 143 novel molecular interactors of RALY. Among these, the protein NONO has been recently identified as an interactor of YB-1 containing complex together with RALY.[17] Several hnRNPs were copurified with RALY, and among these were the hnRNP A1, C1/C2 and K. Although these factors play different roles in the metabolism, they can also interact with proteins involved in DNA damage response pathways.[75,76] It will be interesting to determine whether RALY might change its intracellular localization upon DNA damage, supporting the emerging concept that RNA-binding proteins can be recruited to DNA damage sites and repair process with mechanisms that are still poorly investigated. Treatments with RNase allowed us to categorize RALY interactors into RNA-mediated interaction partners and direct (protein−protein) interactions. Interestingly, 80 identified interactors became enriched in RALY-containing complexes after RNase treatment. These results allow us to speculate cellular RNA to be a strong competitor for RALY, probably because of the high affinity of RALY for RNA. Thus, the interaction of RALY with additional proteins can be enhanced and/or stabilized upon depletion of RNA. Another hypothesis is that the lack of associated RNA changes the folding structure of RALY. These conformational changes might expose hidden domains of RALY allowing for additional interactions with other proteins. Many of the identified proteins are RNA-binding proteins (RBPs) known to be involved in

dx.doi.org/10.1021/pr400193j | J. Proteome Res. 2013, 12, 2869−2884

several processes of the RNA metabolism including rRNA and ncRNA metabolism, and RNP biogenesis. Most rewardingly, however, is the fact that a significant portion of the identified interactors is implicated in mRNA translational control. Our data suggest that RALY might have different functions in mRNA metabolism that need further investigations. Among the proteins identified in this study, eIF4AIII and FMRP showed a direct protein−protein interaction with RALY. The translation initiation factor eIF4AIII, Mago and Y14 are core components of the exon-junction-complex, a dynamic multiprotein complex that plays an essential role in nonsense mediated decay (NMD). The role of FMRP has been thoroughly investigated, especially in the nervous system. The loss of FMRP causes the Fragile X syndrome, the most common form of inherited intellectual disability.[77] In neurons, FMRP is a negative regulator of target mRNA translation important for neuronal development and synaptic function.[78−80] FMRP is mainly found in the cytoplasm, but it shuttles into the nucleus where it binds to its cargo mRNAs.[81] In neurons, both eIF4AIII and FMRP localize to dendrites in RNP complexes containing the double stranded RNA-binding protein Staufen and localized transcripts.[82] Interestingly, eIF4AIII interacts with another member of the NMD machinery, MLN51/Barentsz (Btz), that is also a component of the dendritic mRNP.[83] For this reason, it would be interesting to determine whether RALY is also a component of the molecular machinery involved in mRNA subcellular localization in polarized cells such as neurons. Preliminary results confirm that RALY is present both in the cytoplasm and in distal processes of the oligodendroglial progenitor cell line Oli-neu[84,85] (data not shown). It is tempting to speculate that RALY might remain associated with mRNAs during their transport and subsequent localization. It will be interesting to determine whether RALY can exert any role in local translational and/or RNA stability. Our data provide evidence that RALY interacts with proteins that exert pleiotropic roles in mRNA metabolism.

■ ASSOCIATED CONTENT

Supporting Information

Figure S1. (A) ClustalW alignment of human RALY (Q9UKM9.1), *P. troglodytes* (XP_514591.2), *M. musculus* (Q64012.3), *R. norvegicus* (NP_001011958.1) and *D. rerio* (AAQ97838.1). Identical residues and conservative amino acid changes are marked by asterisks and dots, respectively. The domains schematically represented in Figure 1A are indicated by lines below the sequences: RNA-binding domain (yellow), NLS (red), and GRR (green). (B) Schematic representation of the procedure used to purify and characterize RALY interactors. Cells were transfected with two constructs expressing RALY tagged with the biotin acceptor peptide (BAP) and BirA, respectively. Additional cells were transfected with either RALY-BAP (Ctrl 1) or BirA (Ctrl 2) alone as controls. After 36 h, cells were washed and processed as described in Materials and Methods. Part of the lysate was directly incubated with streptavidin-coated magnetic beads, and the purified proteins were identified by mass spectrometry analysis. To identify proteins interacting with RALY in a RNA-independent way, the remaining of the lysate was treated with either RNase (or DNase in some cases) before purification. Figure S2. (A) Western blot showing the specificity of the purification. 293T cells were transfected with the construct expressing RALY-BAP. The cell lysates were then incubated with streptavidin-coated magnetic beads. After several washing steps, the eluates were run on SDS-PAGE. Western blots were decorated with specific antibodies as indicated. No unspecific bond of the identified proteins is observed. The same results were obtained when 293T cells expressed only BirA in the absence of RALY-BAP. (B) ClustalW alignment of human RALY and human hnRNP C (NP_112604.2). Compared to RALY, hnRNP C protein does not contain the glycine rich region. Figure S3. Venn diagrams depicting (A) overlap between technical replicates, (B) overlap between biological replicates, and (C) overlap between pulldown and control samples. Venn Diagrams were constructed using the VENNY web application. (http://bioinfogp.cnb.csic.es/tools/venny/index.html). Table S1. Complete listing of proteins identified in pulldowns and control samples. This material is available free of charge via the Internet at http://pubs.acs.org.

■ AUTHOR INFORMATION

Corresponding Author

*Phone: +39 0461 283819. Fax: +39 0461 283937. E-mail: macchi@science.unitn.it.

Author Contributions

#S. Tenzer and A. Moro contributed equally to this work.

Notes

The authors declare no competing financial interest.

■ ACKNOWLEDGMENTS

The plasmid to express Bir(A) was kindly provided by Dr. Oscar Burrone (ICGEB-International Centre for Genetic Engineering and Biotechnology, Trieste, Italy). We are grateful to Antonio Casini for technical advice. We thank Dr. Anna Cereseto for her comments on the manuscript and helpful discussion. This work was supported by the Forschungszentrum Immunologie (FZI) and the Naturwissenschaftlich-Medizinisches Forschungszentrum (NMFZ) of the Johannes-Gutenberg University Mainz (to S.T.), the University of Trento (Progetto Biotecnologie), CARITRO (Cassa di Risparmio di Trento e Rovereto) Foundation Grant (all to P.M.) and by the European Community's Seventh Framework Programme [FP7-2007-2013] under Grant Agreement No. HEALTH-F2-2011-256986 (to A.P. and P.M.).

■ REFERENCES

(1) Krecic, A. M.; Swanson, M. S. hnRNP complexes: composition, structure, and function. *Curr. Opin. Cell Biol.* **1999**, *11* (3), 363−71.

(2) Carpenter, B.; MacKay, C.; Alnabulsi, A.; MacKay, M.; Telfer, C.; Melvin, W. T.; Murray, G. I. The roles of heterogeneous nuclear ribonucleoproteins in tumour development and progression. *Biochim. Biophys. Acta* **2006**, *1765* (2), 85−100.

(3) Han, S. P.; Tang, Y. H.; Smith, R. Functional diversity of the hnRNPs: past, present and perspectives. *Biochem. J.* **2010**, *430* (3), 379−92.

(4) Ostareck-Lederer, A.; Ostareck, D. H. Control of mRNA translation and stability in haematopoietic cells: the function of hnRNPs K and E1/E2. *Biol. Cell* **2004**, *96* (6), 407−11.

(5) Weighardt, F.; Biamonti, G.; Riva, S. The roles of heterogeneous nuclear ribonucleoproteins (hnRNP) in RNA metabolism. *Bioessays* **1996**, *18* (9), 747−56.

(6) He, Y.; Smith, R. Nuclear functions of heterogeneous nuclear ribonucleoproteins A/B. *Cell. Mol. Life Sci.* **2009**, *66* (7), 1239−56.

(7) Bailey-Serres, J.; Sorenson, R.; Juntawong, P. Getting the message across: cytoplasmic ribonucleoprotein complexes. *Trends Plant Sci.* **2009**, *14* (8), 443−53.

(8) Kiebler, M. A.; Bassell, G. J. Neuronal RNA granules: movers and makers. *Neuron* **2006**, *51* (6), 685−90.
(9) Percipalle, P.; Raju, C. S.; Fukuda, N. Actin-associated hnRNP proteins as transacting factors in the control of mRNA transport and localization. *RNA Biol.* **2009**, *6* (2), 171−4.
(10) Giorgi, C.; Moore, M. J. The nuclear nurture and cytoplasmic nature of localized mRNPs. *Semin. Cell Dev. Biol.* **2007**, *18* (2), 186−93.
(11) Hirokawa, N. mRNA transport in dendrites: RNA granules, motors, and tracks. *J. Neurosci.* **2006**, *26* (27), 7139−42.
(12) Valverde, R.; Edwards, L.; Regan, L. Structure and function of KH domains. *FEBS J.* **2008**, *275* (11), 2712−26.
(13) Rhodes, G. H.; Valbracht, J. R.; Nguyen, M. D.; Vaughan, J. H. The p542 gene encodes an autoantigen that cross-reacts with EBNA-1 of the Epstein Barr virus and which may be a heterogeneous nuclear ribonucleoprotein. *J. Autoimmun.* **1997**, *10* (5), 447−54.
(14) Michaud, E. J.; Bultman, S. J.; Stubbs, L. J.; Woychik, R. P. The embryonic lethality of homozygous lethal yellow mice (Ay/Ay) is associated with the disruption of a novel RNA-binding protein. *Genes Dev.* **1993**, *7* (7A), 1203−13.
(15) Duhl, D. M.; Stevens, M. E.; Vrieling, H.; Saxon, P. J.; Miller, M. W.; Epstein, C. J.; Barsh, G. S. Pleiotropic effects of the mouse lethal yellow (Ay) mutation explained by deletion of a maternally expressed gene and the simultaneous production of agouti fusion RNAs. *Development* **1994**, *120* (6), 1695−708.
(16) Shav-Tal, Y.; Zipori, D. PSF and p54(nrb)/NonO—multi-functional nuclear proteins. *FEBS Lett.* **2002**, *531* (2), 109−14.
(17) Tsofack, S. P.; Garand, C.; Sereduk, C.; Chow, D.; Aziz, M.; Guay, D.; Yin, H. H.; Lebel, M. NONO and RALY proteins are required for YB-1 oxaliplatin induced resistance in colon adenocarcinoma cell lines. *Mol. Cancer* **2011**, *10*, 145.
(18) Schittek, B.; Psenner, K.; Sauer, B.; Meier, F.; Iftner, T.; Garbe, C. The increased expression of Y box-binding protein 1 in melanoma stimulates proliferation and tumor invasion, antagonizes apoptosis and enhances chemoresistance. *Int. J. Cancer* **2007**, *120* (10), 2110−8.
(19) Ohga, T.; Uchiumi, T.; Makino, Y.; Koike, K.; Wada, M.; Kuwano, M.; Kohno, K. Direct involvement of the Y-box binding protein YB-1 in genotoxic stress-induced activation of the human multidrug resistance 1 gene. *J. Biol. Chem.* **1998**, *273* (11), 5997−6000.
(20) Jurica, M. S.; Licklider, L. J.; Gygi, S. R.; Grigorieff, N.; Moore, M. J. Purification and characterization of native spliceosomes suitable for three-dimensional structural analysis. *RNA* **2002**, *8* (4), 426−39.
(21) Sun, S.; Zhang, Z.; Fregoso, O.; Krainer, A. R. Mechanisms of activation and repression by the alternative splicing factors RBFOX1/2. *RNA* **2012**, *18* (2), 274−83.
(22) Jin, Y.; Suzuki, H.; Maegawa, S.; Endo, H.; Sugano, S.; Hashimoto, K.; Yasuda, K.; Inoue, K. A vertebrate RNA-binding protein Fox-1 regulates tissue-specific splicing via the pentanucleotide GCAUG. *EMBO J.* **2003**, *22* (4), 905−12.
(23) Underwood, J. G.; Boutz, P. L.; Dougherty, J. D.; Stoilov, P.; Black, D. L. Homologues of the *Caenorhabditis elegans* Fox-1 protein are neuronal splicing regulators in mammals. *Mol. Cell. Biol.* **2005**, *25* (22), 10005−16.
(24) Pardo, M.; Lang, B.; Yu, L.; Prosser, H.; Bradley, A.; Babu, M. M.; Choudhary, J. An expanded Oct4 interaction network: implications for stem cell biology, development, and disease. *Cell Stem Cell* **2010**, *6* (4), 382−95.
(25) Kelstrup, C. D.; Young, C.; Lavallee, R.; Nielsen, M. L.; Olsen, J. V. Optimized fast and sensitive acquisition methods for shotgun proteomics on a quadrupole Orbitrap mass spectrometer. *J. Proteome Res.* **2012**, *11* (6), 3487−97.
(26) Paul, F. E.; Hosp, F.; Selbach, M. Analyzing protein−protein interactions by quantitative mass spectrometry. *Methods* **2011**, *54* (4), 387−95.
(27) Pardo, M.; Choudhary, J. S. Assignment of protein interactions from affinity purification/mass spectrometry data. *J. Proteome Res.* **2012**, *11* (3), 1462−74.
(28) Volkel, P.; Le Faou, P.; Angrand, P. O. Interaction proteomics: characterization of protein complexes using tandem affinity purification−mass spectrometry. *Biochem. Soc. Trans.* **2010**, *38* (4), 883−7.
(29) Tate, S.; Larsen, B.; Bonner, R.; Gingras, A. C. Label-free quantitative proteomics trends for protein−protein interactions. *J. Proteomics* **2013**, *81*, 91−101.
(30) Tirat, A.; Freuler, F.; Stettler, T.; Mayr, L. M.; Leder, L. Evaluation of two novel tag-based labelling technologies for site-specific modification of proteins. *Int. J. Biol. Macromol.* **2006**, *39* (1−3), 66−76.
(31) de Boer, E.; Rodriguez, P.; Bonte, E.; Krijgsveld, J.; Katsantoni, E.; Heck, A.; Grosveld, F.; Strouboulis, J. Efficient biotinylation and single-step purification of tagged transcription factors in mammalian cells and transgenic mice. *Proc. Natl. Acad. Sci. U. S. A.* **2003**, *100* (13), 7480−5.
(32) Rudra, D.; deRoos, P.; Chaudhry, A.; Niec, R. E.; Arvey, A.; Samstein, R. M.; Leslie, C.; Shaffer, S. A.; Goodlett, D. R.; Rudensky, A. Y. Transcription factor Foxp3 and its protein partners form a complex regulatory network. *Nat. Immunol.* **2012**, *13* (10), 1010−9.
(33) Vidalino, L.; Monti, L.; Haase, A.; Moro, A.; Acquati, F.; Taramelli, R.; Macchi, P. Intracellular trafficking of RNASET2, a novel component of P-bodies. *Biol. Cell* **2012**, *104* (1), 13−21.
(34) Wisniewski, J. R.; Zougman, A.; Nagaraj, N.; Mann, M. Universal sample preparation method for proteome analysis. *Nat. Methods* **2009**, *6* (5), 359−62.
(35) Tenzer, S.; Docter, D.; Rosfa, S.; Wlodarski, A.; Kuharev, J.; Rekik, A.; Knauer, S. K.; Bantz, C.; Nawroth, T.; Bier, C.; Sirirattanapan, J.; Mann, W.; Treuel, L.; Zellner, R.; Maskos, M.; Schild, H.; Stauber, R. H. Nanoparticle size is a critical physicochemical determinant of the human blood plasma corona: a comprehensive quantitative proteomic analysis. *ACS Nano* **2011**, *5* (9), 7155−67.
(36) Geromanos, S. J.; Vissers, J. P.; Silva, J. C.; Dorschel, C. A.; Li, G. Z.; Gorenstein, M. V.; Bateman, R. H.; Langridge, J. I. The detection, correlation, and comparison of peptide precursor and product ions from data independent LC−MS with data dependant LC−MS/MS. *Proteomics* **2009**, *9* (6), 1683−95.
(37) Silva, J. C.; Denny, R.; Dorschel, C. A.; Gorenstein, M.; Kass, I. J.; Li, G. Z.; McKenna, T.; Nold, M. J.; Richardson, K.; Young, P.; Geromanos, S. Quantitative proteomic analysis by accurate mass retention time pairs. *Anal. Chem.* **2005**, *77* (7), 2187−200.
(38) Giles, K.; Pringle, S. D.; Worthington, K. R.; Little, D.; Wildgoose, J. L.; Bateman, R. H. Applications of a travelling wave-based radio-frequency-only stacked ring ion guide. *Rapid Commun. Mass Spectrom.* **2004**, *18* (20), 2401−14.
(39) Silva, J. C.; Denny, R.; Dorschel, C.; Gorenstein, M. V.; Li, G. Z.; Richardson, K.; Wall, D.; Geromanos, S. J. Simultaneous qualitative and quantitative analysis of the *Escherichia coli* proteome: a sweet tale. *Mol. Cell. Proteomics* **2006**, *5* (4), 589−607.
(40) Silva, J. C.; Gorenstein, M. V.; Li, G. Z.; Vissers, J. P.; Geromanos, S. J. Absolute quantification of proteins by LCMSE: a virtue of parallel MS acquisition. *Mol. Cell. Proteomics* **2006**, *5* (1), 144−56.
(41) Huang da, W.; Sherman, B. T.; Tan, Q.; Collins, J. R.; Alvord, W. G.; Roayaei, J.; Stephens, R.; Baseler, M. W.; Lane, H. C.; Lempicki, R. A. The DAVID Gene Functional Classification Tool: a novel biological module-centric algorithm to functionally analyze large gene lists. *Genome Biol.* **2007**, *8* (9), R183.
(42) Huang da, W.; Sherman, B. T.; Tan, Q.; Kir, J.; Liu, D.; Bryant, D.; Guo, Y.; Stephens, R.; Baseler, M. W.; Lane, H. C.; Lempicki, R. A. DAVID Bioinformatics Resources: expanded annotation database and novel algorithms to better extract biology from large gene lists. *Nucleic Acids Res.* **2007**, *35* (Web Server issue), W169−75.
(43) Bradshaw, R. A.; Burlingame, A. L.; Carr, S.; Aebersold, R. Reporting protein identification data: the next generation of guidelines. *Mol. Cell. Proteomics* **2006**, *5* (5), 787−8.
(44) Patzig, J.; Jahn, O.; Tenzer, S.; Wichert, S. P.; de Monasterio-Schrader, P.; Rosfa, S.; Kuharev, J.; Yan, K.; Bormuth, I.; Bremer, J.; Aguzzi, A.; Orfaniotou, F.; Hesse, D.; Schwab, M. H.; Mobius, W.; Nave, K. A.; Werner, H. B. Quantitative and integrative proteome

analysis of peripheral nerve myelin identifies novel myelin proteins and candidate neuropathy loci. *J. Neurosci.* **2011**, *31* (45), 16369−86.
(45) Pesiridis, G. S.; Lee, V. M.; Trojanowski, J. Q. Mutations in TDP-43 link glycine-rich domain functions to amyotrophic lateral sclerosis. *Hum. Mol. Genet.* **2009**, *18* (R2), R156−62.
(46) Howard, P. K.; Shaw, J.; Otsuka, A. J. Nucleotide sequence of the birA gene encoding the biotin operon repressor and biotin holoenzyme synthetase functions of *Escherichia coli*. *Gene* **1985**, *35* (3), 321−31.
(47) Mallardo, M.; Deitinghoff, A.; Muller, J.; Goetze, B.; Macchi, P.; Peters, C.; Kiebler, M. A. Isolation and characterization of Staufen-containing ribonucleoprotein particles from rat brain. *Proc. Natl. Acad. Sci. U. S. A.* **2003**, *100* (4), 2100−5.
(48) Chen, M.; Zhang, J.; Manley, J. L. Turning on a fuel switch of cancer: hnRNP proteins regulate alternative splicing of pyruvate kinase mRNA. *Cancer Res.* **2010**, *70* (22), 8977−80.
(49) Busch, A.; Hertel, K. J. Evolution of SR protein and hnRNP splicing regulatory factors. *Wiley Interdiscip. Rev.: RNA* **2012**, *3* (1), 1−12.
(50) Chaudhury, A.; Chander, P.; Howe, P. H. Heterogeneous nuclear ribonucleoproteins (hnRNPs) in cellular processes: Focus on hnRNP E1's multifunctional regulatory roles. *RNA* **2010**, *16* (8), 1449−62.
(51) Salton, M.; Elkon, R.; Borodina, T.; Davydov, A.; Yaspo, M. L.; Halperin, E.; Shiloh, Y. Matrin 3 binds and stabilizes mRNA. *PLoS One* **2011**, *6* (8), e23882.
(52) Alexandrov, A.; Colognori, D.; Steitz, J. A. Human eIF4AIII interacts with an eIF4G-like partner, NOM1, revealing an evolutionarily conserved function outside the exon junction complex. *Genes Dev.* **2011**, *25* (10), 1078−90.
(53) Palacios, I. M.; Gatfield, D., St; Johnston, D.; Izaurralde, E. An eIF4AIII-containing complex required for mRNA localization and nonsense-mediated mRNA decay. *Nature* **2004**, *427* (6976), 753−7.
(54) Shibuya, T.; Tange, T. O.; Sonenberg, N.; Moore, M. J. eIF4AIII binds spliced mRNA in the exon junction complex and is essential for nonsense-mediated decay. *Nat. Struct. Mol. Biol* **2004**, *11* (4), 346−51.
(55) Kataoka, N.; Diem, M. D.; Kim, V. N.; Yong, J.; Dreyfuss, G. Magoh, a human homolog of Drosophila mago nashi protein, is a component of the splicing-dependent exon-exon junction complex. *EMBO J.* **2001**, *20* (22), 6424−33.
(56) Kohno, K.; Izumi, H.; Uchiumi, T.; Ashizuka, M.; Kuwano, M. The pleiotropic functions of the Y-box-binding protein, YB-1. *Bioessays* **2003**, *25* (7), 691−8.
(57) Chanarat, S.; Seizl, M.; Strasser, K. The Prp19 complex is a novel transcription elongation factor required for TREX occupancy at transcribed genes. *Genes Dev.* **2011**, *25* (11), 1147−58.
(58) Sihn, C. R.; Cho, S. Y.; Lee, J. H.; Lee, T. R.; Kim, S. H. Mouse homologue of yeast Prp19 interacts with mouse SUG1, the regulatory subunit of 26S proteasome. *Biochem. Biophys. Res. Commun.* **2007**, *356* (1), 175−80.
(59) Chi, M. N.; Auriol, J.; Jegou, B.; Kontoyiannis, D. L.; Turner, J. M.; de Rooij, D. G.; Morello, D. The RNA-binding protein ELAVL1/HuR is essential for mouse spermatogenesis, acting both at meiotic and postmeiotic stages. *Mol. Biol. Cell* **2011**, *22* (16), 2875−85.
(60) Latorre, E.; Tebaldi, T.; Viero, G.; Sparta, A. M.; Quattrone, A.; Provenzani, A. Downregulation of HuR as a new mechanism of doxorubicin resistance in breast cancer cells. *Mol. Cancer* **2012**, *11*, 13.
(61) Till, S. M. The developmental roles of FMRP. *Biochem. Soc. Trans.* **2010**, *38* (2), 507−10.
(62) Zalfa, F.; Bagni, C. Another view of the role of FMRP in translational regulation. *Cell. Mol. Life Sci.* **2005**, *62* (2), 251−2.
(63) Feng, Y.; Absher, D.; Eberhart, D. E.; Brown, V.; Malter, H. E.; Warren, S. T. FMRP associates with polyribosomes as an mRNP, and the I304N mutation of severe fragile X syndrome abolishes this association. *Mol. Cell* **1997**, *1* (1), 109−18.
(64) Sauliere, J.; Murigneux, V.; Wang, Z.; Marquenet, E.; Barbosa, I.; Le Tonqueze, O.; Audic, Y.; Paillard, L.; Roest Crollius, H.; Le Hir, H. CLIP-seq of eIF4AIII reveals transcriptome-wide mapping of the human exon junction complex. *Nat. Struct. Mol. Biol.* **2012**, *19* (11), 1124−31.
(65) Chan, C. C.; Dostie, J.; Diem, M. D.; Feng, W.; Mann, M.; Rappsilber, J.; Dreyfuss, G. eIF4A3 is a novel component of the exon junction complex. *RNA* **2004**, *10* (2), 200−9.
(66) Ferraiuolo, M. A.; Lee, C. S.; Ler, L. W.; Hsu, J. L.; Costa-Mattioli, M.; Luo, M. J.; Reed, R.; Sonenberg, N. A nuclear translation-like factor eIF4AIII is recruited to the mRNA during splicing and functions in nonsense-mediated decay. *Proc. Natl. Acad. Sci. U. S. A.* **2004**, *101* (12), 4118−23.
(67) Wahl, M. C.; Will, C. L.; Luhrmann, R. The spliceosome: design principles of a dynamic RNP machine. *Cell* **2009**, *136* (4), 701−18.
(68) Dreyfuss, G.; Matunis, M. J.; Pinol-Roma, S.; Burd, C. G. hnRNP proteins and the biogenesis of mRNA. *Annu. Rev. Biochem.* **1993**, *62*, 289−321.
(69) Sun, K. H.; Tang, S. J.; Wang, Y. S.; Lin, W. J.; You, R. I. Autoantibodies to dsDNA cross-react with the arginine-glycine-rich domain of heterogeneous nuclear ribonucleoprotein A2 (hnRNP A2) and promote methylation of hnRNP A2. *Rheumatology (Oxford, U. K.)* **2003**, *42* (1), 154−61.
(70) Van Dusen, C. M.; Yee, L.; McNally, L. M.; McNally, M. T. A glycine-rich domain of hnRNP H/F promotes nucleocytoplasmic shuttling and nuclear import through an interaction with transportin 1. *Mol. Cell. Biol.* **2010**, *30* (10), 2552−62.
(71) Khrebtukova, I.; Kuklin, A.; Woychik, R. P.; Michaud, E. J. Alternative processing of the human and mouse raly genes(1). *Biochim. Biophys. Acta* **1999**, *1447* (1), 107−12.
(72) Yang, X. Y.; Ren, C. P.; Wang, L.; Li, H.; Jiang, C. J.; Zhang, H. B.; Zhao, M.; Yao, K. T. Identification of differentially expressed genes in metastatic and non-metastatic nasopharyngeal carcinoma cells by suppression subtractive hybridization. *Cell Oncol.* **2005**, *27* (4), 215−23.
(73) Penalva, L. O.; Keene, J. D. Biotinylated tags for recovery and characterization of ribonucleoprotein complexes. *Biotechniques* **2004**, *37*, (4), 604, 606, 608−10.
(74) Tabb, D. L.; Vega-Montoto, L.; Rudnick, P. A.; Variyath, A. M.; Ham, A. J.; Bunk, D. M.; Kilpatrick, L. E.; Billheimer, D. D.; Blackman, R. K.; Cardasis, H. L.; Carr, S. A.; Clauser, K. R.; Jaffe, J. D.; Kowalski, K. A.; Neubert, T. A.; Regnier, F. E.; Schilling, B.; Tegeler, T. J.; Wang, M.; Wang, P.; Whiteaker, J. R.; Zimmerman, L. J.; Fisher, S. J.; Gibson, B. W.; Kinsinger, C. R.; Mesri, M.; Rodriguez, H.; Stein, S. E.; Tempst, P.; Paulovich, A. G.; Liebler, D. C.; Spiegelman, C. Repeatability and reproducibility in proteomic identifications by liquid chromatography-tandem mass spectrometry. *J. Proteome Res.* **2010**, *9* (2), 761−76.
(75) Lee, S. W.; Lee, M. H.; Park, J. H.; Kang, S. H.; Yoo, H. M.; Ka, S. H.; Oh, Y. M.; Jeon, Y. J.; Chung, C. H. SUMOylation of hnRNP-K is required for p53-mediated cell-cycle arrest in response to DNA damage. *EMBO J.* **2012**, *31* (23), 4441−52.
(76) Haley, B.; Paunesku, T.; Protic, M.; Woloschak, G. E. Response of heterogeneous ribonuclear proteins (hnRNP) to ionising radiation and their involvement in DNA damage repair. *Int. J. Radiat. Biol.* **2009**, *85* (8), 643−55.
(77) De Rubeis, S.; Fernandez, E.; Buzzi, A.; Di Marino, D.; Bagni, C. Molecular and cellular aspects of mental retardation in the Fragile X syndrome: from gene mutation/s to spine dysmorphogenesis. *Adv. Exp. Med. Biol.* **2012**, *970*, 517−51.
(78) Liu-Yesucevitz, L.; Bassell, G. J.; Gitler, A. D.; Hart, A. C.; Klann, E.; Richter, J. D.; Warren, S. T.; Wolozin, B. Local RNA translation at the synapse and in disease. *J. Neurosci.* **2011**, *31* (45), 16086−93.
(79) Dahm, R.; Macchi, P. Human pathologies associated with defective RNA transport and localization in the nervous system. *Biol. Cell* **2007**, *99* (11), 649−61.
(80) Zalfa, F.; Giorgi, M.; Primerano, B.; Moro, A.; Di Penta, A.; Reis, S.; Oostra, B.; Bagni, C. The fragile X syndrome protein FMRP associates with BC1 RNA and regulates the translation of specific mRNAs at synapses. *Cell* **2003**, *112* (3), 317−27.

(81) Kim, M.; Bellini, M.; Ceman, S. Fragile X mental retardation protein FMRP binds mRNAs in the nucleus. *Mol. Cell. Biol.* **2009**, *29* (1), 214−28.
(82) Giorgi, C.; Yeo, G. W.; Stone, M. E.; Katz, D. B.; Burge, C.; Turrigiano, G.; Moore, M. J. The EJC factor eIF4AIII modulates synaptic strength and neuronal protein expression. *Cell* **2007**, *130* (1), 179−91.
(83) Macchi, P.; Kroening, S.; Palacios, I. M.; Baldassa, S.; Grunewald, B.; Ambrosino, C.; Goetze, B.; Lupas, A., St; Johnston, D.; Kiebler, M. Barentsz, a new component of the Staufen-containing ribonucleoprotein particles in mammalian cells, interacts with Staufen in an RNA-dependent manner. *J. Neurosci.* **2003**, *23* (13), 5778−88.
(84) Jung, M.; Kramer, E.; Grzenkowski, M.; Tang, K.; Blakemore, W.; Aguzzi, A.; Khazaie, K.; Chlichlia, K.; von Blankenfeld, G.; Kettenmann, H.; et al. Lines of murine oligodendroglial precursor cells immortalized by an activated neu tyrosine kinase show distinct degrees of interaction with axons in vitro and in vivo. *Eur. J. Neurosci.* **1995**, *7* (6), 1245−65.
(85) White, R.; Gonsior, C.; Kramer-Albers, E. M.; Stohr, N.; Huttelmaier, S.; Trotter, J. Activation of oligodendroglial Fyn kinase enhances translation of mRNAs transported in hnRNP A2-dependent RNA granules. *J. Cell Biol.* **2008**, *181* (4), 579−86.

7.3 MICROARRAY RESULTS

Down regulated genes												
ProbeName	GeneSymbol	FC (abs)	ProbeName	GeneSymbol	FC (abs)	ProbeName	GeneSymbol	FC (abs)	ProbeName	GeneSymbol	FC (abs)
A_23_P109235	RALY	17,26	A_23_P7732	CETN3	2,51	A_23_P319859	EYA2	2,13	A_33_P3250671	TCF7	1,96
A_23_P92730	HSPB3	10,04	A_23_P429977	KCNQ1	2,51	A_24_P114438	OLA1	2,12	A_33_P3319491	AZIN1	1,96
A_24_P262127	RRAD	8,10	A_33_P3248903	WNT7B	2,50	A_33_P3221343	HECTD2	2,12	A_23_P403588	USP47	1,96
A_23_P47924	PTPRR	6,12	A_23_P65518	DACT1	2,49	A_24_P639505	STX6	2,11	A_23_P210581	KCNG1	1,96
A_33_P3303649	MB	5,48	A_24_P938614	CDS1	2,48	A_23_P28466	WDR69	2,10	A_32_P134209	ACVR2B	1,96
A_32_P141238	ANO2	4,60	A_23_P128215	SOCS2	2,48	A_33_P3362296	KCNG1	2,10	A_33_P3280805	LMO7	1,96
A_23_P118392	RASD1	4,28	A_33_P3237260	C11orf53	2,45	A_24_P165423	RBP7	2,10	A_33_P3397905	BET1	1,95
A_24_P175059	ATG5	4,08	A_23_P501538	HOXA3	2,43	A_33_P3251073	TMEM52	2,10	A_23_P135257	PRSS3	1,95
A_33_P3511265	POSTN	3,96	A_33_P3839897	RNU4ATAC	2,43	A_23_P333498	EEPD1	2,10	A_33_P3286151	LOC100132891	1,95
A_33_P3240078		3,63	A_33_P3623118	LOC153577	2,43	A_33_P3301095		2,09	A_23_P398854	DOK7	1,95
A_33_P3232692	IL24	3,61	A_23_P310274	PRSS2	2,42	A_33_P3343616	PHF12	2,09	A_24_P515319	FAM90A7	1,95
A_33_P3290780	IL24	3,59	A_23_P17130	C2orf88	2,41	A_24_P346431	TNS3	2,09	A_33_P3382331	HSPA6	1,95
A_23_P104188	ELF3	3,57	A_24_P403303	PHF20L1	2,40	A_24_P332857	CT47A11	2,08	A_24_P289299	ARHGEF25	1,94
A_23_P372834	AQP1	3,56	A_23_P87964	ESD	2,38	A_33_P3285565	CLDN3	2,08	A_33_P3312039	RAD23B	1,94
A_23_P432947	GREM1	3,39	A_33_P3375002	LOC144481	2,34	A_23_P166297	ABCG1	2,07	A_23_P250102	CAND2	1,94
A_23_P53390	PTPRB	3,25	A_33_P3260722	UVRAG	2,34	A_33_P3332970	CLEC2B	2,07	A_23_P300056	CDC42	1,94
A_23_P33759	DHRS3	3,21	A_23_P27133	KRT15	2,33	A_23_P429998	FOSB	2,05	A_33_P3241204	CALHM3	1,94
A_33_P3293446	KIAA1462	3,20	A_23_P49816	ADAP2	2,33	A_23_P259090	NUDT12	2,05	A_23_P161686	ARHGAP32	1,94
A_33_P3327519	SNORA74A	3,10	A_24_P90900	CTRL	2,30	A_23_P207345	ADAM11	2,05	A_23_P74112	IL28RA	1,93
A_23_P365738	ARC	3,10	A_23_P82503	PEG10	2,30	A_23_P119916	WNT6	2,05	A_33_P3306973		1,93
A_24_P236091	ENO2	3,09	A_33_P3214105	ATF3	2,30	A_23_P26511	GDPD3	2,04	A_23_P40096	PROC	1,93
A_33_P3846653	KRT19P2	3,08	A_24_P225616	RRM2	2,30	A_23_P171296	MPP1	2,03	A_33_P3367917	SSH2	1,93
A_23_P66798	KRT19	3,01	A_33_P3274319	TMEM52	2,29	A_23_P98844	ARHGEF25	2,02	A_33_P3379967	HLA-F	1,92
A_24_P392110	PSG8	2,97	A_24_P52697	H19	2,27	A_23_P149121	DIRAS3	2,02	A_23_P5163	ATP13A1	1,92
A_33_P3220919	ADRBK2	2,95	A_23_P69738	RASL11B	2,26	A_23_P94736	ST6GALNAC4	2,01	A_33_P3419460	VAPA	1,92
A_23_P431305	FAM69B	2,92	A_23_P16944	SDC1	2,24	A_23_P91221	PKIG	2,00	A_23_P62081	SCG5	1,92
A_33_P3403576	FCGR2A	2,92	A_24_P205045	ERC2	2,24	A_23_P60599	UGT1A6	2,00	A_23_P214079	SPINK1	1,92
A_23_P160159	SLC2A5	2,87	A_23_P70448	HIST1H1A	2,24	A_23_P215461	LIMK1	2,00	A_23_P301521	KIAA1462	1,92
A_33_P3287348	CHN2	2,85	A_23_P100022	SV2B	2,23	A_33_P3302075	UGT1A8	2,00	A_33_P3280801	LMO7	1,92
A_23_P151506	PLEK2	2,80	A_24_P33895	ATF3	2,22	A_23_P105923	DIO3	1,99	A_23_P28953	DNMT3B	1,91
A_23_P114903	HSPA6	2,79	A_33_P3331831	DKFZp451A211	2,22	A_23_P255104	LHFPL2	1,99	A_24_P10137	C13orf15	1,91
A_33_P3378514	PDE5A	2,76	A_23_P373927	ERP44	2,22	A_33_P3329974	CGN	1,99	A_23_P395426	DIDO1	1,91
A_32_P65616	PRL	2,74	A_33_P3320538	NUPL1	2,21	A_24_P945194	PDCD6IP	1,98	A_23_P67569	LPPR3	1,90
A_23_P203267	TRIM29	2,72	A_23_P209288	CUL3	2,20	A_23_P361584	TMEM154	1,98	A_33_P3261565	ZRANB1	1,90
A_24_P177279	CSDC2	2,68	A_23_P205959	ALDH1A3	2,17	A_23_P82859	OSGIN2	1,98	A_32_P108156	MIR155HG	1,89
A_33_P3319870	GREM1	2,58	A_33_P3260614	PLCB2	2,15	A_23_P326319	C16orf45	1,98	A_23_P301372	TAPT1	1,89
A_33_P3214586	ARTN	2,57	A_23_P101642	PTPRH	2,15	A_23_P7582	TCF7	1,97	A_24_P378019	IRF7	1,89
A_23_P7250	CDS1	2,55	A_23_P34915	ATF3	2,13	A_24_P125283	HDAC5	1,97	A_24_P141332	CAMK2G	1,89
A_23_P379649	BMF	2,55	A_23_P157793	CA9	2,13	A_23_P115064	CRABP2	1,97	A_23_P99386	TNFSF11	1,89

ProbeName	GeneSymbol	FC (abs)
A_33_P3278906	PHF20L1	1,89
A_33_P3288074	LOC730202	1,88
A_33_P3379922	PROC	1,88
A_23_P151820	RIN3	1,88
A_33_P3231878	PIK3C2A	1,87
A_33_P3305158	ZNF621	1,87
A_24_P911607	WNT7B	1,87
A_23_P371410	PRKACB	1,87
A_23_P29257	H1F0	1,86
A_23_P27795	SPINT2	1,86
A_23_P115573	SHISA4	1,86
A_24_P237389	EIF1AX	1,85
A_24_P222872	UGT1A6	1,85
A_23_P107963	FUT1	1,85
A_33_P3314659	SPEF2	1,84
A_24_P48495	LYPD3	1,84
A_33_P3413905	ADM2	1,84
A_23_P25566	GPR183	1,83
A_23_P99741	CDKL1	1,83
A_33_P3410194	H3F3B	1,83
A_23_P53668	NFYB	1,83
A_23_P132763	VGLL3	1,82
A_23_P143143	ID2	1,82
A_23_P25194	HRK	1,82
A_33_P3216277	LOC100131354	1,81
A_23_P8452	LFNG	1,81
A_23_P211909	PLS1	1,80
A_23_P65386	OTUB2	1,80
A_23_P34930	BCAS2	1,80
A_23_P311885	L3MBTL3	1,80
A_23_P46903	CAMK2G	1,80
A_24_P318073	RPUSD4	1,80
A_33_P3245178	BEX2	1,80
A_33_P3310293	PKIG	1,80
A_24_P151582	TEF	1,80
A_23_P11915	GDAP2	1,80
A_23_P23966	ZNF488	1,80
A_32_P203430	ZNF30	1,79
A_23_P315815	NRG1	1,79
A_24_P250227	NR1D1	1,79
A_24_P203056	BCL7A	1,78

ProbeName	GeneSymbol	FC (abs)
A_23_P217054	DCAF10	1,78
A_24_P389608	C10orf47	1,78
A_33_P3394605	HMG20B	1,78
A_24_P921933	SRSF1	1,78
A_24_P296254	ARHGAP11A	1,78
A_24_P392151	C11orf86	1,78
A_23_P336198	GLCCI1	1,78
A_33_P3245006	DAK	1,77
A_23_P109322	PCP4	1,77
A_33_P3368358	NEDD9	1,77
A_24_P369898	MYO15B	1,77
A_33_P3284345	NRG1	1,77
A_24_P921897	HOOK1	1,76
A_23_P103371	ADC	1,76
A_33_P3543133	LOC283624	1,76
A_33_P3283122	WWC2	1,76
A_33_P3407356	LOC731656	1,76
A_23_P124619	S100A14	1,76
A_24_P865226	LOC440356	1,76
A_24_P226755	TOX	1,75
A_23_P151059	FAM90A1	1,75
A_32_P524904	C11orf86	1,75
A_33_P3215929	PRR5	1,75
A_23_P90804	MAP4K4	1,75
A_33_P3256920	WNT7B	1,74
A_23_P129188	CALML4	1,74
A_33_P3244021	MAVS	1,74
A_23_P148047	PTGER4	1,74
A_24_P241318	DCAF4	1,74
A_33_P3251685	PDP2	1,74
A_24_P234415	STAC	1,74
A_33_P3306264	LYPD3	1,74
A_24_P913115	PTEN	1,74
A_33_P3313622	MIR17HG	1,73
A_33_P3252834	PHLDA3	1,73
A_23_P214411	GLO1	1,73
A_33_P3394599	HMG20B	1,73
A_23_P255257	DCAF12	1,73
A_24_P139208	USP25	1,73
A_23_P256413	CMTM7	1,73
A_23_P2317	DDN	1,72

ProbeName	GeneSymbol	FC (abs)
A_24_P331704	KRT80	1,72
A_32_P118586	FAM116A	1,72
A_33_P3276282	PTPRF	1,72
A_33_P3288219	FLJ45684	1,72
A_24_P48069	DOK4	1,72
A_33_P3323298	JUN	1,72
A_24_P254551	ARHGEF9	1,72
A_23_P216935	NCRNA00287	1,72
A_33_P3794213	LOC338653	1,72
A_33_P3338360	SCARNA13	1,72
A_33_P3364112	FRS2	1,72
A_33_P3328903	LOC100506533	1,72
A_24_P11061	CSAG1	1,71
A_23_P145514	IL20RA	1,71
A_23_P255376	CCDC109B	1,71
A_23_P85716	FCGR2A	1,71
A_24_P233786	FAM129A	1,71
A_33_P3243702	KLHL30	1,71
A_23_P14986	HSD11B2	1,71
A_23_P250385	HIST1H1B	1,71
A_23_P395172	ABHD2	1,70
A_23_P88630	BLM	1,70
A_32_P80597	ELOVL6	1,70
A_24_P943613	TBC1D1	1,70
A_23_P80382	PRR5	1,70
A_24_P250650	RABL2A	1,70
A_33_P3419234	DCAF4	1,70
A_33_P3317880	ZNF252	1,70
A_24_P151727	NONO	1,70
A_33_P3316248		1,70
A_24_P99046	STK38L	1,69
A_23_P15394	CD68	1,69
A_33_P3323463	HSPA8	1,69
A_33_P3325866	FBXL17	1,69
A_33_P3380897	ATP6V1C1	1,69
A_24_P291978	ADCK2	1,69
A_24_P356601	HEXIM1	1,69
A_33_P3256952	EGLN3	1,69
A_33_P3415683		1,69
A_24_P86868	METTL10	1,69
A_23_P47077	BAG3	1,68

ProbeName	GeneSymbol	FC (abs)
A_23_P201939	PPM1J	1,68
A_32_P84242	FAM169A	1,68
A_23_P210554	SPATA2	1,68
A_23_P218770	RAC2	1,68
A_33_P3257678	HIST2H3A	1,68
A_33_P3389298	ZNF30	1,68
A_32_P152437	AKAP12	1,68
A_23_P256244	OXR1	1,68
A_23_P115261	AGT	1,67
A_24_P391431	TAF9B	1,67
A_23_P161399	MXI1	1,67
A_33_P3265224	CEP68	1,67
A_33_P3329088	PRSS8	1,67
A_23_P48936	SMAD3	1,67
A_23_P216568	C9orf6	1,67
A_23_P61810	BAIAP2	1,67
A_23_P203743	GAB2	1,66
A_23_P41629	ADAMTS16	1,66
A_23_P99747	CDKL1	1,66
A_23_P102364	NGEF	1,66
A_23_P113161	C1orf21	1,65
A_23_P152107	UBE2I	1,65
A_23_P403955	TARDBP	1,65
A_23_P35684	INPP5F	1,65
A_23_P58506	ELL2	1,65
A_33_P3422133	ADAP1	1,65
A_23_P375147	RC3H2	1,65
A_23_P7361	ELOVL6	1,65
A_24_P943957	PIKFYVE	1,65
A_24_P929754	MKNK2	1,65
A_23_P88580	ARID3B	1,64
A_23_P93938	NACAD	1,64
A_24_P235305	ZNF706	1,64
A_23_P43898	EPHX4	1,64
A_23_P163458	EHD4	1,64
A_23_P30784	ABT1	1,64
A_33_P3251522	AQPEP	1,64
A_23_P142310	MKNK2	1,64
A_33_P3332066	METTL10	1,64
A_23_P11224	MMGT1	1,64
A_24_P782308	NEDD4L	1,64

ProbeName	GeneSymbol	FC (abs)
A_24_P226116	NAA15	1,63
A_23_P133293	MCTP1	1,63
A_23_P133739	HUS1B	1,63
A_23_P201863	CDK18	1,63
A_32_P88415	MYOZ3	1,63
A_23_P158880	STARD5	1,63
A_23_P167509	CYFIP2	1,63
A_33_P3219454		1,63
A_24_P402825	CACNA2D3	1,62
A_23_P74737	EYA3	1,62
A_23_P211345	TBX1	1,62
A_23_P346969	PIK3CB	1,62
A_24_P212811	ANKRD34A	1,62
A_24_P100830	AMN1	1,62
A_33_P3226177	CYFIP2	1,62
A_23_P344988	ICK	1,62
A_23_P404821	KIAA1147	1,62
A_23_P377664	ALS2	1,62
A_23_P133536	CAPSL	1,62
A_24_P383609	NANOS1	1,61
A_23_P152353	EARS2	1,61
A_23_P38167	GPRC5C	1,61
A_23_P111311	AKAP12	1,61
A_33_P3346688	HSPA8	1,61
A_23_P319423	KCNK5	1,61
A_24_P81298	PPP6C	1,61
A_23_P135248	CCL27	1,61
A_23_P31765	PKIA	1,60
A_24_P340800	ZNF621	1,60
A_23_P28598	DLX2	1,60
A_23_P130359	ARHGAP28	1,60
A_24_P92183	PABPC1L	1,60
A_23_P37127	FOXA1	1,60
A_23_P168610	TSPAN13	1,60
A_33_P3323074	AGPAT4	1,60
A_24_P226008	MGLL	1,60
A_23_P217845	RGS16	1,60
A_33_P3359268	HMG20B	1,59
A_23_P32175	LHX6	1,59
A_24_P274795	CDCA7L	1,59
A_23_P46131	GRRP1	1,59

ProbeName	GeneSymbol	FC (abs)
A_23_P259272	WSB2	1,59
A_23_P257256	GRK6	1,59
A_23_P79518	IL1B	1,59
A_33_P3278868	HEATR5A	1,59
A_23_P17275	DNAJC27	1,59
A_23_P18384	ARMC8	1,59
A_23_P432573	MRGPRF	1,59
A_23_P35871	E2F8	1,58
A_24_P227069	GPAM	1,58
A_24_P148043	FAM20B	1,58
A_23_P358597	POPDC3	1,58
A_24_P346855	MKI67	1,58
A_23_P393401	PDXDC2P	1,58
A_23_P15108	YPEL3	1,58
A_23_P345081	ZNF655	1,58
A_32_P141724	COMMD7	1,58
A_24_P943472	NR1D2	1,58
A_24_P325520	SORT1	1,58
A_23_P317465	RAB8B	1,57
A_33_P3251144	CDCA7L	1,57
A_32_P33083	VCX2	1,57
A_33_P3841368	LOC286161	1,57
A_23_P348183	C6orf223	1,57
A_23_P80040	PROCR	1,57
A_23_P147431	LYN	1,57
A_24_P286935	ARL3	1,57
A_23_P314191	ZDHHC17	1,57
A_33_P3780901	SBNO1	1,57
A_24_P303193		1,57
A_23_P162322	WNT10B	1,57
A_23_P78802	PRKD2	1,57
A_32_P131050	ZNF148	1,57
A_23_P52761	MMP7	1,57
A_23_P151710	PTGER2	1,57
A_32_P525524	ITPRIPL1	1,56
A_24_P941268	CA5B	1,56
A_23_P80062	TAF4	1,56
A_33_P3371999	TPPP	1,56
A_23_P250735	CBX7	1,56
A_23_P125265	KPNA2	1,56
A_24_P101786	THADA	1,56

ProbeName	GeneSymbol	FC (abs)
A_24_P202139	METTL9	1,56
A_33_P3651994	GNL3LP1	1,56
A_33_P3345031		1,56
A_23_P46539	PSRC1	1,56
A_24_P921155	C3orf17	1,55
A_23_P420196	SOCS1	1,55
A_33_P3264875	GRK6	1,55
A_24_P137897	IFRD1	1,55
A_33_P3389926		1,55
A_23_P360626	PLD6	1,55
A_24_P191312	SLC1A4	1,55
A_24_P50801	NRP2	1,55
A_23_P94128	NEIL2	1,55
A_23_P8913	CA2	1,55
A_23_P54758	GDE1	1,55
A_33_P3269388	MBOAT7	1,54
A_24_P248606	ACSL3	1,54
A_24_P239606	GADD45B	1,54
A_33_P3300965	HOXC6	1,54
A_33_P3271273	HOXB2	1,54
A_33_P3298099		1,54
A_23_P201079	PRDM2	1,54
A_33_P3306504	ISYNA1	1,54
A_23_P1523	RHOD	1,54
A_33_P3240507	KCTD12	1,54
A_23_P150018	DUSP5	1,54
A_24_P172768	GMFB	1,54
A_23_P120103	KCNS3	1,54
A_32_P203300	EIF4E	1,54
A_24_P85478	ARIH1	1,54
A_23_P8339	MRPL18	1,54
A_23_P117782	LARP6	1,54
A_23_P214080	EGR1	1,54
A_23_P389919	WHSC1	1,54
A_23_P320578	RGS16	1,54
A_24_P228717	RAC2	1,54
A_33_P3343485	HIP1	1,54
A_33_P3421626	KIAA1147	1,54
A_33_P3347971	TPD52	1,54
A_23_P431179	HIST1H4A	1,54
A_24_P17870	HCP5	1,54

ProbeName	GeneSymbol	FC (abs)
A_33_P3324909	JUND	1,54
A_23_P304237	RAPGEF1	1,54
A_23_P214766	HIVEP2	1,54
A_23_P5131	ISYNA1	1,53
A_23_P401361	PITPNM2	1,53
A_23_P55256	ZNF652	1,53
A_33_P3211569	ERBB3	1,53
A_32_P219279	ELFN2	1,53
A_23_P105313	EIF2B1	1,53
A_24_P189997	PCSK6	1,53
A_33_P3237567		1,53
A_33_P3359753	C1orf96	1,53
A_23_P48585	SALL2	1,53
A_33_P3316505	SNORA73A	1,53
A_32_P87568	ENAH	1,53
A_33_P3252809	FAM118A	1,53
A_33_P3339361	ARHGAP11A	1,53
A_24_P415280	SEC61A2	1,53
A_23_P67367	DHDH	1,53
A_33_P3238455	SRSF6	1,53
A_33_P3355407	RNU105A	1,53
A_33_P3254695	RNU105A	1,52
A_32_P74955	ARID2	1,52
A_23_P75149	SFXN4	1,52
A_23_P32064	NELF	1,52
A_24_P926960	MEGF6	1,52
A_24_P280029	PDXP	1,52
A_33_P3290082	HPS4	1,52
A_33_P3217704	KIAA1539	1,52
A_33_P3269359	SPPL3	1,52
A_33_P3361546	TFAP2A	1,52
A_23_P64932	RIC8B	1,52
A_32_P183609	ASB1	1,52
A_23_P96087	H1FX	1,52
A_24_P166789	IMPAD1	1,52
A_24_P175460	CAMSAP1	1,52
A_23_P401709	C20orf196	1,52
A_33_P3236993	ARVCF	1,52
A_24_P393838	TOMM20	1,52
A_23_P106194	FOS	1,52
A_33_P3287959	RASA4	1,52

ProbeName	GeneSymbol	FC (abs)
A_33_P3311205	PRPF40B	1,52
A_23_P338505	C19orf40	1,51
A_33_P3384452	TFDP1	1,51
A_32_P216548	LDLRAP1	1,51
A_24_P229164	HIP1R	1,51
A_23_P309701	PTPN2	1,51
A_33_P3321522		1,51
A_33_P3233378		1,51

ProbeName	GeneSymbol	FC (abs)
A_33_P3323718	UACA	1,51
A_33_P3373144		1,51
A_23_P140450	SLC27A2	1,51
A_23_P74290	GBP5	1,51
A_23_P46852	OBFC1	1,51
A_23_P127915	STK33	1,51
A_23_P167005	GPR160	1,51
A_23_P75790	C11orf9	1,51

ProbeName	GeneSymbol	FC (abs)
A_24_P920188	ZNF24	1,51
A_23_P502142	FYN	1,51
A_33_P3296198	C5orf63	1,51
A_24_P161463	ZNFX1-AS1	1,51
A_23_P312246	CCDC82	1,51
A_24_P345679	MLF1	1,51
A_32_P416583	NLRC5	1,51
A_23_P216894	MAPKAP1	1,51

ProbeName	GeneSymbol	FC (abs)
A_24_P149902	SUFU	1,51
A_23_P94103	SCARA5	1,51
A_23_P101374	CYP2S1	1,51
A_24_P321511	GOLT1B	1,50
A_33_P3336287	SEC61A2	1,50
A_24_P237486	MECP2	1,50
A_32_P42574	C1orf198	1,50
A_33_P3214466	MESP1	1,50
A_24_P943106	U2SURP	1,50

Up regulated genes												
ProbeName	GeneSymbol	FC (abs)	ProbeName	GeneSymbol	FC (abs)	ProbeName	GeneSymbol	FC (abs)	ProbeName	GeneSymbol	FC (abs)
A_23_P500000	SCEL	12,18	A_23_P13548	CHRDL2	2,68	A_23_P142878	ATOH8	2,33	A_33_P3229083	HIST1H2BK	2,21
A_23_P91910	PLSCR4	9,28	A_23_P156408	C6orf155	2,66	A_32_P78681	GLP2R	2,33	A_33_P3283824	SLC39A8	2,20
A_23_P204304	PTPRO	5,40	A_33_P3221408	NTNG1	2,63	A_23_P7144	CXCL1	2,32	A_23_P344531	SYNPO	2,20
A_23_P95930	HMGA2	5,16	A_23_P145238	HIST1H2BK	2,62	A_23_P207507	ABCC3	2,32	A_24_P784765	CD59	2,20
A_23_P29773	LAMP3	5,02	A_33_P3255304	GGT5	2,61	A_33_P3253214		2,32	A_24_P106542	RSPO3	2,19
A_23_P20484	FGL1	3,84	A_32_P162250	ARHGAP18	2,61	A_33_P3379916	GLS	2,32	A_33_P3391796	NOG	2,19
A_33_P3250939	RAB3C	3,63	A_33_P3599591	PAPPA	2,60	A_33_P3361636	MGP	2,32	A_33_P3372099	DDIT4L	2,19
A_33_P3314559	RAB3C	3,61	A_23_P324340	DISP2	2,60	A_23_P137856	MUC1	2,32	A_23_P156289	OSMR	2,18
A_24_P303420	LOC221442	3,57	A_23_P135990	SLCO2A1	2,58	A_23_P164089	RFFL	2,31	A_23_P168882	TP53INP1	2,18
A_24_P88696	SCG2	3,51	A_23_P314101	SUSD2	2,57	A_33_P3246763	AANAT	2,31	A_33_P3337134	ABLIM2	2,17
A_32_P46214	SLC9A9	3,50	A_32_P122226	AMDHD1	2,56	A_23_P363769	KRT86	2,31	A_33_P3232965	TDRD6	2,17
A_33_P3415240	LOC730091	3,43	A_23_P125233	CNN1	2,55	A_23_P371266	DNM3	2,31	A_33_P3253812		2,17
A_33_P3317543	GTF2IRD2	3,43	A_33_P3418025	CTSO	2,55	A_33_P3265222	KIAA1324	2,30	A_33_P3230478	C1S	2,17
A_23_P255672	ABLIM2	3,40	A_23_P91104	KCNK3	2,54	A_33_P3406661	TMEM63C	2,30	A_23_P152305	CDH11	2,16
A_24_P290286	P4HA3	3,37	A_23_P212756	GRK4	2,53	A_33_P3294946	LOC100506173	2,30	A_33_P3775848	CLIC2	2,16
A_33_P3318852	TBC1D8B	3,28	A_23_P121665	SORCS2	2,51	A_24_P3783	HIST1H2BM	2,29	A_33_P3258478	LOC100506173	2,16
A_33_P3268304	LIMS2	3,25	A_33_P3296862	C16orf89	2,50	A_23_P502590	KIR2DS4	2,28	A_32_P229618	DLG2	2,16
A_23_P10206	HAS2	3,17	A_33_P3246833	IL1RN	2,48	A_23_P418785	STXBP5L	2,27	A_32_P59302	HIVEP3	2,15
A_23_P17192	RAPGEF4	3,15	A_32_P80850	COL14A1	2,48	A_23_P216023	ANGPT1	2,26	A_23_P151805	FBLN5	2,15
A_23_P406025	PRUNE2	3,10	A_33_P3366221	NTNG1	2,47	A_23_P416608	LAMP2	2,26	A_23_P209564	CYBRD1	2,14
A_24_P822704	TMEM198	3,09	A_33_P3884179	LOC100506123	2,47	A_23_P120153	RNF149	2,25	A_33_P3271156	SPOCK3	2,14
A_32_P209960	CIITA	3,08	A_23_P211957	TGFBR2	2,46	A_23_P27734	NPAS1	2,25	A_33_P3346966	SPAG16	2,13
A_23_P116235	MDK	2,94	A_24_P678104	STMN3	2,45	A_23_P93180	HIST1H2BC	2,25	A_32_P119033	PLCXD3	2,13
A_23_P59616	GTF2IRD2	2,93	A_33_P3229241	HIST2H2BF	2,45	A_24_P49260	SPTLC3	2,25	A_23_P101093	COPZ2	2,13
A_32_P60065	F2RL2	2,91	A_23_P218626	NEU4	2,44	A_23_P8013	HIST1H2BL	2,25	A_23_P2492	C1S	2,13
A_23_P39766	GLS	2,90	A_24_P48204	SECTM1	2,43	A_23_P111041	HIST1H2BI	2,24	A_23_P150053	ACTA2	2,13
A_23_P63343	UTS2	2,86	A_23_P350001	GUCY1A2	2,41	A_23_P111054	HIST1H2BB	2,24	A_24_P257478	COL25A1	2,12
A_24_P196528	CRB1	2,85	A_23_P200670	WDR78	2,40	A_23_P45999	FBXO2	2,24	A_32_P46571	RHBDL2	2,12
A_23_P116414	PLA2G16	2,85	A_23_P88351	ATL1	2,40	A_23_P63432	RHBDL2	2,23	A_24_P68908	LOC344887	2,11
A_33_P3289296	TMEM37	2,85	A_32_P129950	NHLRC3	2,38	A_24_P146211	HIST1H2BD	2,23	A_23_P348146	SLAIN1	2,11
A_33_P3354374	LOC100507410	2,82	A_33_P3708413	MFAP5	2,38	A_33_P3290443	SCARNA9	2,22	A_33_P3298216	MYO16	2,11
A_33_P3280157	SNORD116-19	2,79	A_23_P71855	C5	2,38	A_23_P36611	APAF1	2,22	A_23_P366216	HIST1H2BH	2,11
A_23_P42282	C4B	2,78	A_23_P3221	SQRDL	2,36	A_32_P107876	FRAS1	2,22	A_24_P261417	DKK3	2,11
A_23_P97541	C4BPA	2,76	A_23_P56578	VIT	2,36	A_24_P360206	PCDHA11	2,22	A_33_P3270346	KIR2DL5A	2,11
A_32_P156851	RCAN2	2,76	A_32_P4018	ROR1	2,35	A_33_P3233843	IL6ST	2,22	A_23_P118203	ZG16B	2,11
A_23_P46936	EGR2	2,76	A_23_P164057	MFAP4	2,35	A_33_P3284129	LYPD1	2,21	A_23_P139527	HPD	2,11
A_32_P69166	ANKRD42	2,75	A_23_P77415	OSGIN1	2,34	A_24_P388786	DNAH5	2,21	A_23_P355067	TMCO1	2,10
A_23_P83028	RECK	2,72	A_23_P12363	ROR1	2,34	A_23_P167983	HIST1H2AC	2,21	A_24_P54174	TNFRSF1B	2,09
A_23_P216361	COL14A1	2,72	A_23_P133712	CYP39A1	2,34	A_33_P3345210	TLCD2	2,21	A_33_P3256793	KIAA1324	2,09

ProbeName	GeneSymbol	FC (abs)
A_33_P3399980	TYRP1	2,09
A_24_P110558	C5orf53	2,08
A_33_P3253501	HIST2H2BF	2,07
A_33_P3233580	KIAA1217	2,07
A_23_P107775	TMEM190	2,07
A_33_P3367392	FAM167B	2,06
A_23_P4082	CCT6B	2,06
A_33_P3354464	LOXL1	2,06
A_23_P307860	SVOPL	2,05
A_23_P353035	IGFBP7	2,05
A_23_P59069	HIST1H2BO	2,05
A_23_P157914	MAMDC2	2,04
A_33_P3679876	LOC340037	2,04
A_33_P3309491	PTPRU	2,04
A_32_P37592	SCARNA17	2,04
A_32_P86763	TGM2	2,04
A_23_P318396	CELF1	2,04
A_23_P107247	CACNA1G	2,03
A_23_P89431	CCL2	2,03
A_32_P183918	MGC39372	2,03
A_23_P23611	AMY1C	2,02
A_24_P51909	CPLX1	2,02
A_23_P209625	CYP1B1	2,02
A_23_P405129	LTBP2	2,02
A_24_P55148	HIST1H2BJ	2,02
A_33_P3420466	MATN3	2,01
A_33_P3261293	DKK3	2,01
A_33_P3246623	CCDC18	2,01
A_24_P137434	DCBLD2	2,01
A_33_P3368900		2,01
A_23_P19987	IGF2BP3	2,01
A_32_P47754	SLC2A14	2,01
A_23_P350698	ANKFN1	2,00
A_23_P3956	C1QTNF1	2,00
A_33_P3258452	C12orf5	1,99
A_23_P40866	ZBTB20	1,99
A_23_P204751	ACCN2	1,99
A_32_P114284	IKZF2	1,99
A_23_P12572	CASP7	1,98
A_23_P36531	TSPAN8	1,98
A_23_P145529	PKIB	1,98

ProbeName	GeneSymbol	FC (abs)
A_23_P370544	ANKAR	1,98
A_23_P328766	ZNF519	1,98
A_24_P325107	FAM160B1	1,97
A_23_P144348	SLIT2	1,97
A_23_P201808	PPAP2B	1,96
A_33_P3357759	HEATR7B1	1,96
A_33_P3640101	LOC400684	1,96
A_24_P34155	RUNX1	1,95
A_24_P14260	CARD8	1,95
A_33_P3259775	DOCK5	1,95
A_33_P3420078	LRP11	1,95
A_24_P33982	MILR1	1,95
A_24_P414658		1,95
A_23_P127891	BDNF	1,94
A_23_P53176	FOLR1	1,94
A_33_P3233841	IL6ST	1,93
A_23_P141306	GLP2R	1,93
A_33_P3278774		1,93
A_33_P3300267	VIT	1,92
A_23_P109171	BFSP1	1,92
A_33_P3209522	SLFN5	1,92
A_33_P3317103	CCDC157	1,92
A_24_P229389	DKFZP686I15217	1,92
A_33_P3383696	SPEG	1,92
A_23_P106617	WFDC1	1,92
A_24_P926195	MAN1A2	1,91
A_33_P3288589		1,91
A_33_P3282641	LOC344887	1,91
A_33_P3349145	TTLL1	1,91
A_32_P78491	ETV1	1,91
A_33_P3240532	RGL1	1,90
A_33_P3482466		1,90
A_24_P166443	HLA-DPB1	1,90
A_33_P3398406	GLP2R	1,90
A_32_P110872	A2LD1	1,90
A_23_P122443	HIST1H1C	1,90
A_23_P170857	IL1RAP	1,90
A_23_P156687	CFB	1,89
A_23_P300484	OBSL1	1,89
A_23_P394064	PTRF	1,89
A_23_P55706	RELB	1,89

ProbeName	GeneSymbol	FC (abs)
A_23_P502470	IL6ST	1,89
A_33_P3301709	GNG4	1,89
A_23_P212339	FYCO1	1,88
A_23_P69383	PARP9	1,88
A_32_P489130	BRWD3	1,88
A_33_P3871347	SNED1	1,88
A_33_P3415395	SPTLC3	1,88
A_33_P3353552	SLC48A1	1,88
A_33_P3213822	KCNK2	1,88
A_23_P94403	TYRP1	1,88
A_24_P166663	CDK6	1,88
A_23_P29953	IL15	1,88
A_33_P3233834	IL6ST	1,88
A_33_P3290343	CYP1B1	1,87
A_33_P3282840	RPS29	1,87
A_23_P30126	FGFBP1	1,87
A_23_P85693	GBP2	1,87
A_24_P658427	NFIB	1,86
A_23_P168669	CROT	1,86
A_33_P3309643		1,86
A_23_P167997	HIST1H2BG	1,86
A_23_P215790	EGFR	1,86
A_23_P111402	RSPO3	1,85
A_33_P3381666	ABLIM2	1,85
A_23_P134237	RARRES2	1,85
A_33_P3341601	WDR86	1,85
A_23_P200741	DPT	1,84
A_33_P3218832	RIMS1	1,84
A_23_P201628	LAMC1	1,84
A_23_P207213	ALDH3A1	1,84
A_24_P225534	RHBDL2	1,84
A_23_P101407	C3	1,83
A_33_P3244669	TMEM30A	1,83
A_32_P198731	NEURL1B	1,83
A_33_P3318581	PLOD2	1,83
A_33_P3287338	IL6ST	1,82
A_23_P141394	WIPI1	1,82
A_24_P213548	MAN1A2	1,82
A_33_P3227788	PANK1	1,82
A_23_P62890	GBP1	1,82
A_24_P205994	EPGN	1,82

ProbeName	GeneSymbol	FC (abs)
A_23_P105002	ROM1	1,81
A_33_P3256425	BICD1	1,81
A_23_P96965	SYNC	1,81
A_33_P3385957	TTLL1	1,81
A_33_P3324206	HR	1,81
A_33_P3226050	GATSL3	1,80
A_24_P380536	CD164	1,80
A_33_P3285334	LOC100130417	1,80
A_23_P133236	PCDHB14	1,80
A_33_P3415087	CLCN5	1,80
A_23_P350512	ADAM12	1,80
A_23_P29057	KCNJ6	1,80
A_33_P3878772	JAK2	1,80
A_23_P205200	DHRS12	1,80
A_24_P233917	KIAA0494	1,80
A_23_P200325	RABGAP1L	1,80
A_23_P114740	CFH	1,79
A_24_P86240	BMP2K	1,79
A_23_P356526	TRIM5	1,79
A_23_P43684	BNC2	1,79
A_23_P17855	TRIOBP	1,79
A_24_P243749	PDK4	1,78
A_23_P502797	WDFY1	1,78
A_24_P161018	PARP14	1,78
A_24_P187774	SVEP1	1,78
A_33_P3230166	NALCN	1,78
A_23_P112289	TMOD1	1,78
A_32_P133916	BNC2	1,78
A_33_P3298024	ABCC3	1,78
A_33_P3365193	AMY1C	1,78
A_23_P315364	CXCL2	1,78
A_33_P3289705	GOLGB1	1,78
A_32_P214340		1,77
A_33_P3232527	EDEM3	1,77
A_33_P3313899	LOC728228	1,77
A_33_P3249674	LOC541472	1,77
A_33_P3402694	STXBP5L	1,77
A_23_P216094	ASPH	1,77
A_23_P83403	LIMCH1	1,77
A_23_P69908	GLRX	1,77
A_23_P19663	CTGF	1,77

ProbeName	GeneSymbol	FC (abs)
A_33_P3338693	SNAP25	1,76
A_24_P940166	PAPSS2	1,76
A_33_P3238433	ALDH3A1	1,76
A_32_P232214	LOC388630	1,76
A_33_P3396444	PTGR1	1,76
A_33_P3347869	C3	1,76
A_24_P270033	MPZL3	1,76
A_23_P105619	TMEM116	1,75
A_23_P67127	TMEM145	1,75
A_24_P941166	ZNF425	1,75
A_33_P3219651	BMPER	1,75
A_23_P62901	BTG2	1,75
A_33_P3344127	HIST1H2AC	1,75
A_33_P3402611		1,75
A_23_P91829	DCBLD2	1,75
A_23_P154605	SULF2	1,75
A_33_P3645465	LOC282997	1,75
A_33_P3316878	CHPF	1,75
A_23_P147839	EPHA5	1,75
A_33_P3352970	IRAK2	1,75
A_23_P360079	NCKAP5	1,75
A_24_P372625	RNF141	1,75
A_33_P3320079	NFIB	1,75
A_33_P3331726	LOC647979	1,74
A_24_P130363	C18orf1	1,74
A_23_P300150	NFATC1	1,74
A_23_P156061	LNPEP	1,74
A_23_P217564	ACSL4	1,74
A_33_P3214665	MAP2	1,73
A_33_P3345816	GPER	1,73
A_32_P130788	SAMD13	1,73
A_33_P3217230	ZNF91	1,73
A_24_P208045	EDEM3	1,73
A_23_P161424	PLXDC2	1,73
A_33_P3210218	GALNT1	1,73
A_23_P8640	GPER	1,73
A_23_P112061	HGSNAT	1,72
A_24_P153456	ZDHHC11	1,72
A_24_P115621	EIF4EBP2	1,72
A_23_P202978	CASP1	1,72
A_23_P254756	CD164	1,72

ProbeName	GeneSymbol	FC (abs)
A_23_P113825	NACC2	1,72
A_23_P327022	MDFIC	1,72
A_33_P3364864	NAMPT	1,72
A_33_P3394272	C6orf176	1,72
A_23_P92042	ITPR1	1,71
A_24_P199655	VANGL1	1,71
A_33_P3388822	ZNF233	1,71
A_33_P3413671	ABL2	1,71
A_23_P386320	MFI2	1,71
A_23_P433798	PODNL1	1,71
A_23_P216448	NFIB	1,71
A_33_P3294901	SULT1A4	1,71
A_23_P130815	KIR2DS2	1,70
A_33_P3308347	ADAMTS8	1,70
A_24_P160413	MTMR9LP	1,70
A_23_P23947	MAP3K8	1,70
A_33_P3441639	LOC145694	1,70
A_33_P3363260	PGM2L1	1,70
A_23_P422724	PPIC	1,70
A_23_P70897	ZCWPW1	1,70
A_33_P3331856	PDE1C	1,70
A_23_P163227	CKMT1A	1,69
A_23_P121064	PTX3	1,69
A_33_P3241428	OBSL1	1,69
A_23_P106241	TRIP11	1,69
A_33_P3235410	PTPLA	1,69
A_33_P3324755	LOC100128788	1,69
A_24_P229531	OBFC2A	1,69
A_24_P112447	ENTPD7	1,69
A_24_P81900	SLC2A3	1,69
A_23_P309381	HIST2H2AA4	1,69
A_33_P3306272	KIAA0825	1,69
A_23_P60837	PDE3A	1,69
A_24_P115511	RAB14	1,69
A_23_P332960	TMEM80	1,69
A_32_P68050	NEK1	1,69
A_23_P167081	REST	1,68
A_23_P428184	HIST1H2AD	1,68
A_33_P3540143	IL17RA	1,68
A_33_P3295358	ANGPTL4	1,68
A_23_P45871	IFI44L	1,68

ProbeName	GeneSymbol	FC (abs)
A_23_P54918	LDHD	1,68
A_33_P3412353	ZNF268	1,68
A_33_P3290562	GLI3	1,68
A_23_P205531	RNASE4	1,68
A_24_P161973	ATP11A	1,67
A_33_P3413098	LOC100129550	1,67
A_23_P326204	SGMS2	1,67
A_33_P3330264	CXCL1	1,67
A_24_P133253	KITLG	1,67
A_23_P39955	ACTG2	1,67
A_24_P332081	JAKMIP3	1,67
A_33_P3370404	PANX1	1,67
A_23_P56703	C2orf89	1,67
A_23_P146417	C9orf5	1,67
A_23_P8834	EPHX2	1,67
A_23_P25503	FNDC3A	1,66
A_33_P3284763	DMD	1,66
A_23_P154962	RIMBP3	1,66
A_33_P3384548		1,66
A_33_P3415092	CLCN5	1,66
A_33_P3295108	GANC	1,66
A_23_P34537	EPHX1	1,66
A_33_P3308432	MORN1	1,66
A_33_P3311551	WLS	1,66
A_33_P3320082	NFIB	1,66
A_23_P401606	EDIL3	1,66
A_23_P342709	FBXO15	1,66
A_23_P134384	PHF14	1,66
A_24_P309594	SLC48A1	1,66
A_33_P3419691	GATS	1,66
A_23_P7212	CFI	1,66
A_23_P387471	MICB	1,66
A_33_P3280521	MFAP3L	1,66
A_23_P34877	RBM15	1,66
A_23_P60166	DEPTOR	1,66
A_33_P3396339		1,66
A_33_P3231750	ZNF738	1,66
A_23_P163235	CKMT1A	1,66
A_23_P145874	SAMD9L	1,66
A_33_P3223495	FRY	1,65
A_33_P3259092	FKTN	1,65

ProbeName	GeneSymbol	FC (abs)
A_33_P3818959	SAMD11	1,65
A_23_P213620	PPP2R2B	1,65
A_23_P9523	RBKS	1,65
A_33_P3226832	F3	1,65
A_33_P3411427	ZNF837	1,65
A_23_P329261	KCNJ2	1,65
A_32_P160883	NEDD4	1,65
A_33_P3409447	AKAP11	1,65
A_24_P350576	TNIK	1,65
A_33_P3209646	WDFY2	1,65
A_23_P57268	CXADR	1,65
A_23_P64873	DCN	1,65
A_33_P3296940	FNDC3B	1,65
A_23_P210425	MYL9	1,65
A_24_P12435	NCOA7	1,64
A_23_P45087	ZNF107	1,64
A_24_P66679	NAA30	1,64
A_33_P3369436	LOC100130111	1,64
A_23_P353005	RNF217	1,64
A_33_P3340847	CARD6	1,64
A_23_P102950	RSPH1	1,64
A_23_P336644	TOR1AIP2	1,64
A_23_P201979	CREM	1,64
A_32_P128391	LOC728431	1,64
A_23_P145957	TPK1	1,64
A_23_P99163	DRAM1	1,64
A_33_P3257279	TMEM145	1,64
A_23_P7402	PDZD2	1,63
A_23_P426021	SEL1L3	1,63
A_23_P208293	PVRL2	1,63
A_23_P404481	S1PR1	1,63
A_33_P3293266	TMEM175	1,63
A_32_P427222	HEATR7B1	1,63
A_33_P3865368	LOC254896	1,63
A_33_P3299220	ADAMTSL4	1,63
A_23_P139704	DUSP6	1,63
A_33_P3313075		1,63
A_23_P218358	FBXW10	1,63
A_23_P98402	SIDT2	1,63
A_24_P191417	NAB1	1,63
A_23_P211631	FBLN1	1,63

ProbeName	GeneSymbol	FC (abs)
A_33_P3243069	KIAA0040	1,63
A_24_P295010	SERPINB9	1,63
A_32_P234145	SHC4	1,62
A_33_P3413701	ERAP1	1,62
A_23_P166508		1,62
A_24_P316005	RABGAP1L	1,62
A_32_P25737	CHIC1	1,62
A_23_P45304	XK	1,62
A_24_P257579	EPB41L4A	1,62
A_23_P352266	BCL2	1,62
A_32_P30649	ETV5	1,62
A_33_P3381318	FAM160A1	1,62
A_23_P153676	TLE2	1,62
A_33_P3238402		1,62
A_24_P541919	DENND5B	1,62
A_33_P3209831	ZNF345	1,62
A_23_P417415	ACOT11	1,61
A_33_P3296707	FAM127C	1,61
A_33_P3227472	SDSL	1,61
A_33_P3419399	ZC3H12D	1,61
A_23_P86021	SELENBP1	1,61
A_23_P82379	CACNA2D1	1,61
A_24_P38276	FZD1	1,61
A_33_P3404954	SLC38A6	1,61
A_33_P3277447	SLC26A2	1,61
A_32_P181638	BVES	1,61
A_23_P40611	TCN2	1,61
A_33_P3289845	IGFL1	1,61
A_23_P72059	VSIG10	1,61
A_23_P119478	EBI3	1,61
A_33_P3310104	SERPINB5	1,61
A_23_P99063	LUM	1,61
A_33_P3352103	LYPLAL1	1,61
A_24_P147461	SERPINB8	1,60
A_23_P302060	IFNE	1,60
A_23_P386254	NKX3-2	1,60
A_23_P501080	ZNF92	1,60
A_24_P295245	ASPH	1,60
A_23_P99661	ARHGEF40	1,60
A_33_P3741059	LOC100506459	1,60
A_33_P3373259	CACNA2D3	1,60

ProbeName	GeneSymbol	FC (abs)
A_32_P187663	ZNF596	1,60
A_23_P113777	ITGBL1	1,60
A_23_P69810	AGPAT9	1,60
A_24_P184305	BBS1	1,60
A_33_P3212490	DICER1	1,60
A_24_P370670	ZMYM6NB	1,60
A_32_P96692	POLH	1,59
A_33_P3280950	LOC144571	1,59
A_24_P217834	HIST1H3D	1,59
A_24_P941912	DTX3L	1,59
A_23_P121875	C5orf28	1,59
A_33_P3390823		1,59
A_23_P142830	PLA2R1	1,59
A_33_P3419696	FGF2	1,59
A_33_P3407606		1,59
A_33_P3333317	OPTN	1,59
A_24_P280113	IL13RA1	1,59
A_23_P207879	CARD14	1,59
A_33_P3418209	ITGBL1	1,59
A_23_P316472	DNHD1	1,59
A_33_P3327956	ZNF605	1,59
A_33_P3289865	PLCL1	1,58
A_33_P3259890	FLJ35946	1,58
A_24_P374943	CXADR	1,58
A_24_P355493	LHPP	1,58
A_24_P928052	NRP1	1,58
A_23_P65230	TMTC4	1,58
A_23_P104054	C1orf9	1,58
A_33_P3336422	LOC729013	1,58
A_33_P3344204	ZDHHC11	1,58
A_23_P258944	DNAJB9	1,58
A_33_P3401156	ETV1	1,58
A_33_P3324186	LOC642366	1,58
A_33_P3221448	ZNF264	1,58
A_23_P108751	FHL2	1,58
A_32_P20454	COPA	1,57
A_23_P329198	OBFC2A	1,57
A_33_P3381948	WTIP	1,57
A_23_P4160	NBR2	1,57
A_33_P3666884	PNPLA7	1,57
A_33_P3269806	ZNF616	1,57

ProbeName	GeneSymbol	FC (abs)
A_33_P3254141	LOC285696	1,57
A_23_P500410	ATP6V1G2	1,57
A_24_P192727	KAZALD1	1,57
A_23_P337934	FBLIM1	1,57
A_23_P252962	ITSN1	1,57
A_33_P3396214	KREMEN2	1,57
A_23_P107612	RAB27B	1,57
A_24_P223124	FNDC3B	1,57
A_23_P383118	ZSWIM5	1,57
A_33_P3306103	CALCRL	1,57
A_33_P3294608	MVP	1,57
A_23_P66311	DNASE1	1,57
A_33_P3367596	CLCN4	1,57
A_32_P63562	MIG7	1,57
A_23_P252764	SMARCA2	1,57
A_33_P3418668	PAR-SN	1,57
A_32_P94160	PRKAA2	1,57
A_33_P3308749	LAMA4	1,56
A_23_P34827	HCN3	1,56
A_33_P3263890	PRRX1	1,56
A_32_P217655	LOC645166	1,56
A_33_P3299421	ZNF530	1,56
A_33_P3391375	LANCL3	1,56
A_24_P49349	RABGAP1L	1,56
A_23_P113034	C10orf11	1,56
A_24_P150791	JPH3	1,56
A_33_P3607359	LOC399815	1,56
A_23_P151307	RAPGEF3	1,56
A_23_P161125	MOV10	1,56
A_23_P58036	MCCC1	1,56
A_33_P3421913	CADM1	1,56
A_32_P108826	ZBTB41	1,56
A_33_P3415440	MAP3K2	1,56
A_23_P327698	LMBRD2	1,56
A_33_P3214720	ZC3H12A	1,56
A_33_P3352958	ENDOV	1,56
A_23_P59798	MKRN1	1,56
A_33_P3280066	PTRF	1,55
A_32_P80741	C8orf22	1,55
A_23_P311010	SPRY3	1,55
A_23_P74088	MMP23B	1,55

ProbeName	GeneSymbol	FC (abs)
A_33_P3387861	CENPN	1,55
A_33_P3253832		1,55
A_23_P114689	ASAP3	1,55
A_33_P3331267		1,55
A_33_P3364060	HR	1,55
A_23_P26865	MYH3	1,55
A_23_P319598	C4BPB	1,55
A_33_P3409337	C14orf45	1,55
A_23_P73208	GABPB2	1,55
A_23_P146922	GAS6	1,54
A_33_P3395369	AMD1	1,54
A_33_P3243857	ADAM10	1,54
A_24_P185854	DMD	1,54
A_23_P32036	C9orf95	1,54
A_23_P1014	C1orf97	1,54
A_23_P155417	ABHD14B	1,54
A_32_P85539	HCFC2	1,54
A_23_P125423	C1R	1,54
A_24_P3045	CASP10	1,54
A_24_P300777	ADAM8	1,54
A_33_P3385782	ZNF713	1,54
A_33_P3231739	ELOVL2	1,54
A_33_P3338186	HEXDC	1,54
A_33_P3213772	SRGAP2	1,54
A_23_P151297	TENC1	1,54
A_23_P55011	SLC38A10	1,53
A_23_P33364	SH3D19	1,53
A_33_P3263417	FLJ43663	1,53
A_23_P342138	ADAMTSL1	1,53
A_23_P145485	ULBP2	1,53
A_33_P3357949	ETV1	1,53
A_32_P221256	MGC70870	1,53
A_33_P3233165	CCDC104	1,53
A_33_P3349646	PCDH7	1,53
A_33_P3304668	COL1A1	1,53
A_23_P118615	ABCA8	1,53
A_23_P398566	NR4A3	1,53
A_23_P374902	CLDND2	1,53
A_33_P3218559		1,53
A_33_P3414122	ZNF260	1,53
A_23_P59855	ZNF138	1,53

ProbeName	GeneSymbol	FC (abs)
A_23_P19852	IQCE	1,53
A_23_P84576	ANTXR1	1,53
A_23_P88184	BTBD7	1,53
A_23_P115922	EIF4EBP2	1,52
A_24_P18105	ASPH	1,52
A_23_P250136	GRIK2	1,52
A_33_P3243153	GFPT1	1,52
A_23_P44195	MSI2	1,52
A_23_P51487	GBP3	1,52
A_23_P11843	LRRN2	1,52
A_33_P3244194	PTPLB	1,52
A_32_P2392	GOLGA8A	1,52
A_33_P3711933	ARHGAP42	1,52
A_23_P35230	CD46	1,52
A_33_P3227716	GATSL3	1,52
A_32_P124708	ONECUT2	1,52

ProbeName	GeneSymbol	FC (abs)
A_23_P206501	CLEC18B	1,52
A_33_P3284939	TMEM189	1,52
A_32_P191895		1,52
A_33_P3259938	LOC100130547	1,52
A_23_P144384	GALNT7	1,52
A_23_P357811	MBNL1	1,52
A_33_P3260575	CERCAM	1,52
A_24_P167338	RAB30	1,52
A_33_P3237977	LARP6	1,52
A_33_P3307197	PTGFRN	1,52
A_23_P397417	TMEM188	1,52
A_33_P3367830	EFEMP2	1,52
A_33_P3400828	NXNL2	1,52
A_23_P93881	SYPL1	1,51
A_23_P211047	BACH1	1,51

ProbeName	GeneSymbol	FC (abs)
A_23_P210210	EPAS1	1,51
A_23_P136978	SRPX2	1,51
A_23_P167401	PCDHB11	1,51
A_24_P307572	ANKRD13A	1,51
A_23_P21162	TCTEX1D2	1,51
A_32_P190303	LONRF2	1,51
A_33_P3243332	ARHGAP42	1,51
A_33_P3212615	TFPI	1,51
A_33_P3249364	TMTC1	1,51
A_23_P71037	IL6	1,51
A_23_P305140	C10orf32	1,51
A_23_P100654	ZBTB4	1,51
A_33_P3228325	SP100	1,51
A_33_P3535175		1,51
A_24_P321068	SLC31A1	1,51

ProbeName	GeneSymbol	FC (abs)
A_32_P197561	EBF1	1,51
A_33_P3240912	MAGT1	1,51
A_33_P3397658	SYNPO	1,51
A_33_P3257518	FLJ22447	1,51
A_24_P45367	NIPAL3	1,51
A_23_P149858	ELOVL3	1,50
A_33_P3739260	CAP2	1,50
A_33_P3238685	TET2	1,50
A_24_P406754	LOXL4	1,50
A_23_P166526	RIBC2	1,50
A_23_P114414	LONRF3	1,50
A_33_P3219572	LONRF3	1,50
A_23_P129556	IL4R	1,50
A_23_P8522	TMEM106B	1,50
A_23_P41854	CARD6	1,50

7.4 MATERIALS AND METHODS

Constructs

The sequences of the primers used in this study are listed in the Supplementary Table 1. RT-PCR was performed on total RNA isolated from HeLa cells using the TRIzol reagent (Invitrogen). Raly cDNA was amplified with the Phusion High-Fidelity DNA polymerase (New England BioLabs) and then cloned in frame with either EGFP (pEGFP-N1, Clontech), dsRED (pDsRED, Clontech) or in the same vector in frame with HA lacking EGFP. Point mutations were created using the QuickChange site-directed mutagenesis kit (Stratagene) according to the manufacturer's protocol.

BAP-tagged RALY was created using two complementary primers, which were annealed and cloned in frame to RALY cDNA in the pEGFP-N1 vector lacking the EGFP-coding sequence. BAP-tagged RALY was created as previously described (Petris, Vecchi et al. 2011). The construct to express RALY lacking the glycine-rich region (RALY-ΔGRR) was created using the site-directed mutagenesis kit (Finnzymes, Thermo Scientific) according to the manufacturer's protocol with the following primers: 5′- gagaacacaacttctgaggcaggc and 5′-ctgctccaagcggctcagcagggc.

The list of all the primers is reported in supplementary in Appendix 7.5.

Competition assay

For the antibody competition assay, the RALY full-length cDNA was cloned into pGEX-T (Amersham Biosciences, Buckinghamshire, UK), for expression as a GST fusion protein in the *E. coli* strain Rosetta (Novagen, Madison, WI, USA) and purified with MagneGSTProtein Purification System (Promega). 5 µg of anti-RALY antibody (Bethyl) were incubated with 30 µg of purified GST-RALY full length fusion protein for 2h at 4°C in Detector Block (KPL, Gaithersburg, MA, USA). As a positive control, 5 µg of anti-RALY antibody were incubated for 2h at 4°C in Detector Block. The two solutions were tested on western blots using HeLa cells lysate.

Cell cultures, transient transfections, silencing

Hek293T, HeLa and MCF7 cells grown in DMEM supplemented with 10% FCS. Ovcar 3 cells were grown in DMEM/DMEM F-12 (50/50) supplemented with 10% FCS as previously described (Vidalino, Monti et al. 2012). OliNeu cells were grown in SATO medium (ref Trotter) added 2% FCS. All the cell lines were transfected using the TransIT transfection reagent (Mirus, Bio LLC) according to the manufacturer’s protocol.

For the silencing, the cells were transfected with the specific pool of siRNA for RALY: ON-target plus SMART pool (Thermo Scientific Dharmacon) using INTERFERin transfection reagent (Polyplus Transfection). Then the cells were incubated for 72 hours. Metabolic stress was induced using 0.5 mM Na-arsenite (Sigma) for 1 hour (Kedersha, Chen et al. 2002; Vessey, Vaccani et al. 2006).

Immunocytochemistry and fluorescence microscopy

Cells grown on cover slips were washed in pre-warmed PBS and then fixed in 4% PFA for 15 min at room temperature. Immunocytochemistry was carried out as previously described (Goetze, Tuebing et al. 2006). The following primary antibodies were used: rabbit polyclonal anti-RALY (dilution 1:500; Bethyl Laboratories); mouse polyclonal anti-RALY (dilution 1:100, Abcam). For the other antibody see supplementary in Appendix 7.5. Alexa 594- Alexa 688- and Alexa 488-coupled goat anti-mouse and anti-rabbit IgG were used as secondary antibodies (dilution 1:500, Life Technology). Microscopy analysis was performed using the Zeiss Observer Z.1 Microscope implemented with the Zeiss ApoTome device and the pictures were acquired using AxioVision imaging software package (Zeiss). Confocal images were acquired using the Leica confocal microscope. Images were not modified other than adjustments of levels, brightness and magnification.

Preparation of cell extracts and Western blot

Cells were washed with pre-warmed PBS, lysed in lysis RIPA buffer plus proteinase inhibitor and phosphatase inhibitor mixture (Roche), or lysed with NEHN lysis buffer [20 mM HEPES pH 7.5, 300 mM NaCl, 0.5 % NP-40, 20% glycerol, 1 mM EDTA, phosphatase and protease inhibitors (Roche)] and incubated for 30 minutes in ice. Then the lysate were centrifugated at 10000 g for 5 min a 4°C. Then the surnatant were stocked at -80°C.

Equal amounts of proteins were separated by 10 or 12% SDS-PAGE and blotted onto nitrocellulose (GE Healthcare). Western blots were probed with anti-mouse- and anti-rabbit-HRP secondary antibodies, scanned and analyzed with the Image Lab software (BioRad). The list of antibodies used is in supplementary in Appendix 7.5.

iBioPQ

All the Material and Method for the technique are reported in article "Proteome-Wide Characterization of the RNA-Binding Protein RALY-Interactome Using the in Vivo-Biotinylation-Pulldown-Quant (iBioPQ) Approach." (Tenzer, Moro et al. 2013)

Polyribosome analysis and pharmacological treatments

Polyribosome analysis was performed as described in (Provenzani, Fronza et al. 2006). Briefly, HeLa cells grown on 10 cm Petri's dishes were incubated with DMEM supplemented with cycloheximide (0.01 mg/ml) for 3 minutes then washed 3 times with cold PBS. Cells were then lysed with the lysis buffer [10 mM NaCl, 10 mM MgCl2, 10 mM Tris-HCl ph 7.5, 0.1% Triton X-100, 1U of RNase Lock (Fermentas), 1 mM DTT, 0.01 mg/ml cycloheximide, 0.1% NaDeoxycholate]. The cell extracts were loaded onto 5-20% w/w density gradient of sucrose and centrifuged at 40.000xg for 160 min at 4°C. For RNase treatment, the extracts were incubated with 100 ug/ml RNase A for 15 minutes, and then loaded to the sucrose gradient. EDTA was added to the cell lysate at the final concentration of 100 mM. The treatment with puromycin (100 μg/ml) was performed for 3 hours. One ml of each fractions was collected, proteins precipitated with TCA and the pellets were resuspended in RIPA buffer (Thermo Scientific). For the starvation experiments, HeLa cells were incubated for 24 hours in DMEM without FCS.

Microarray analysis

HeLa cells were grown on 10 cm Petri dishes. Total RNA was extracted from 4 biological replicates using the Agilent Total RNA Isolation Mini kit (Agilent Technologies, Milan, Italy) according to the manufacturer's protocol. RNA was quantified using the NanoDrop spectrophotometer (NanoDrop Technologies, Wilmington, DE, USA) and its quality was assessed by the Agilent 2100 Bioanalyzer. Hybridization, blocking and washing were performed according to Agilent protocol "One-Color Microarray-Based Gene Expression Analysis (Quick Amp Labeling)". Hybridized microarray slides were then scanned with an Agilent DNA Microarray Scanner (G2505C) at 5-micron resolution with the manufacturer's software (Agilent ScanControl 8.1.3). The scanned TIFF images were analyzed numerically using Feature Extraction (Agilent) and Genespring (Agilent), to derive the information regarding gene fold-change.

RealTime PCR

The RNA was purified from cells grown in a 10 cm dish using the commercial kit RNeasy Mini Kit (Quiagen). Then the RNA was retrotranscripted in cDNA by RevertAid First Strand cDNA Sunthesis Kit (Thermo Scientific Fermentas). For the RealTime PCR was used the KAPA PROBE FAST qPCR Kit (KAPA Biosystems) and the specific primers and probe for RALY, Actin, GAPDH, PTPRR, PLSCR4, PTPRO, SCEL, HSPB3, RRAD sold by IDT (TEMA ricerca). The plate with all the samples was incubated in BioRad C1000 Thermo Cycler for 40 cycles of reaction. The result was analyzed with Bio-Rad CFX Manager version 2.1.

Cell cultures and pharmacological treatments

MCF7 cells were grown in DMEM supplemented with 10% FCS. After 24 hours the medium was changed with DMEM whit 10% FCS supplemented with 1,5 ng/μl Doxorubicin. The cells were incubated for 2, 4, 8, 12 or 16 hours before lyses. For the treatment with MG132 after primary incubation the cell was treated with 1,5 ng/ μl Doxo and 10 ng/ μl MG132.

7.5 SUPPLEMENTARY

7.5.1 List of primers

Construct	Sequence[a]
$RALY_{1-306}$	5'- ctcagatctatgtccttgaagcttcaggca 5'- tttaccggttgcaaggccccatcatccgc
$RALY_{1-142}$	5'- ctcagatctatgtccttgaagcttcaggca 5'- tttaccggtaccgccctgggcactggcac
$RALY_{132-306}$	5'- ctcagatctatgcgtctgtcgcccgtgccagtg 5'- tttaccggttgcaaggccccatcatccgc
$RALY_{\Delta GRR}$	5'- ctcagatctatgtccttgaagcttcaggca 5'- cggaccggtacctccatcacccttcttctt
$RALY_{HA}$	5' - agaattc**atgtacccatacgatgttccagattacgct**tccttgaagcttcaggcaagcaatg 5' - ttgcggccgcttactgcaaggccccatcatccg
$RALY_{RFP}$	5'- gggaattccttgaagcttcaggcaagcaat 5'- aaaaggtaccttactgcaaggccccatcatccg
$RALY_{BAP}$	5′- gagaacacaacttctgaggcaggc 5′- ctgctccaagcggctcagcagggc
Del-NLS1	5' - cgggtcaaaactaacgtacctgtc 5' - cgggaccgccctgggcactg
Del-NLS2	5' - gggggtggcgccggcggcggc 5' - gggattggccttttgctccgcagc
$NLS\text{-}1_{PR/AA}$	5' - agggcggtccctgtgaagcgaGCAGCGgtcacagtccctttggtccgg 5' - ccggaccaaagggactgtgaccgctgctcgcttcacagggaccgccct
$NLS\text{-}2_{RR/AA}$	5' - cgggtcacagtccctttggtcGCTGCAgtcaaaactaacgtacctgtc 5' - gacaggtacgttagttttgactgcagcgaccaaagggactgtgacccg
$NLS\text{-}3_{KK/AA}$	5' - aaggccaatccagatggcaagGCTGCAggtgatggaggtggcgccggc 5' - gccggcgccacctccatcacctgcagccttgccatctggattggcctt

[a] The restriction enzyme sites are underlined; HA sequence is in bold.

7.5.2 List of antibodies

Antibodies	Company	Dilution for SDS-PAGE	Dilution for IF
Rabbit anti-RALY	Bethyl	1:5000	1:250
Mouse anti-RALY	Sigma		1:100
Rabbit anti-Casc3	HomeMade	1:5000	1:250
Mouse anti-hnRNP A1	Genetex	1:5000	
Mouse anti-p53	SantaCruz	1:5000	1:500
Rabbit anti-γH2AX	Cell Signaling	1:5000	1:250
Mouse anti-RPL26	Cell Signaling	1:5000	
Rabbit anti-PABP	AbCam	1:5000	
Rabbit anti-Actin	SantaCruz	1:5000	
Rabbit anti-Actinin	SantaCruz	1:10000	

The list of antibody used for the publications are not reported in this table.

ACKNOWLEDGE

Perhaps a four-year period is a short time to conclude successfully a project, BUT these four years were full of new experiences and connections of people beyond my expectations. All this heterogeneous network of people, that has grown more and more, has represented my little world and now, at the end of my long experience, it becomes very difficult to thank everybody.

The first person who I want to thank is my boss prof. Paolo Macchi. I don't know why he decided to accept me in his lab and probably, he has repented of his choice several times. Nevertheless, despite our frequent different opinions I was very happy to work with him, because I learned so much and I hope to learn even more in the near future: he is my mentor and I hope that our collision can continue☺.

I then thank all people with whom I have collaborated: In primis Betty for the thesis' revision and for helping me solves all the bureaucratic problems during these years. I would like to thank my referees, prof.s Jacqueline Trotter and Stefano Ferrari, for the time spent on the revision of my thesis, for their priceless suggestions and for the support they gave me during my entire project.

My gratitude goes to all people who supported me during my PhD: my colleagues of the 25th cycle, with whom I shared my joys and sorrows of being a PhD student; the other students of the PhD program in Biomolecular Sciences (in particular AC, SZ, CZ, NB, SW) ; all professors who helped me resolve my problems, my doubts and my questions (prof. Cereseto, Inga, Jousson, Provenzani, Guella, Demichelis); all researchers and the Postdocs at Cibio for their advice and support (FD, LV, YC, AB, MG, PB, GV, etc.). I'd like to thank all bachelor students (Alex, Federica, Maria, Patrick), who have had the fortune (or misfortune) to have me as their supervisor. Last but not least, I would like to thanks to the people whom I shared these years outside the works (NP, MP, IZ, MS, etc); with them I shared my time, my concerns and more yet☺. Thank you everybody for the wonderful time that I spent with all of you.

In conclusion, I address my special thanks to my parents Elda and Giancarlo, who lovely supported me especially during the hardest moments of my staying in Trento; thanks to my brother Alessandro: he's my inspiration, he, and our brotherly competition often forced me to improve, that's why I challenge him to reach the same goal in four/five years! Finally, I want to thank my best friends Sabrina, Alberto, Mattia, Ashwant, Micaela e Paola; they are the core of my world, and without them I could not have achieved this important result of my life and scientific career.

In the end, thank you my little world!!!